IMPLICATIONS OF ENVIRONMENTAL CHANGE FOR WETLAND VULNERABILITY AND CARBON STORAGE IN COASTAL LOUISIANA

AN ABSTRACT

SUBMITTED ON THE 6 DAY OF AUGUST 2018

TO THE DEPARTMENT OF EARTH AND ENVIRONMENTAL SCIENCES

IN PARTIAL FULFILLMENT OF THE REQUIREMENTS

OF THE SCHOOL OF SCIENCE AND ENGINEERING

OF TULANE UNIVERSITY

FOR THE DEGREE

OF

DOCTOR OF PHILOSOPHY

BY

Krista L. Jankowski

APPROVED:

Torbjörn E. Törnqvist, Ph.D.
Committee Chair

Mead A. Allison, Ph.D.

Matthew L. Kirwan, Ph.D.

Brad E. Rosenheim, Ph.D.

IMPLICATIONS OF ENVIRONMENTAL CHANGE FOR WETLAND VULNERABILITY AND CARBON STORAGE IN COASTAL LOUISIANA

DISSERTATION ABSTRACT

Natural systems can be altered, over a wide range of time scales, through changes in environmental conditions. In the Mississippi Delta, which has been shaped by changes in sediment deposition and sea level at the land-ocean interface over the Holocene, changes to environmental conditions lead to state changes that can be observed in both modern ecosystems and the depositional record. Alluvial strata (which comprise the bulk of the world's sedimentary record) can provide insight into past triggers for ecosystem state changes and can be compared to modern monitoring data to paint a fuller picture of system response to environmental change. Given the large potential impact of anthropogenic climate change on natural systems, this combination of modern and paleo-environmental information may improve our ability to predict future conditions.

This dissertation explores coastal and delta plain ecosystem responses to environmental change, particularly relative sea-level rise over annual to millennial timescales (Chapters 2 and 3) and rates of carbon storage by organic and clastic deposits in the Mississippi Delta (Chapter 4). Chapter 2 describes the results of an analysis of how subsidence and relative sea-level rise affect modern wetlands in coastal Louisiana. Using 274 rod surface-elevation table – marker horizon records, GPS measurements, and satellite altimetry data from the Gulf of Mexico, this chapter assesses present-day wetland vulnerability given current environmental conditions.

Chapter 3 describes an analysis of how changes in past environmental conditions, specifically variable rates of relative sea-level rise, impacted marshes in the Mississippi Delta throughout the Holocene. Using 355 sediment cores, this chapter identifies relative sea-level rise tipping points that lead to marsh collapse and a state shift from marsh to open water. Using ^{14}C dating, foraminiferal assemblage analysis, and stable isotope geochemistry, this chapter also estimates the time necessary for reestablishment of

terrestrial conditions after an initial marsh collapse and conversion to open water at one selected location. Together, these results provide a framework for projecting likely marsh response to future increased rates of relative sea-level rise in coastal Louisiana. The combination of these studies provides a more complete picture of modern and future wetland vulnerability in coastal Louisiana and provides unique insights into the limitations of short-term observational studies of marsh conditions for projecting long-term outcomes in response to environmental change.

Chapter 4 describes the results of a comparative analysis of carbon storage rates in organic and clastic deposits within the Holocene sedimentary record near Bayou Lafourche in the Mississippi Delta. Using ^{14}C and OSL dating, elemental analysis, and bulk density measurements collected from three sediment cores, this chapter calculates carbon storage rates to determine the relative carbon storage efficiency of these deposits. This chapter provides an important comparison to similar work in deltaic deposits of the Wax Lake Delta. Furthermore, the high rates of carbon storage within the dominantly clastic deposits, which are interpreted as a proxy for planned sediment diversions in the region, provide an estimate for future carbon storage potential by these coastal restoration efforts.

IMPLICATIONS OF ENVIRONMENTAL CHANGE FOR WETLAND VULNERABILITY

AND CARBON STORAGE IN COASTAL LOUISIANA

A DISSERTATION

SUBMITTED ON THE 06 DAY OF AUGUST 2018
TO THE DEPARTMENT OF EARTH AND ENVIRONMENTAL SCIENCES

IN PARTIAL FULFILLMENT OF THE REQUIREMENTS

OF THE SCHOOL OF SCIENCE AND ENGINEERING

OF TULANE UNIVERSITY

FOR THE DEGREE

OF

DOCTOR OF PHILOSOPHY

BY

Krista L. Jankowski

APPROVED:

Torbjörn E. Törnqvist, Ph.D.
Committee Chair

Mead A. Allison, Ph.D.

Matthew L. Kirwan, Ph.D.

Brad E. Rosenheim, Ph.D.

Table of Contents

List of Tables

List of Figures

1. Introduction

The modern landscape of coastal Louisiana, including the Mississippi Delta plain, has been formed and subsequently altered through the complex interactions of natural and human processes. While North American watersheds have drained into the Gulf of Mexico since the early Cretaceous (Buffler, 1991) and the region is underlain by an extensive, largely compaction-free Pleistocene-aged deposit (Fisk, 1938), it is Holocene deposition that has arguably defined coastal Louisiana and the Mississippi Delta plain.

Dating back to the 1930s, geologic research on the Holocene Mississippi Delta plain (e.g. Trowbridge, 1930; Russell, 1936; Fisk, 1938) revealed that great swaths of coastal Louisiana's land were a result of the overlapping deposits of abandoned Mississippi River delta lobes. In the 1940s and 1950s, further research (e.g. Russell, 1940; Fisk, 1944; Fisk et al., 1954; Fisk and McFarlan, 1955; Kolb and Van Lopik, 1958) refined the understanding of the processes behind these deposits, known as delta cycling, that involved the progradation of a delta lobe in one location followed by subsequent river path abandonment and shift of deposition to another area following avulsion.

Reworking of delta sediments through transgressive events following delta abandonment (Penland et al., 1988) and deposition of riverine sediments through overbank flooding, crevasse splays, and distributary systems has further altered the Holocene geology of the region (e.g. Saucier, 1994; Roberts, 1997). Organic deposits, notably thick peat beds, also underlie the Mississippi Delta plain (Fisk, 1960; Frazier and Osanik, 1969; Kosters et al., 1987) and formed through the anaerobic burial of alluvial and/or coastal wetland vegetation (e.g. Tye and Kosters, 1986; Kosters et al., 1987; Kosters, 1989) linked to changes in sea-level rise through the Holocene.

Historically, marshes in the Mississippi Delta plain existed at the intersection of fluvial and coastal influences. Freshwater marshes adjacent to the natural levees of the Mississippi River and the proximal portion of its distributaries were maintained through periodic flooding that supplied freshwater and sediment to the alluvial plain, while salt marshes benefitted from tidal transport of marine sediments and nutrients onto the marsh surface. Salinity was also mediated by the interaction of freshwater and saltwater throughout these marsh systems. Importantly, overbank flooding as well as levee breaching by crevasse splays provided marshes with freshwater, nutrients, and sediments that helped alleviate salt stress, allowing marsh vegetation to thrive. These clastic and organic contributions helped maintain marsh surface elevation and allowed marshes to persist, even as relative sea level rose through time.

Since the start of the 20th century, significant environmental changes – in particular, man-made changes – have led to remarkable land loss in coastal Louisiana. In the past ~80 years, the state of Louisiana has suffered ~5000 km^2 of land loss with very little land building (concentrated around the mouth of the Atachafalaya River) to counteract it (Couvillion et al., 2017). A decades long history of river leveeing by the US Army Corps of Engineers and significant upstream damming to provide flood protection for Midwestern communities has decreased sediment supply to the delta and alluvial plain (e.g. Blum and Roberts, 2009) resulting in less clastic deposition to support land building and marsh maintenance. Extensive land use changes have resulted from oil and gas exploration and development in the region, including the alteration of hydrology and marsh integrity due to dredging of navigation canals (Day et al., 2000), and altered rates of subsidence due to subsurface fluid extraction (Kolker et al., 2011).

Rapid marsh loss in coastal Louisiana not only alters the state in map view but also increases migration pressures on indigenous coastal populations (Maldanado et al., 2013) and significantly decreases the value of ecosystem services provided by wetlands, including wildlife habitat and storm protection (Costanza et al., 2014) and carbon storage (DeLaune and White, 2012). Furthermore, the issue of large scale land loss is only exacerbated by the interconnectedness of these ecosystems, with initially localized marsh collapse often expanding to larger areas as the overall system is weakened (Fagherazzi, 2013; Ortiz et al., 2017).

Given the importance of these coastal ecosystems and the threats to their persistence in the landscape, many studies have been undertaken to characterize current coastal conditions in an attempt to project future outcomes. For instance, modern wetlands are at risk from the impacts of current and future climate change, particularly relative sea-level rise (RSLR) (e.g. USGCPR, 2017). In order to better understand what the future may hold for coastal marshes in Louisiana, it is important to have a clear baseline of current conditions and short-term vulnerability. Over the past 30 years, surface-elevation tables have been used to track changes in surface elevation and vertical accretion in both natural and experimentally manipulated marsh settings (e.g. Ford and Grace, 1998; Lane et al., 2006; Day et al., 2011; Cahoon et al., 2011). These studies have traditionally been limited in size, with, generally fewer than 20 surface-elevation table sites in use for a given study, prompting calls (Lovelock, et al., 2015; Webb et al., 2013) for large-scale, regionally continuous monitoring. Such a large-scale monitoring effort could significantly add to our understanding of marsh vulnerability to environmental change in coastal Louisiana.

To more effectively predict future marsh response to increasing rates of RSLR, records of response to Holocene changes in sea level are important as it is not assured that observations for the past 5–10 years will translate into longer-term wetland resilience. In the Mississippi Delta plain, alluvial strata contain information about past changes including the timing and location of delta building and progradation (e.g. Fisk, 1938; Roberts, 1997; Shen et al, 2015; Chamberlain et al., 2018) and delta switching events (e.g. McFarlan, 1961; Frazier, 1974; Saucier, 1964; Törnqvist et al., 1996).

Environmental responses to changes in Holocene sea level, including rapid RSLR events, are also recorded in alluvial strata (Törnqvist et al., 2004a; Törnqvist et al., 2004b; González and Törnqvist, 2009). However, there is potential for additional insights to be extracted from the alluvial record, in conjunction with these previous sea-level studies, to answer questions about the link between RSLR and Holocene landscape evolution. For instance, we know that some sites have drowned and then had terrestrial conditions being re-established, but it is not well understood what changes to environmental conditions, and at what rates, lead to these outcomes, as well as their implications for a coastal Louisiana at risk due to anthropogenic climate change and RSLR.

Environmental change can also impact geochemical cycles. Organic carbon (OC) is exchanged between the terrestrial, marine, and atmospheric reservoirs on short (annual to decadal) and long (centennial to millennial) time scales. It is well-known that organic-rich deposits, such as peats derived from coastal marshes, accumulate carbon at rapid rates of ~200 $g/m^2/yr$ (Chmura et al., 2003; Baustian et al., 2017) in modern ecosystems. What is less well-known is whether this modern (annual to decadal time scale) OC accumulation rate is representative of long-term (centennial to millennial time scale) OC storage rates for organic rich deposits. Furthermore, it is unknown how deposition in different subdelta environments (e.g., inland, freshwater swamps in the delta plain, flood basins, and crevasse splays) compare in terms of OC storage rates over longer time scales. The rich alluvial record in the Mississippi Delta plain, with extensive peat beds and diversion-like crevasse-splay deposits, could be analyzed to determine how carbon storage for these different deposits compare and to examine possible implications for the global carbon cycle as well as coastal restoration efforts.

from marshes in North America and Europe suggests that concerns about marsh vulnerability to sea-level rise may have been overstated (Kirwan et al., 2016). However, these authors also acknowledge the "limits to marsh adaptability in places such as coastal Louisiana", a region they recognize as underrepresented in their study. With present-day relative sea-level rise (RSLR) rates among the highest in the world (12 ± 8 mm yr^{-1}), coastal Louisiana may provide a window into the future for similar settings worldwide given global sea-level predictions with similar rates later in this century.

Louisiana's coastal wetland loss (~5000 km^2 between 1932 and 2010; Couvillion et al., 2011) is a complex problem, impacted by decreased sediment supply due to river leveeing and damming (Blum and Roberts, 2009), dredging of navigation canals (Day et al., 2000), and subsurface fluid extraction (Kolker et al., 2011). The resilience of coastal wetlands is influenced by a number of feedbacks (FitzGerald et al., 2008; Fagherazzi et al., 2012) and for these ecosystems to persist, surface elevation must be gained at a rate that equals or exceeds that of RSLR, particularly since landward migration is not always possible (Kirwan and Megonigal, 2013). Short-term (annual to decadal) resilience often involves non-linear responses to environmental factors that may be detrimental over longer timescales. For example, RSLR may induce short-term positive surface-elevation change (SEC) through increased mineral deposition during inundation (Reed, 1995). Modest environmental stress from RSLR may spur increased plant productivity (Morris et al., 2002), organic matter accretion, and trapping of clastic sediment (Fagherazzi et al., 2012) in some cases, although for wetlands with limited elevation capital (i.e., low initial elevation as is the case in coastal Louisiana) prolonged inundation decreases plant productivity (Kirwan and Guntenspergen, 2012). Importantly, vertical accretion (VA) at the wetland surface can be partially or entirely offset by subsidence, including shallow subsidence (SS). Therefore, the interplay between these two variables determines whether net surface-elevation gain occurs (Cahoon et al., 1995) (Fig. 2.1).

An influential attempt to model marsh dynamics (Morris et al., 2002) found that salt marshes may be able to withstand RSLR rates up to ~12 mm yr^{-1}, given optimal primary productivity and high sediment loading in a mesotidal environment with monotonic RSLR. A subsequent synthesis of five numerical models (Kirwan et al., 2010) concluded that marshes with suspended sediment concentrations of >20 mg l^{-1} and a tidal range of <1 m – conditions applicable to coastal Louisiana – may not become vulnerable to drowning until RSLR rates are on the order of ~10 mm yr^{-1}. However, observational evidence to test these

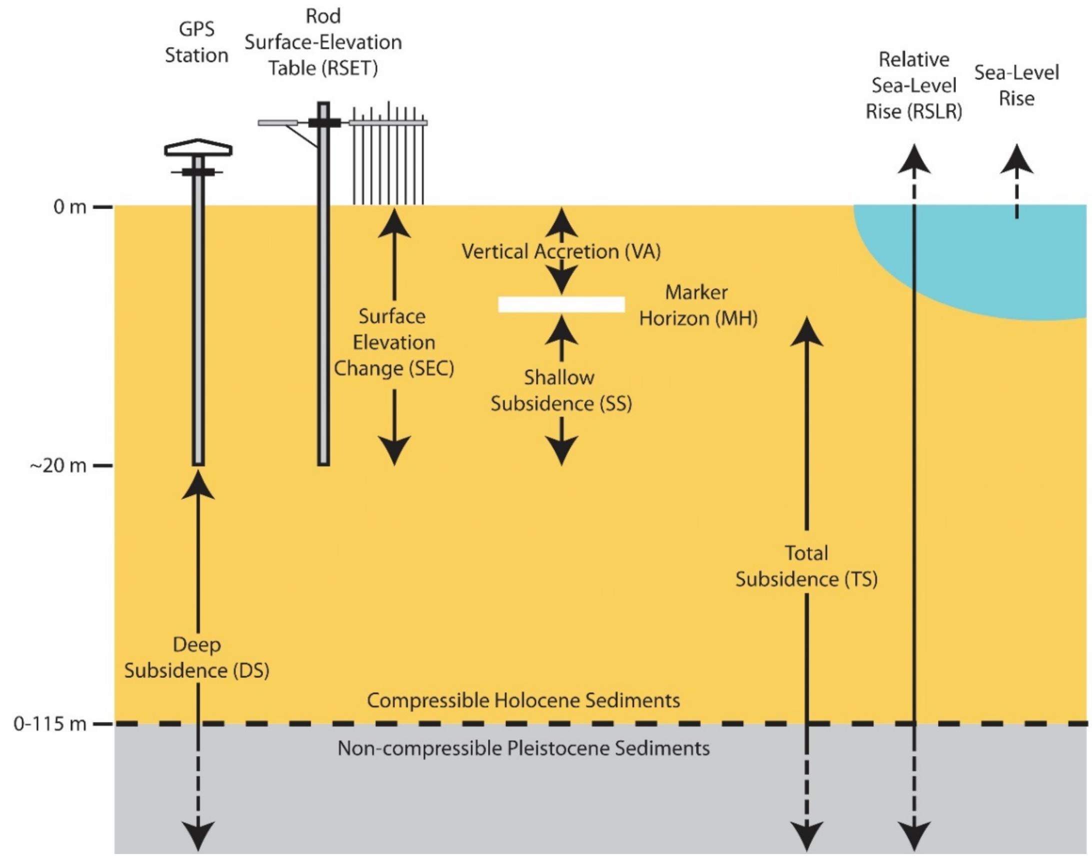

Figure 2.1. Relationship between study variables. Representation of surface-elevation change, vertical accretion, shallow subsidence (vertical accretion – surface-elevation change), deep subsidence, total subsidence (shallow subsidence + deep subsidence), sea-level rise, and relative sea-level rise (total subsidence + sea-level rise) as used in this study. When the vertical accretion rate exceeds the rate of relative sea-level rise there is an accretion surplus; when the vertical accretion rate is less than the rate of relative sea-level rise there is an accretion deficit. Figure is not to scale. Modified from Webb et al., 2013.

model results is sparse. Currently available SEC rates are derived from relatively small case studies in coastal Louisiana (Ford and Grace, 1998; Lane et al., 2006; Day et al., 2011; Cahoon et al., 2011) (<20 sites; Appendix A, Table A2) and have produced results that are inconclusive as to whether RSLR outpaces wetland surface-elevation gain. Additionally, the complex feedbacks of multiple variables (e.g., vegetation type and initial elevation) vary among wetland sites, limiting the usefulness of data from a small number of sites to elucidate broader trends. Thus, it is increasingly clear that much larger datasets are required to address this problem (Kirwan et al., 2016; Lovelock et al., 2015).

Here we test the hypothesis that wetlands in coastal Louisiana are keeping up with present-day rates of RSLR. We evaluate 274 new records (Fig. 2.2) derived from rod surface elevation table – marker horizon (RSET-MH) measurements, a well-established method for studying coastal wetland change (Webb et al., 2013). Our dataset, provided through Louisiana's Coastwide Reference Monitoring System (CRMS) (Steyer et al., 2003), is an order of magnitude larger than any currently available regionally continuous dataset worldwide (Appendix A, Table A2). The size and density of this dataset therefore offer unprecedented opportunities for studying present-day coastal wetland dynamics along with its uncertainties, spatial patterns, and the delicate interplay between VA, SS, and SEC (Fig. 2.1). We find that many wetland sites across coastal Louisiana, and especially those concentrated in its westernmost portion, exhibit an accretion deficit that results in vulnerability to modern rates of RSLR.

2.3 Results

2.3.1 Calculated rates

SEC rates exhibit substantial variability among individual sites (s.d. = 7.4 mm yr^{-1}; Table 2.1). Mean (5.7 mm yr^{-1}) and median (5.8 mm yr^{-1}) SEC rates are higher in the Mississippi Delta than in the Chenier Plain (-0.2 and -0.5 mm yr^{-1}, respectively) (Fig. 2.2a, Table 2.1). This difference is statistically significant according to a one-way ANOVA test ($F(1,272) = 43.5$, $p = 2.2E-10$). It is important to note that SEC rates are expressed with respect to the base of the RSET rod, which may itself be subsiding. This would make our measured rates upper limits for the true SEC values. However, recent studies (Yu et al., 2012; Wolstencroft et al., 2014; Karegar et al., 2015) allow us to estimate deeper subsidence rates for sites

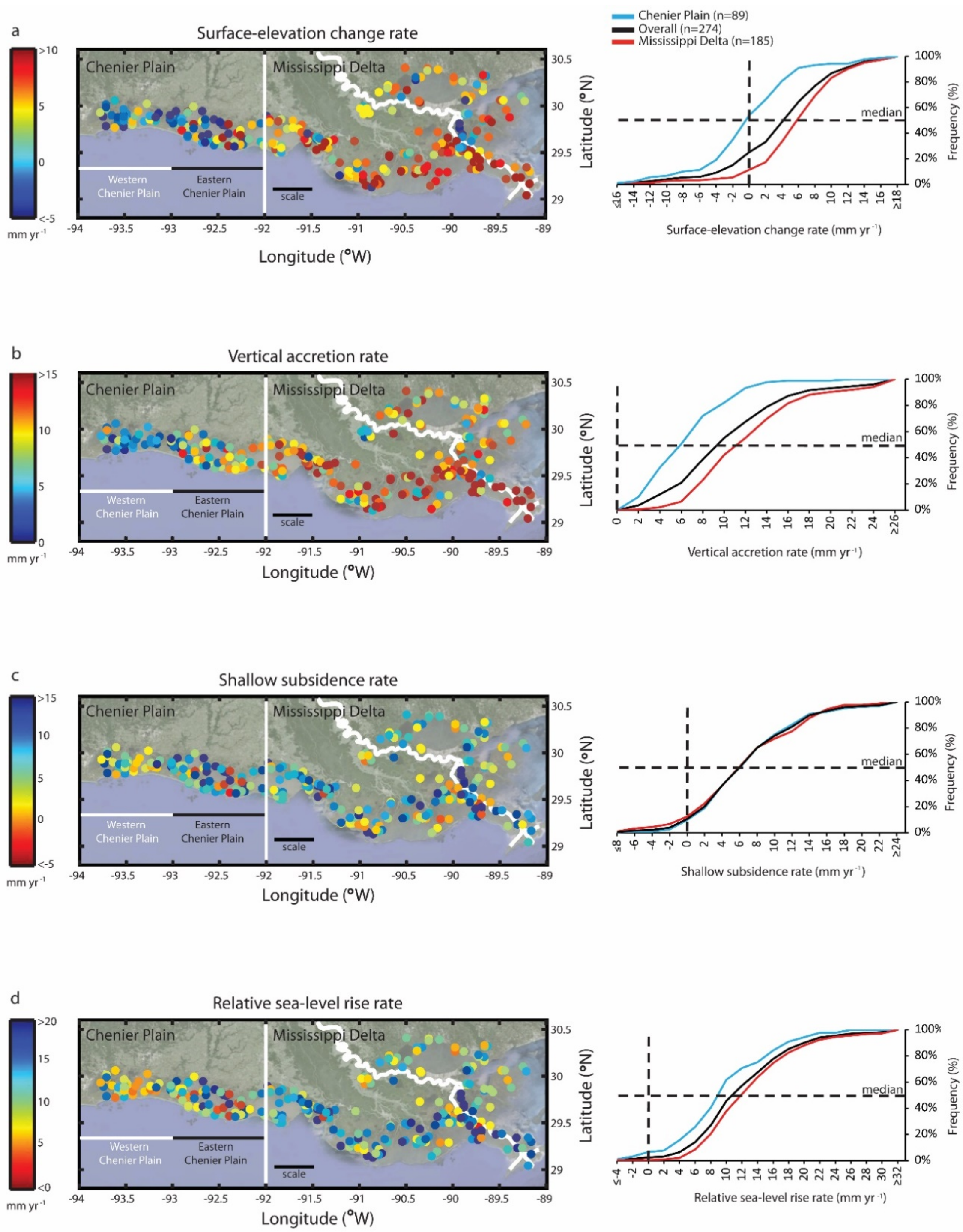

Figure 2.2. Spatial pattern and cumulative frequency distribution of present-day wetland conditions in coastal Louisiana. Rates of **a**, surface-elevation change; **b**, vertical accretion; **c**, shallow subsidence; and **d**, relative sea-level rise at 274 sites. Frequency histograms of these datasets are provided in Appendix A, Fig. A1. Scale bar is 50 km.

anchored below the Pleistocene surface where rates are comparatively stable, as discussed in more detail below.

VA rates also vary widely (s.d. = 7.8 mm yr^{-1}; Table 2.1). Mean (12.8 mm yr^{-1}) and median (11.3 mm yr^{-1}) VA rates in the Mississippi Delta are considerably higher than in the Chenier Plain (6.3 and 5.9 mm yr^{-1}, respectively) (Fig. 2.2b, Table 2.1); this difference is also statistically significant ($F(1,272) = 48.3$, $p = 2.7E-10$). In contrast with previous studies (Fagherazzi et al., 2012), our results do not show a significantly higher VA rate for wetlands at lower elevations as compared to those at higher elevations. This is likely due to the narrow elevation range among the sites (-0.2 m to 0.6 m, Supplementary Data 2.1), a reflection of the microtidal regime in coastal Louisiana. No meaningful differences in SEC and VA rates between wetland types were observed (Appendix A, Table A3).

2.4 Discussion

Differences in SEC and VA rates between the Mississippi Delta and the Chenier Plain (Appendix A, Fig. A1) may be related to the differing geomorphological features and processes in each region (e.g., proximity to riverine sediment inputs, connectivity to the Gulf of Mexico, impact of chenier ridges and impoundments). The trend of SEC and VA rates within the Chenier Plain, decreasing from east to west (Figs. 2.2a, b), supports this interpretation. The areas with higher SEC and VA rates in the Mississippi Delta likely reflect deposition during frontal passage and tidal exchange (Roberts et al., 2015), storm events (Tweel and Turner, 2012), or major floods (Falcini et al., 2012).

Our results show a high spatial variability of SS rates with no geographic trend (Fig. 2c). We find that median Mississippi Delta (6.0 mm yr^{-1}) and Chenier Plain (5.8 mm yr^{-1}) SS rates are strikingly similar (Fig. 2.2c, Table 2.1). Previous work has suggested that subsidence rates increase with the thickness of Holocene strata (Karegar et al.,2015; Meckel et al., 2006; Törnqvist et al., 2008; Blum and Roberts, 2012). Holocene deposits are generally much thicker (32.8 ± 22.5 m) in the Mississippi Delta than in the Chenier Plain (5.8 ± 3.5 m) (Fig. 2.3), yet the SS rates for the two regions are indistinguishable. This indicates that SS rates are primarily controlled by shallow sediment compaction known to vary rapidly over short distances (Törnqvist et al., 2008), and fully captured in the 5-10 m thick Holocene veneer of the Chenier Plain. The median SS rate for Mississippi Delta sites anchored in the consolidated Pleistocene substrate

Table 2.1. Rates of change in coastal Louisiana wetlands

Overall surface-elevation change rate (mm yr^{-1}) (n=274)		Mississippi Delta surface-elevation change rate (mm yr^{-1}) (n=185)		Chenier Plain surface-elevation change rate (mm yr^{-1}) (n=89)	
Mean	3.8	Mean	5.7	Mean	-0.2
Median	4.1	Median	5.8	Median	-0.5
Standard Deviation	7.4	Standard Deviation	7.2	Standard Deviation	6.3
Minimum	-41.0	Minimum	-41.0	Minimum	-17.3
Maximum	46.0	Maximum	46.0	Maximum	22.5
Overall vertical accretion rate (mm yr^{-1}) (n=274)		**Mississippi Delta vertical accretion rate (mm yr^{-1}) (n=185)**		**Chenier Plain vertical accretion rate (mm yr^{-1}) (n=89)**	
Mean	10.7	Mean	12.8	Mean	6.3
Median	9.5	Median	11.3	Median	5.9
Standard Deviation	7.8	Standard Deviation	8.4	Standard Deviation	3.7
Minimum	0.2	Minimum	1.6	Minimum	0.2
Maximum	83.7	Maximum	83.7	Maximum	20.6
Overall shallow subsidence rate (mm yr^{-1}) (n=274)		**Mississippi Delta shallow subsidence rate (mm yr^{-1}) (n=185)**		**Chenier Plain shallow subsidence rate (mm yr^{-1}) (n=89)**	
Mean	6.8	Mean	7.1	Mean	6.5
Median	6.0	Median	6.0	Median	5.8
Standard Deviation	7.9	Standard Deviation	8.7	Standard Deviation	6.3
Minimum	-39.4	Minimum	-39.4	Minimum	-11.2
Maximum	60.7	Maximum	60.7	Maximum	22.9
Overall total subsidence rate (mm yr^{-1}) (n=274)		**Mississippi Delta total subsidence rate (mm yr^{-1}) (n=185)**		**Chenier Plain total subsidence rate (mm yr^{-1}) (n=89)**	
Mean	10.0	Mean	11.2	Mean	7.5
Median	8.7	Median	10.0	Median	6.8
Standard Deviation	8.3	Standard Deviation	8.8	Standard Deviation	6.3
Minimum	-35.0	Minimum	-35.0	Minimum	-10.2
Maximum	65.8	Maximum	65.8	Maximum	23.9
Overall relative sea-level rise rate (mm yr^{-1}) (n=274)		**Mississippi Delta relative sea-level rise rate (mm yr^{-1}) (n=185)**		**Chenier Plain relative sea-level rise rate (mm yr^{-1}) (n=89)**	
Mean	12.0	Mean	13.2	Mean	9.5
Median	10.7	Median	12.0	Median	8.8
Standard Deviation	8.3	Standard Deviation	8.8	Standard Deviation	6.3
Minimum	-33.0	Minimum	-33.0	Minimum	-8.2
Maximum	67.8	Maximum	67.8	Maximum	25.9

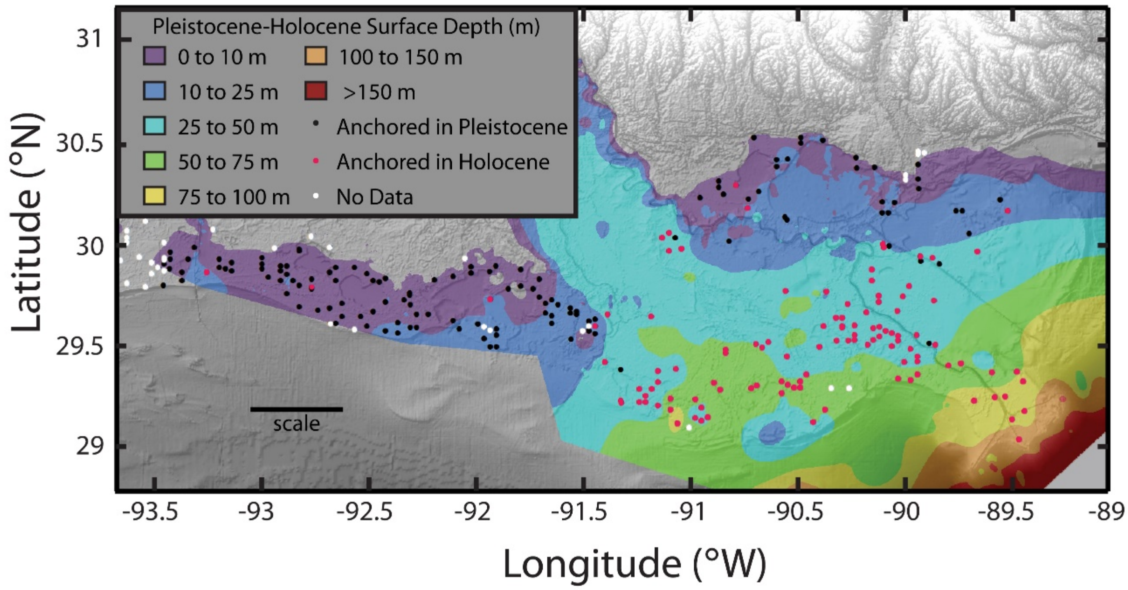

Figure 2.3. Surface-elevation table rod depth compared to the depth of the Pleistocene-Holocene contact in coastal Louisiana. Depths are with respect to North American Vertical Datum of 1988. Because the surface elevation at the 274 sites used in this study ranges from -0.2 to 0.6 m, the map (Heinrich et al., 2016) can be interpreted as a Holocene isopach map. Scale bar is 50 km.

(6.1 mm yr^{-1}, n = 64, mean depth of Pleistocene surface 10.1 m; Fig. 2.3) is remarkably similar to the median SS rate for all Mississippi Delta sites, confirming that the majority of SS is occurring in the shallowest portion of the Holocene succession. Taking into account the limited thickness of Holocene strata in the Chenier Plain, we conclude that SS occurs mainly in the uppermost 5-10 m.

In order to assess whether wetlands are keeping pace with RSLR, the rate of RSLR must be determined with respect to the land surface. Tide gauges measure RSLR with respect to benchmarks that in settings like coastal Louisiana are typically anchored a few tens of meters below the land surface. In view of our finding that shallow subsidence accounts for a large proportion of total subsidence (and, thus, RSLR), tide gauges in this region do not capture the full amount of RSLR. Therefore, unlike most previous studies that have relied on tide gauges, we calculate the rate of RSLR with respect to the land surface for each individual site by adding an estimate of the deep subsidence (DS) rate and the present-day rate of sea-level rise in the Gulf of Mexico to the known SS rate. In the Mississippi Delta, RSET-MH measurements of SS and GPS measurements of DS are complementary, given that GPS anchor depths (mostly >15 m; Appendix A, Table A4) are generally comparable to mean RSET rod depths (22.9 ± 6.3 m). GPS records show that DS rates increase toward the coast (Karegar et al., 2015) with an approximately linear trend (Blum and Roberts, 2012). We use this relationship (Fig. 2.4) to quantify the DS rate as a function of latitude at the Mississippi Delta sites. For Chenier Plain sites, a rate of 1 mm yr^{-1} is used to characterize DS, based on GPS data from outside the Mississippi Delta (Karegar et al., 2015) and supported by glacial isostatic adjustment modeling for the central US Gulf Coast (Wolstencroft et al., 2014), in turn constrained by high-resolution Holocene RSL data (Yu et al., 2012). The sum of SS and DS yields the total subsidence (TS) rate (Fig. 2.1) for each site (Table 2.1) and we find that SS accounts for 60% and 85% (on average) of TS in the Mississippi Delta and Chenier Plain, respectively. Finally, we add the mean rate of sea-level rise in the Gulf of Mexico from 1992-2011 satellite altimetry data (2.0 ± 0.4 mm yr^{-1}) (Letetrel et al., 2015). The mean present-day rate of RSLR is 12.0 ± 8.3 mm yr^{-1} overall (Fig. 2.2d, Table 2.1) and 13.2 ± 8.8 and 9.5 ± 6.3 mm yr^{-1} in the Mississippi Delta and the Chenier Plain, respectively. These rates are slightly higher than previously published rates of RSLR (Penland and Ramsey, 1990) of ~12 and 6 mm yr^{-1} as obtained from tide-gauge records in the two regions, respectively. It should be noted, however, that our methodology is fundamentally different. Tide gauges measure RSLR with respect to an anchor point well

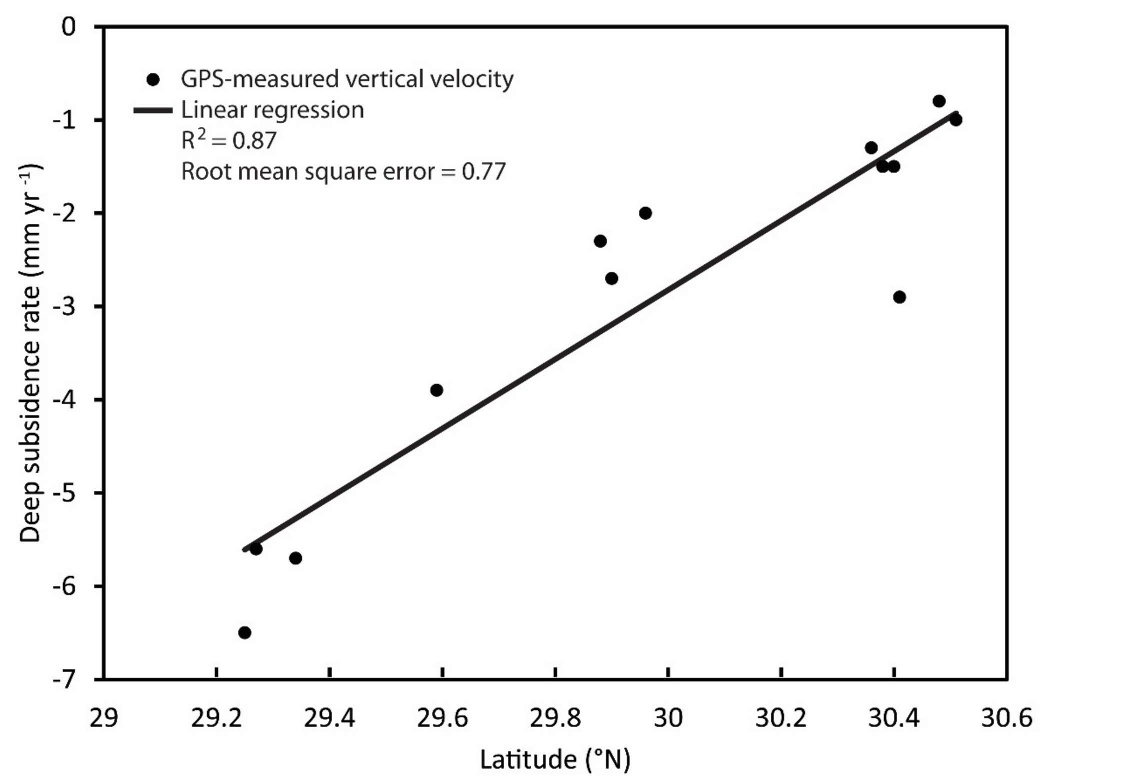

Figure 2.4. Deep subsidence rates in the Mississippi Delta. Linear regression of vertical velocity at 13 GPS stations (Karegar et al., 2015) (see Appendix A, Table A4) versus latitude within the Mississippi Delta. For each of the 185 Mississippi Delta sites, the deep subsidence (DS) rate was estimated by solving the linear model equation as a function of latitude.

below the land surface and therefore do not capture the SS component. The relatively high rates that were recorded nevertheless can most likely be attributed to the fact that the published tide-gauge data cover a time interval considerably older than our records. It has been shown (Kolker et al., 2011) that the high rates of oil and gas extraction between 1950 and 1980 were a likely contributor to the anomalously high rates of RSLR during that time period.

We assess present-day coastal wetland vulnerability by plotting RSLR rates vs. VA rates and find that the data in the Mississippi Delta generally cluster around a 1:1 line (Fig. 2.5a). Sites that fall slightly below the 1:1 line may also persist, as a limited accretion deficit can be counteracted by increased productivity in the short term. Therefore, we consider sites with an accretion deficit of >2 mm yr^{-1} below the present-day RSLR rate particularly vulnerable. In the Mississippi Delta, 35% of sites exhibit such an accretion deficit. In contrast, despite the lower rates of RSLR, the Chenier Plain (Fig. 2.5b) is currently facing accretion deficits at 58% of the sites. The Chenier Plain exhibits a higher concentration of vulnerable sites in its western portion, where 64% of sites are not keeping up with RSLR. These findings are consistent with the sustained wetland loss in this area (Couvillion et al., 2011), although it is important to note that our analysis does not specifically consider the possible impact of smaller scale geomorphological features (e.g., alluvial ridges, chenier ridges) on inundation patterns. Both regions feature striking juxtapositions (Supplementary Data 2.1) with highly vulnerable sites that are in close proximity to sites where the VA rate currently exceeds the rate of RSLR.

We should stress that our assessment of wetland vulnerability is highly conservative. First, the methodology excludes any sites with negative VA (i.e., erosion), thus inflating mean VA rates. Second, the sites are inherently biased toward stability because RSET-MH stations tend not to be located in rapidly degrading settings (e.g., wetlands that are currently converting to open water). Finally, while the mean rate of sea-level rise in the Gulf of Mexico appears to have remained below the global mean over the past few decades (Roberts et al., 2015), it is far from certain that this will continue to be the case in the future, considering, for example, increasing rates of Antarctic ice melt (Mitrovica et al., 2009; DeConto and Pollard, 2016).

Our conclusions therefore represent a best-case scenario for coastal Louisiana and it remains to be seen whether observations for the past 5-10 years will translate into longer-term wetland resilience. While

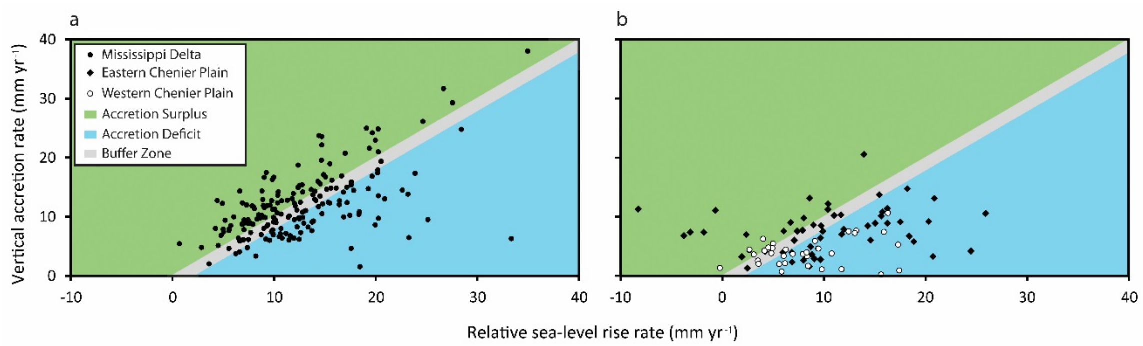

Figure 2.5. Vulnerability of coastal Louisiana wetlands to present-day rates of relative sea-level rise. **a**, Mississippi Delta; **b**, Chenier Plain. Sites that fall within the accretion surplus field have vertical accretion rates that exceed the rate of relative sea-level rise. Sites within the gray buffer zone have an accretion deficit that is <2 mm yr^{-1} and are assumed herein not to be vulnerable (although this is uncertain). Sites that fall below this buffer zone have an accretion deficit >2 mm yr^{-1} and are considered vulnerable given current rates of relative sea-level rise. Outliers in the Mississippi Delta (n = 5, with 4 experiencing an accretion surplus) are not shown for ease of comparison between the two regions.

the inevitable increase in the rate of RSLR may be counteracted in carefully selected portions of the Mississippi Delta by means of major sediment diversions (Paola et al., 2011), the Chenier Plain is already in serious jeopardy due to its isolation from the primary sediment source (i.e., the Mississippi River) and less favorable topographic conditions (i.e., chenier ridges). This is particularly the case in the western Chenier Plain which represents a highly vulnerable ~3000 km^2 area where accretion deficits are currently already substantial. Since coastal Louisiana is currently experiencing rates of RSLR that will become increasingly common across the globe in the future, our findings may provide a less optimistic perspective on the fate of coastal wetlands worldwide than what recent studies have suggested.

2.5 Methods

2.5.1 Data source and selection criteria

The Coastwide Reference Monitoring System (CRMS) (Steyer et al., 2003) has been operational since 2006 and at present consists of 391 sites across coastal Louisiana. At each CRMS site, SEC, VA, and vegetation data (among others) are collected through a partnership of the United States Geological Survey and Louisiana's Coastal Protection and Restoration Authority; all raw data used in this study are publicly available online (CPRA, 2016). A subset of 274 CRMS sites (Fig. 2.3, Table 2.1) was selected based on the following criteria: (1) they have never had to be re-established due to damage; (2) they have a continuous VA record from one set of marker horizons (MH); and (3) the monitoring period is ≥ 5 years. Vegetation monitoring results were used to investigate possible differences between wetland types (Visser et al., 2002) (Appendix A, Table A3).

2.5.2 Data collection

Data collection was overseen by United States Geological Survey and Coastal Protection and Restoration Authority staff through the CRMS program and followed the RSET-MH methodology (Cahoon et al., 2002). A rod was driven vertically into wetland sediments to the point of refusal (mean coastwide rod depth is 20.6 ± 6.8 m) and secured with a PVC-pipe-bounded concrete casing at the surface (Folse et al., 2014). During each site visit the RSET arm was attached to the rod and in each of 4 directions, 9 pins were lowered to rest on the wetland surface, for a total of 36 pin height measurements per site visit. Initial pin heights provide a baseline. SEC, measured biannually, was determined by taking the difference between site visit and baseline pin heights and then taking the mean of all 36 measurements.

Vertical accretion (VA) measurements were carried out using a liquid N_2 cryo-coring methodology (Cahoon and Lynch, 1996). During the first 36 months after CRMS site establishment, measurements were taken every 6 months. Four measurements were taken from each of 3 MHs which comprise the first establishhed VA plot set (known as “Plot Set 1”). Measurements were then repeated every 18 months until the MH were no longer intact and the plot set no longer yielded data (Folse et al., 2014). All sites included in this study have complete VA records through Fall 2015. A mean of the 12 VA measurements was calculated after each site visit. SEC and VA rates were calculated using linear regression. SS is defined as VA minus SEC (Reed, 1995) relative to a fixed vertical reference point (i.e., the rod depth), or the amount of SEC that does not result from the addition/subtraction of material at the land surface (Fig. 2.2).

CRMS protocols require SEC and VA data collection to be conducted from a raised boardwalk with access from the same location during each site visit to ensure that personnel do not disturb the site. Whenever possible, measurements at a given site are taken by the same individuals as previous measurements to ensure consistency and familiarity with site conditions. Finally, data is entered and all data is subsequently verified before being released to ensure data quality (Folse et al., 2014). These steps limit potential error during data collection.

2.5.3 Statistical analyses

To examine the potential effect of including highly noisy records (i.e., records for sites with significant scatter around the linear trend of SEC or VA) on our statistical analyses, we compared the results using the full dataset (n = 274) to a dataset with the highest SEC and/or VA root mean square error records removed (n = 227). While this reduced the standard deviation in several cases, the mean and median values were essentially unchanged. As a result, we did not omit any CRMS sites from our statistical analysis due to noisiness.

Descriptive statistics were calculated for overall SEC, VA, and SS rates, as well as for the Mississippi Delta and the Chenier Plain separately (Table 2.1). One-way Analysis of Variance (ANOVA) tests were carried out to determine if differences in mean SEC, VA, and SS rates were statistically significant for the Mississippi Delta and Chenier Plain data subsets, as well as for different wetland types (Appendix A, Table A4; Appendix A, Fig. A5).

2. Vulnerability of Louisiana's coastal wetlands to present-day rates of relative sea-level rise

This work has been published and this chapter presents that work as found in:

Jankowski, K. L., Törnqvist, T. E., & Fernandes, A. M. (2017). Vulnerability of Louisiana's coastal wetlands to present-day rates of relative sea-level rise. Nature Communications, 8, 14792.

2.1 Abstract

Coastal Louisiana has lost about 5000 km^2 of wetlands over the past century and concern exists whether remaining wetlands will persist while facing some of the world's highest rates of relative sea-level rise (RSLR). Here we analyze an unprecedented dataset derived from 274 rod surface elevation table-marker horizon stations, to determine present-day surface-elevation change, vertical accretion, and shallow subsidence rates. Comparison of vertical accretion rates with RSLR rates at the land surface (present-day RSLR rates are 12 ± 8 mm yr^{-1}) shows that 65% of wetlands in the Mississippi Delta (SE Louisiana) may keep pace with RSLR, whereas 58% of the sites in the Chenier Plain (SW Louisiana) do not, rendering much of this area highly vulnerable to RLSR. At least 60% of the total subsidence rate occurs within the uppermost 5-10 m, which may account for the higher vulnerability of coastal Louisiana wetlands compared to their counterparts elsewhere.

2.2. Introduction

Coastal wetlands provide exceptionally valuable ecosystem services, including wildlife habitat, food production, biogeochemical cycling, and storm-related disturbance regulation (Costanza et al., 2014). Globally, 64-71% of wetlands (including coastal wetlands) have been lost since 1900 AD (Davidson, 2014). Louisiana is home to 40% of wetlands in the contiguous United States, yet has suffered 80% of the total wetland loss (Bourne, 2000). A recent analysis of surface-elevation change and vertical accretion data

3. Holocene coastal marsh drowning and re-emergence in response to relative sea-level rise

3.1 Introduction

Ecosystem resilience is defined as the magnitude of disturbance that a system can experience before it shifts from an initial state to an alternate state (Holling, 1973) and is directly related to the environmental conditions affecting that ecosystem. Changes to external forcings, such as inter-annual climate variability or the rate of relative sea-level (RSL) rise, can trigger rapid environmental changes (e.g., Hoegh-Guldberg, 1999, Breshears et al., 2005), whether those changes are due to a distinct disturbance event or are the result of more gradual shifts to external forcings on decadal to centennial timescales. For ecosystems where the cumulative effect of gradual environmental change moves the system past a disturbance threshold, the resulting shift from an initial state and set of environmental conditions to an alternate state with different environmental conditions may be non-linear (Gunderson et al., 2002) and drastic (e.g. Scheffer and Carpenter, 2003; Steneck et al., 2002). For marsh ecosystems, this concept of shifting state after reaching a disturbance threshold may have important implications in a world with increasing rates of relative sea-level (RSL) rise.

We can use a conceptual model (Fig. 3.1) to consider the impacts of rising rates of RSL on a coastal marsh ecosystem characterized by very low elevations and with very low elevation gradients. To remain in a terrestrial state, coastal marshes require the rate of organic and/or clastic accretion to equal or exceed the rate of RSL rise. Ecosystem responses to changes in the external forcings that control this balance vary depending on the degree and duration of the change and can be characterized by shifts between two equilibria (Fig. 3.1 a) or even multiple equilibria (Fig 3.1 b) depending on ecosystem conditions. The modest environmental stress experienced by marshes facing increasing rates of RSL rise may initially increase plant productivity (Morris et al., 2002), organic matter accretion, and trapping of clastic sediments (Fagherazzi et al., 2012), allowing these ecosystems to persist on annual to decadal

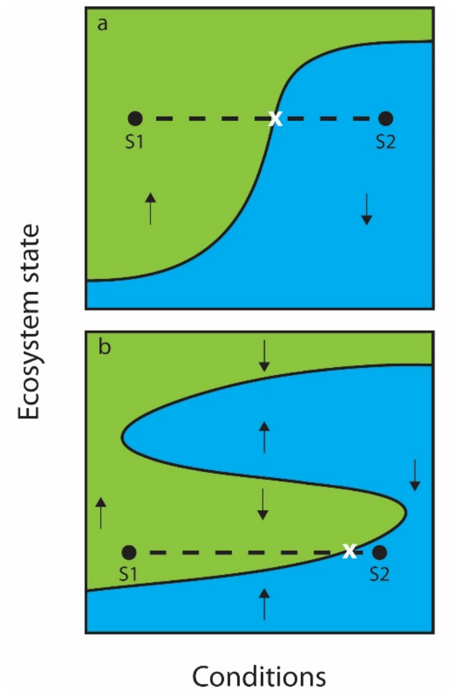

Figure 3.1. Conceptual model of potential environmental responses for a marsh ecosystem. A marsh begins at an initial state (S1), in this case as a terrestrial ecosystem, and maintains the initial state through changes in conditions (along the dashed line) until it reaches a tipping point (white X) so that there is a state shift and the ecosystem shifts to an open water condition (blue field) and maintains this alternate state (S2) until the external forcings reverse to a more favorable condition leading to recovery and re-establishment of a terrestrial ecosystem. Figure is modified from Scheffer et al., 2001.

timescales (Chapter 2). This continues until a threshold is reached and increasing RSL rise rates can no longer be withstood. When the sustained RSL rise-related stress results in more frequent flooding and causes vegetation stress and/or die-back (Mendelssohn et al., 1981; DeLaune et al., 1983), it can lead to vegetation mortality and root network structure collapse (DeLaune et al., 1994). This is an example of a RSL rise rate threshold being reached, where the ecosystem has a non-linear response as reflected by catastrophic marsh drowning (Couvillion and Beck, 2013) and conversion to open water.

The rates of RSL rise that trigger drowning remain poorly constrained due to uncertainties associated with models and difficulty of assessing the short observational record. Theoretical models have suggested that marshes can keep up with rates of RSL rise of ~10 mm/yr (Morris et al., 2002) or higher depending on local conditions such as suspended sediment concentration (SSC) and tidal range (Kirwan et al., 2016). However, surface-elevation change and vertical accretion measurements from 185 sites across the Mississippi Delta (Chapter 2) showed that modern marshes are facing mean rates of RSL rise of ~13 mm/yr over the period of observation (6-10 years), with approximately 1/3 of these sites currently at risk of drowning. A recent remote sensing-based study (Couvillion and Beck, 2013) predicts probable marsh resilience to intermittent inundation depths of between ~150-350 mm above mean water level, depending on marsh type (e.g. intermediate, brackish, or saline). This highlights that ecosystem history also plays a key role in evaluating resilience: as part of a 20 year long study, a Mississippi Delta marsh was observed to collapse after being overwhelmed by modern RSL rise rates (Day et al., 2011). This marsh persisted for several decades prior to and through the observation period (e.g. Cahoon et al., 1995; Rybczyk et al., 2002) before finally collapsing, suggesting that observed marsh persistence in a time of increasing rates of RSL rise may be heavily influenced by the duration of the observation window and that gradual environmental change may lead to impacts that are simply not observable over annual to decadal time scales. Therefore, the question remains what differences in marsh response to RSL rise may exist between annual to decadal and centennial to millennial timescales.

To evaluate the resilience of wetlands on centennial to millennial timescales, we examine marsh persistence over a range of RSL rise rates over the last 8.5 kyr, including the rapid rise during the early Holocene. This time period is of particular interest because the high rates of sea-level rise observed prior to ~7 kyr ago due to the rapid, final retreat of the Laurentide Ice Sheet (e.g., Carlson et al., 2008) are similar to those expected by the end of this century (USGCRP, 2017) and a record of marsh response to those RSL rise rates could inform projections of coastal stability in light of anthropogenic climate change and the resulting accelerated RSL rise.

Using a RSL record, derived from 72 sea-level index points (SLIPs) collected from across the Mississippi Delta (Fig. 3.2), and a set of 355 sediment core records (72 from the SLIP boreholes, and 283 from additional boreholes which lack direct age control; Appendix B, Table B1) we characterize environmental change due to RSL rise over the past 8.5 kyr. Facies and facies succession analysis is used to identify instances of state shift between terrestrial and open water conditions and, when linked with our RSL record, can be used to better understand the rates of RSL rise that may serve as threshold rates for those state shifts. We use these data to investigate marsh drowning and re-emergence in the Mississippi Delta. First, we examine whether a threshold rate of RSL rise exists that leads to marsh systems shifting to open water in the Mississippi Delta through the Holocene. Second, given that all our boreholes were drilled on land, we know that once-drowned sites can re-establish terrestrial conditions, so we also estimate how long that process takes.

In order to accomplish these tasks, we use a number of different data sources. First, we identify common sedimentary facies (Table 3.1) within the 355 boreholes, interpret the facies successions (Table 3.2) and then compare these sedimentary records of paleo-environmental change across the Mississippi Delta. Second, we combine our facies successions analysis with our SLIP-derived RSL curve (Fig 3.3) to estimate rates of RSL rise experienced at the Pleistocene-Holocene transition horizon, which is defined here geologically as the top of the Holocene paleosol overlying the Pleistocene basement sediments, for the 283 additional boreholes. This allows for the determination of which threshold rates of RSL rise are associated with a state shift from terrestrial marsh to open water within the Mississippi Delta during the Holocene. Whereas there are a number of mechanisms that can lead to marsh loss that are not directly tied to RSL rise, particularly lateral marsh edge erosion (Fagherazzi, 2013), a strong relationship between RSL rise rate and the occurrence of marsh drowning in our boreholes would suggest drowning is the mechanism for the state shift from terrestrial to open water in our stratigraphic record.

We are also interested in estimating the amount of time it takes for terrestrial conditions to return

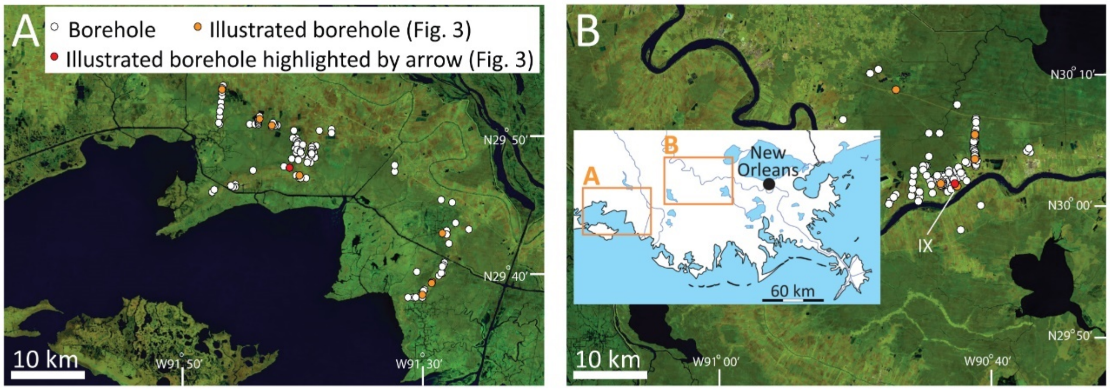

Figure 3.2. Distribution of the 355 boreholes across the Mississippi Delta that were used for the paleo-marsh analysis. Note that the distance between the two regions that were investigated (A, B) is about 100 km and that boreholes within these two regions are scattered up to 40 km apart. This circumvents sampling bias associated with local conditions that may not be representative for a wider region. The location of the 15 boreholes illustrated in Fig. 3.4 is shown in orange or red. The location of the Lutcher IX core is indicated (B).

Table 3.1. Facies classification of Holocene strata.

Facies unit	Sediment texture[1]	Matrix color	Oxidized Fe	Recognizable fossil remains	Sedimentary structures
Swamp peat[2]	Peat, clayey peat	Dark brown, brown, gray brown	Absent	Woody material	Absent
Marsh peat[3]	Peat, clayey peat	Dark brown, brown, gray brown	Absent	Herbaceous material	Absent
Undifferentiated peat	Peat, clayey peat	Dark brown, brown, gray brown	Absent	Absent	Absent
Well-drained swamp mud[2]	Clay, silty clay, silty clay loam	Gray, brown gray	Present	Absent	Absent
Poorly-drained swamp mud[2]	Humic clay, clay, silty clay, silty clay loam	Gray, brown gray	Absent	Woody material	Sand lenses possible
Marsh mud[3]	Humic clay, clay, silty clay, silty clay loam	Gray, brown gray	Absent	Herbaceous material	Sand lenses possible
Lagoonal mud	Clay, silty clay, silty clay loam, silt loam, sandy loam, very fine sand, fine sand[4]	Gray	Absent	Shells and shell fragments (e.g., Rangia cuneata)	Laminations possible
Undifferentiated mud	Humic clay, clay, silty clay, silty clay loam	Gray, brown gray	Absent	Absent	Absent
Paleosol	Slightly humic silty clay loam	Dark gray	Absent	Absent[5]	Absent

1. Descriptions of clastic facies follow the United States Department of Agriculture texture classification system.
2. Freshwater environment.
3. Dominantly intermediate, brackish, or saline environments, although occasionally freshwater conditions may occur.
4. Sandy layers are sometimes encountered in the lagoonal facies that are otherwise generally mud-dominated.
5. Intruded roots are occasionally present, but organic matter is generally highly decomposed.

Table 3.2. Facies successions associated with basal Holocene strata.

Facies succession	**Pleistocene-Holocene transition**	**Terrestrial facies**	**Lagoonal facies**	**Interpretation**
Fully terrestrial	Paleosol overlain by terrestrial mud or peat	Overlie the paleosol and extend throughout the core	Absent	No evidence for marsh drowning
Gradually drowned	Paleosol overlain by terrestrial mud or peat	Overlie the paleosol and extend ≥30 cm before lagoonal mud is encountered	Overlie ≥30 cm of terrestrial facies	Marsh drowning occurred over centennial timescales
Rapidly drowned	Paleosol overlain by terrestrial mud or peat, or by lagoonal mud	If present, overlie the paleosol and extend <30 cm before lagoonal mud is encountered	Overlie paleosol or <30 cm of terrestrial facies	Marsh drowning occurred over multidecadal or shorter timescales

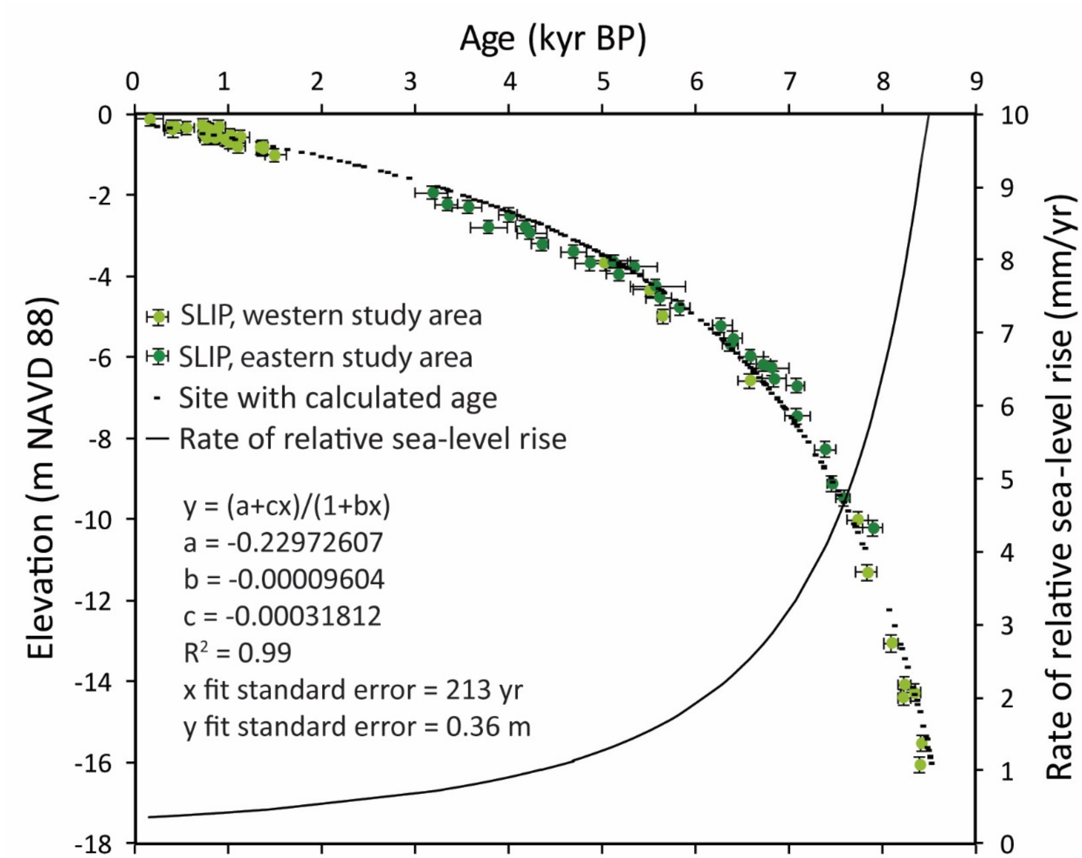

Figure 3.3. Relative sea-level rise record and relative sea-level rise rise rates for the Holocene Mississippi Delta. Directly dated sites (SLIPs, n=72) are indicated with green dots and shown with age and elevation errors. Sites with calculated ages (n=283) are indicated with small black dots and show the form of the relative sea-level curve (equation and parameters inset in figure). The rate of relative sea-level rise is indicated with the black solid line, though our record truncates at 0.15 cal kyr B.P., thus missing the modern relative sea-level acceleration.

after initial drowning. To identify facies successions where an initially terrestrial site converts to open water and then returns to terrestrial facies we use a combination of stratigraphic analyses and ^{14}C dating (as above) along with microfossil and stable isotope analyses to track environmental change through time. We can then use these data sets to characterize marsh ecosystem response to variable RSL rise rates (Fig 3.3) and make an estimate of the duration of the recovery back to a terrestrial ecosystem at a previously drowned site.

3.2 Methods

3.2.1 Sea-level index points and the RSL curve

This study relies on a high resolution ~8.5 kyr RSL rise record (Fig. 3.3) derived from 72 sea-level index points (SLIPs) from across the Mississippi Delta (Fig. 3.2). SLIPs are recognized in the core stratigraphy as organic-rich basal peat deposits which overlie a Holocene-aged, transgressive wetland paleosol (Törnqvist et al., 2004a; Vetter et al., 2017) atop a highly consolidated, virtually compaction-free Pleistocene substrate (Fisk, 1938). These peats, which form in response to a rising groundwater level (Jelgersma, 1961), are indicative of a point in the coastal landscape between mean sea level and mean high water (Van de Plassche, 1986) and therefore represent a past sea-level elevation. $\delta^{13}C$ ratios (Chmura et al., 1987; Törnqvist et al., 2004b), plant macrofossils (Törnqvist et al., 2004a), and foraminiferal assemblages (Li et al., 2012) are used to infer paleo-environmental conditions and indicate that the majority of basal peats formed in brackish to intermediate (i.e., intertidal) environments. This interpretation limits the uncertainty of pinpointing RSL using basal peats because of the microtidal (~30 cm) regime of the Mississippi Delta that likely persisted through most of the study period (Hill et al., 2011).

For each SLIP, the age was determined by ^{14}C dating of plant macrofossils within the basal peat bed (see Yu et al., 2012 for further details). To develop the RSL rise record, the paleo-elevation of the basal peat was defined by the midpoint of the ^{14}C sample interval that was then adjusted based on the indicative range for the basal peat and underlying paleosol as relative to a reference water level (a value calculated as the mean of mean tide level and mean higher high water; Yu et al., 2012). The 72 SLIPs were plotted (Fig. 3.3) with respect to North American Vertical Datum of 1988 (NAVD 88) with paleo-elevations that range from 0.23 to 15.62 m below the datum (Appendix B, Table B1).

The curve fitting software package TableCurve2D, version 5.01.02 (www.sigmaplot.com.uk/products/tablecurve2d/tablecurve2d.php), was used to fit and rank 3665 equations to obtain the RSL curve using the central values of the SLIPs (see Yu et al., 2012 for further details). Since the Holocene RSL history of the Mississippi Delta region is dominated by glacial isostatic adjustment (Love et al., 2016), we only considered curves characterized by monotonic RSL rise. Whereas subtle, century-scale RSL fluctuations with amplitudes of a few decimeters (Gonzalez and Törnqvist, 2009) likely existed, they would have a minor impact on the most important portion of our RSL record when rates of RSL rise were the highest (i.e., the effect would be limited to subtle accelerations and decelerations). The RSL fits were graphically evaluated and assessed for goodness of fit (R^2) and the standard error between the data and the fitted curve. Our selected RSL model takes the form y=(a+cx)/(1+bx). The RSL rise rate at any point along the curve is determined by calculating the first derivative of this RSL curve (Fig. 3.3).

3.2.2 Facies and facies succession analyses

Initial stratigraphic analysis of paleo-environmental change was conducted using the 72 SLIP cores. This analysis used detailed descriptions of texture (USDA soil classification system), organic matter content, color, presence of plant or other fossil remains, and oxidation state to determine sedimentary facies within each borehole at 10 cm increments. Each SLIP record features an organic-rich marsh facies that immediately overlies the paleosol at the Pleistocene-Holocene transition, though the facies that overlie the SLIPs vary widely, ranging from marsh and swamp muds to sediments deposited under open water conditions (Table 3.1).

Facies successions (Table 3.2, Fig. 3.4) with terrestrial facies and no evidence for drowning are classified as fully terrestrial. Facies successions that exhibit a terrestrial to open water state change are classified as drowned. Facies successions lacking clear evidence for either fully terrestrial or drowned status are classified as inconclusive. These classifications were then combined with the RSLR curve to determine which rates of RSLR are threshold rates for marsh drowning.

3.2.3 Estimating ages from the RSL curve

Using core log records, the facies analysis was extended to 283 additional boreholes (Appendix B,

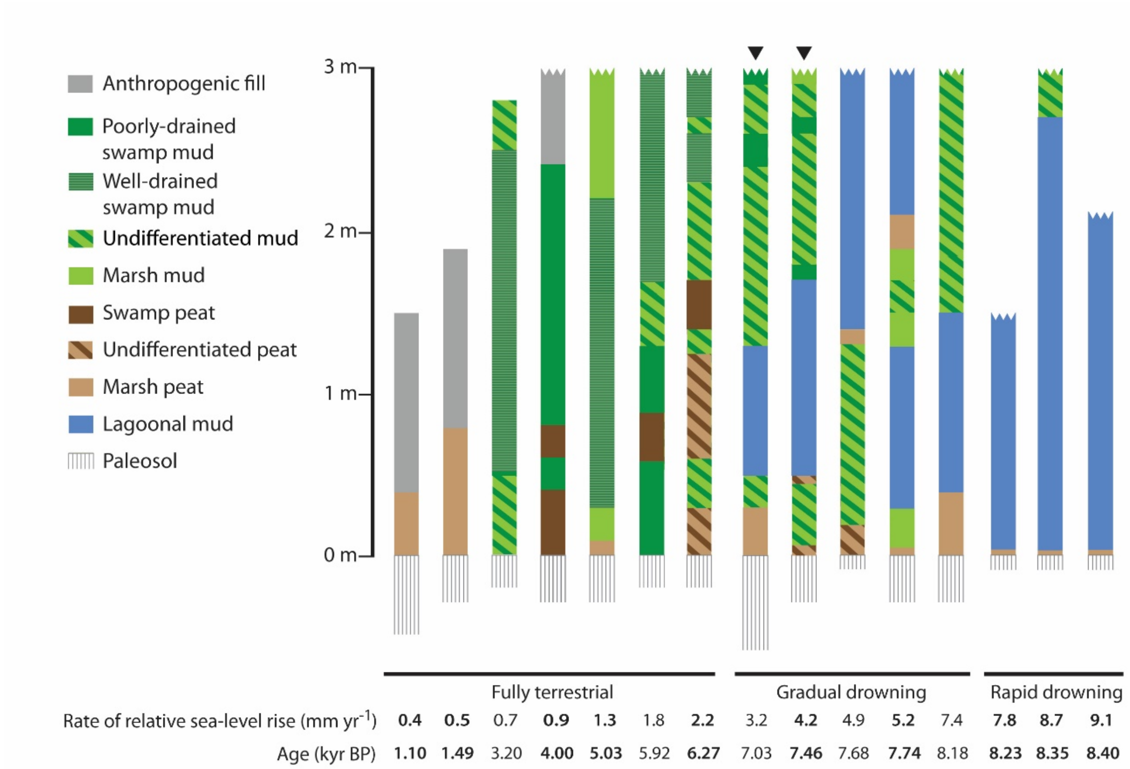

Figure 3.4. Characteristic transgressive facies successions from the past 8500 years.
A selection of 15 representative sedimentary logs features the transition from a wetland paleosol to basal Holocene facies (commonly marsh peat in these examples, although freshwater facies are common in the younger portion of the record) and the overlying succession (details about facies units are provided in Table 3.1). For ease of comparison, the logs have been adjusted vertically so as to align the top of the paleosol and arranged with increasing age (and depth) from left to right (in reality, the elevation of the top of the paleosol decreases from ~0.5 to 16 m below NAVD 88). The serrated pattern is used for logs that do not extend all the way to the land surface. For each log, the weighted mean calibrated age (in cal kyr BP) of the basal facies that drape the paleosol and the rateof RSL rise (the first derivative of the equation in Fig. 3.2) is provided. Directly dated cores are indicated in bold; for the other cores the age of the basal Holocene facies was calculated by means of the equation in Fig. 3.2. Note the extremely rapid transgression of lagoonal mud over marsh peat at the three oldest sites (>8.2 cal kyr BP), the more gradual transgression at the next five sites, and the absence of indicators for open-water conditions once basal ages are <6.8 cal kyr BP. Also note that the two logs marked by arrows with largely similar stratigraphy are ~100 km apart (their locations are shown in Fig. 3.1). Additional sedimentary logs are shown for the western and eastern study areas separately in Fig. 3.8.

Table B1) from across the Mississippi Delta (Fig. 3.2) which lack direct age constraints but have a stratigraphically similar transition overlying the paleosol which is interpreted to mark the Pleistocene-Holocene transition. The impact of local conditions for each borehole (e.g., distance to active distributaries, differences in hydrology) resulting in individual sedimentary record variability is minimized due to the large number of observations in this study and the spatial distribution of the data (>100 km from the eastern to the western extent of borehole sites) in the Mississippi Delta (Fig. 3.2). To be included in the set of 283 additional these boreholes had to meet a number of criteria. First, if the core log indicated a gradually or rapidly drowned facies succession over the basal terrestrial unit it was included regardless of whether the record extended all the way to the land surface or not. Second, if a core log exhibited a fully terrestrial facies succession, the record must extend to the land surface to be included. Boreholes that extended to the land surface but did not contain recognizable terrestrial or lagoonal facies are still included in the data set, but these boreholes are termed inconclusive. All 283 additional boreholes included in the analysis were located within the Mississippi Delta and featured an intact paleosol at the Pleistocene-Holocene transition without indications of erosion. For each core log that met these criteria, the elevation of the top of the intact paleosol was used to solve the Holocene sea-level curve equation in order to predict an age for the base of the Holocene succession in that borehole. Due to the tight age-depth relationship in our RSLR record (Fig. 3.3), estimated ages (standard error = ~0.2 kyr) were assigned to the facies transition at the top of the paleosol in these additional 283 undated core logs, and the rate of RSLR was estimated for each site. The predicted age of each additional borehole had to fall within the ^{14}C age range of 72 SLIP sites. Sites with a predicted age of <0.15 or >8.42 cal kyr B.P. were excluded from our analysis. The same facies (Table 3.1) and facies succession analysis (Table 3.2, Fig. 3.4) was applied to these 283 additional boreholes.

3.2.4 Environmental change analysis

An in-depth analysis of environmental change at a single location was conducted using a ~6 m long core (Lutcher IX), collected near Lutcher, LA (Fig. 3.2 b). The surface elevation at the site, 3.1 m above NAVD 88, was determined from LIDAR data. This site was selected due to stratigraphic evidence for marsh drowning (i.e., lagoonal mud with brackish mollusks) and the eventual re-appearance of terrestrial facies. The stratigraphy of Lutcher IX was described in the field using the methods outlined in the previous section, and major facies changes served as the basis for further sampling. ^{14}C samples (charcoal fragments and plant macrofossils) were collected from 4 organic-rich horizons within the stratigraphy (Table 3.3) corresponding with the base, midpoint, and top of the basal peat bed located between 1350-1375 cm depth in the core, and the base of an organic-rich unit between 970-973 cm. The ^{14}C samples were then measured using accelerator mass spectrometry at the University of California, Irvine. The ^{14}C ages were calibrated using OxCal software version 4.3 (Bronk Ramsey, 2009) using the IntCal13 calibration curve (Reimer et al., 2013) and the weighted mean age along with 1σ uncertainty are reported in this study (Table 3.3).

3.2.4.1 Microfossil analysis

Foraminiferal analysis was used to refine the environmental change analysis of the Lutcher IX core. Targeted sampling (modeled after Nevitt, 2009) was used to select a total of 20 sampling horizons within the borehole, with a 2 cm^3 sediment sample collected from each horizon. Each of the 20 samples was washed and sieved using seven sieve sizes (850 µm to 63 µm mesh) prior to examination using a Wild M5 binocular microscope.

We used the shape and composition (calcareous vs. agglutinated) of the foraminiferal tests (shells) to identify individual specimens to the most specific level possible (genus or species). For the specimens which lacked a test due to poor preservation (e.g., bioturbation or exposure to acidity), the pseudo-chitinous linings were used for identification.

The relative abundance of foraminifera taxa was determined using a frequency system (Kohl et al., 2004) where the abundance of each taxon for each sieve size was determined (ranging from very rare to very abundant) and then combined to calculate the overall abundance for each taxon in each sample. Biofacies were designated based upon the first, second, and third most dominant taxa in a given sample. Changes between biofacies within the borehole were used to track paleo-environmental transitions as foraminiferal assemblages vary based upon environmental conditions (e.g. salinity, water depth, temperature, turbidity, food availability, and pH) (Phleger, 1970; Murray, 1973; Murray, 2006; Culver et al., 2012). Based upon the habitat requirements of present-day foraminiferal assemblages, facies determinations were refined.

Table 3.3. Radiocarbon ages for the Lutcher IX borehole. This site is located in UTM Zone 15R with coordinates 3324860 m N, 720880 m E. Site elevation 3.1 m.

Sample name	Depth below surface (cm)	Material dated	Age (^{14}C yr B.P.)	UCIAMS laboratory number
Lutcher IX-1a	1360-1362	2 charcoal fragments	6900 ± 25	159370
Lutcher IX-1b	1360-1362	6 charcoal fragments	6840 ± 25	159371
Lutcher IX-1c	1360-1362	12 Scirpus fragments	6795 ± 20	159372
Lutcher IX-2a	970-973	3 charcoal fragments	5115 ± 15	187166
Lutcher IX-2b	970-973	3 charcoal fragments	5120 ± 15	187167
Lutcher IX-3	1350-1352	several charcoal fragments	6680 ± 20	187168
Lutcher IX-4	1372-1374	several charcoal fragments	6835 ± 25	187169

3.2.4.2 Stable isotope analysis

Samples were collected adjacent to microfossil samples for $\delta^{13}C$ analysis. Each sample was oven-dried at 50ºC, homogenized, and acid-treated using 10% HCl to remove carbonates. Samples were then rinsed four times in deionized water to bring them to a neutral pH, re-dried, and re-homogenized. Decarbonated sediment samples were then loaded into tin capsules and analyzed for $\delta^{13}C$ on a Carlo Erba 2500-II Elemental Analyzer coupled to a Thermo DeltaPlus XL isotope ratio mass spectrometer at the College of Marine Science, University of South Florida.

3.3 Results

3.3.1 Sea-level rise record

Our Holocene relative sea-level record (Fig. 3.3) covers the period from approximately 8.4 to 0.15 cal kyr B.P. As shown by Li et al. (2012), the earliest part of the record exhibits rapid rates of RSL rise that gradually decrease through the Holocene. Our curve shows changes of RSL rise rates through the Holocene that start at about 10 mm/yr in the earliest portion of the record (~8.4 cal kyr B.P.) and rapidly drop to approximately 4 mm/yr (~7.5 cal kyr B.P.) before gradually decreasing to <1 mm/yr in the most recent portion (after ~4.0 cal kyr B.P.) of the record. The model underestimates observed RSL rise rates in the most recent portion (i.e. the last ~2.0 kyr) of the record, but the facies analysis below shows that this does not have any significant implications for our threshold analysis.

Observed facies successions are illustrated using a subset of 15 representative boreholes from across the Mississippi Delta (Fig. 3.4) which were selected in order to illustrate the variety of sedimentary records over the wide range of RSL rise rates within this study. There are nine facies (Table 3.1) that make up the sedimentary record in these core logs. The base of each core log is marked by the transition between the paleosol and the basal terrestrial facies (most often peat). Above this initial horizon, the facies successions observed vary with swamp and marsh peats, swamp and marsh muds, and lagoonal muds identified based on the criteria laid out in Table 3.1. Some portions of the core logs lacked evidence that allowed for a definitive facies designation and are therefore labeled “undifferentiated”. It is important to note that these facies may represent either terrestrial or open water deposition.

Whereas the facies and their thicknesses vary from core to core, we identify three major facies succession categories. Fully terrestrial facies successions are comprised of terrestrial facies throughout the borehole (Fig. 3.4) with undifferentiated facies, if present, limited to <50 cm in thickness. Shifts between swamp and/or marsh peat facies and swamp and/or marsh mud facies are common.

All boreholes with a RSL rise rate <2 mm/yr exhibit a fully terrestrial facies succession and lack indicators of open-water conditions (e.g., shells of the brackish mollusk Rangia cuneata). For core logs with a RSL rise rate <3 mm/yr (n=286), 90% (n=257) still fall within the fully terrestrial (i.e., never drowned) facies succession classification which dominate the past ~6.9 cal kyr B.P. (Supplementary Data 3.1). Facies successions for the remaining 10% of boreholes with an RSL rise rate of <3 mm/yr are either inconclusive (6%, n=16) or exhibit drowned facies successions (4%, n=12) (Fig. 3.5).

Drowned facies successions are identified wherever lagoonal facies are observed, indicating a previously terrestrial system that shifted to open water. The occurrence of fully terrestrial records decreases substantially as the RSL rise rate increases (Appendix B, Table B1; Fig. 3.5). For core log records with a RSL rise rate of ≥3 mm/yr (n=70), 81% of boreholes (n=57) exhibit drowned facies successions (Fig. 3.4) as reflected by shells and shell fragments within lagoonal muds. Only 9% (n=6) of boreholes with a RSLR rate of ≥3 mm/yr exhibit fully terrestrial facies successions and 10% (n=7) of boreholes have inconclusive facies successions. Given the stark contrast between the fate of marshes experiencing RSL rise rates <3 mm/yr, which largely remain terrestrial, and those experiencing RSL rise rates ≥3 mm/yr, which largely exhibit signs of a state change from terrestrial to open facies, we interpret the RSL rise rate of 3 mm/yr to be a threshold rate for drowning within this system.

Importantly, these results are not limited to the 15 representative cores (Fig. 3.4) nor are they spatially dependent. Facies successions from an additional 20 cores (Fig. 3.6), including 10 each from the eastern and western study areas, exhibit the same relationship between RSL rise rate and fully terrestrial, gradually drowned, and rapidly drowning facies successions. Drowned facies successions are distributed across both the eastern and western study areas (Fig. 3.7), indicating that the results are not tied to local conditions affecting a few cores but rather represent a larger trend in marsh response to rates of RSL rise in the Mississippi Delta. Additionally, the results show that the relationship between the decreased occurrence

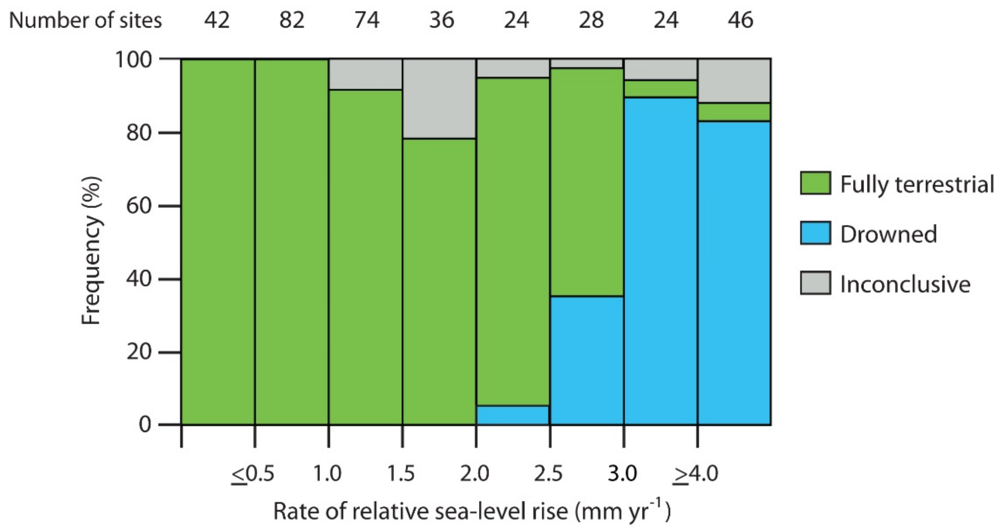

Figure 3.5. Frequency of facies succession occurrence related to relative sea-level rise rate. The relative proportion of facies successions (Table 3.4) is determined for eight increments of rates of RSL rise to identify the tipping point for marsh drowning. The abrupt increase in the proportion of drowned sites between 2.5 and 3.0 mm/yr illustrates the non-linear nature of the marsh response to the rate of RSL rise. Similar plots are shown for the western and eastern study areas separately in Fig. 3.8.

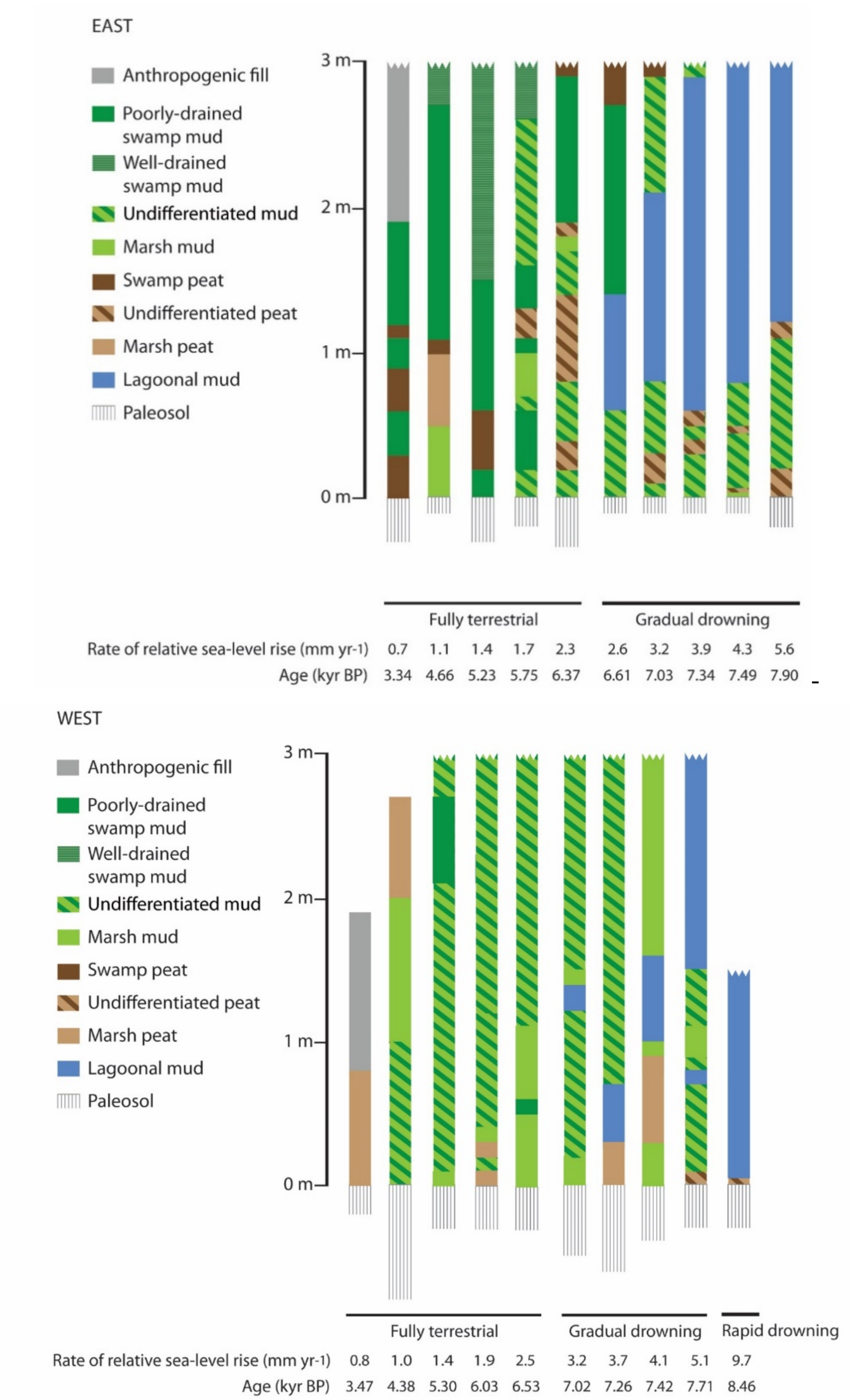

Figure 3.6. Characteristic transgressive facies successions in the western (a) and eastern (b) study areas. A selection of 10 additional sedimentary logs features the transition from a wetland paleosol to basal Holocene facies and the overlying succession. For legend and further details, see Fig. 3.4.

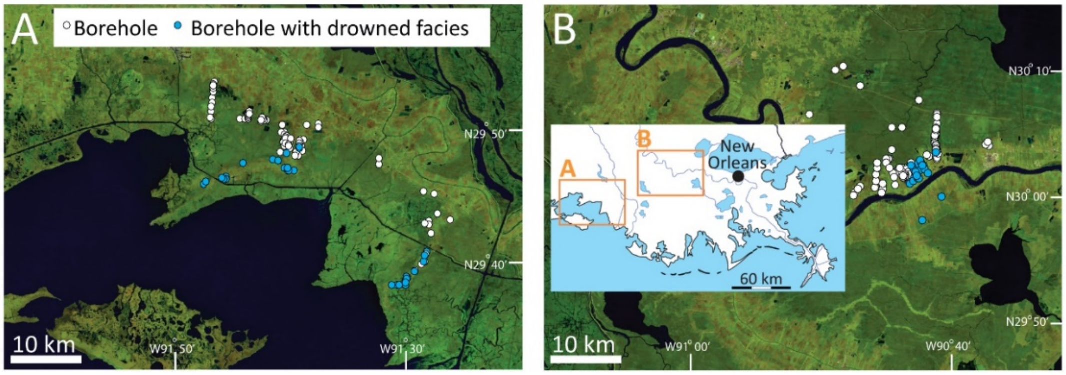

Figure 3.7. Spatial distribution of drowned sites in the western (a) and eastern (b) study areas.

of fully terrestrial facies coincides with increased rates of RSL rise in both the eastern and western study areas (Fig. 3.8), again indicating the robustness of the results.

Furthermore, our results (Fig. 3.4) indicate that the stratigraphy of core logs with drowned facies successions can vary widely in terms of the thickness of initial terrestrial deposition (e.g. marsh peat and marsh mud) ranging from 0 m to 1.5 m (Appendix B, Table B1), with 56% of pre-drowning terrestrial packages at thicknesses >0.3 m and 44% at thicknesses of ≤0.3 m. The duration of marsh persistence for the sites that eventually flooded can be estimated from the thickness of the drowned marsh facies, assuming that vertical accretion initially kept pace with the rate of RSL rise and using a reduction in thickness by a conservative factor of 2.5 due to postdepositional compaction (Van Asselen, 2011). This suggests (Table 3.4) that marsh drowning prior to 8.2 kyr B.P. typically occurred in ~50 years, while between 8.2 and 6.8 cal kyr B.P. marshes were able to persist ~300 years on average.

3.3.2 Marsh persistence, drowning, and marsh re-establishment

The sediment core taken at the Lutcher IX site extends an existing borehole transect (Törnqvist et al., 2004b) and captures a record of paleo-environmental change, from marsh drowning to terrestrial re-establishment. The stratigraphic record at Lutcher IX can be correlated to adjacent sites (Lutcher IV – VIII; Törnqvist et al., 2004b) via largely continuous peat beds (Fig. 3.9). Microfossil and stable isotope analyses (Steinmetz, 2015) provide additional details about the paleoenvironmental evolution of the site. Lutcher IX exhibits a drowned facies succession (Fig. 3.10) with a basal peat bed overlain by a lagoonal mud facies (based on foraminiferal biofacies evidence) and a subsequent appearance of Rangia shells.

The ^{14}C dating results for Lutcher IX provide ages (Table 3.3) of ~7.6 cal kyr B.P. for the base, and ~7.5 cal kyr B.P. for the top of the basal peat, respectively. Lutcher IX has a 100 cm thick package of very fine sand above the open water facies, which is then overlain by humic clays that transition into a 20 cm thick organic rich layer clay bed, the base of which yields a ^{14}C age of ~5.8 cal kyr B.P. (Table 3.3).

Microfossil analysis (Fig. 3.10; after Steinmetz, 2015) show that foraminifera are absent below the basal peat, likely because these species of foraminifera only occur in brackish to saline waters. Above the paleosol, the H. wilberti biofacies occurs within the basal peat, suggesting that the marsh which produced the peat was likely fringing marsh (Kane, 1967) and formed in an environment with a salinity of 5-18 psu

Table 3.4. Thickness and estimated lifespan of drowned marsh facies.

	Drowned marsh facies – all sites[1]			Drowned marsh facies – selected sites[2]		
	Median (mean) thickness (m)	Median (mean) lifespan (years)[3]	Number of observations	Median (mean) thickness (m)	Median (mean) lifespan (years)	Number of observations
Gradual drowning (post-8.2 cal kyr BP)	0.30 (0.43)	212 (282)[4]	51	0.50 (0.58)	310 (372)	25
Rapid drowning (pre-8.2 cal kyr BP)	0.10 (0.18)	25 (50)	17	0.15 (0.34)	46 (98)	8

1. All sites (n = 68) that feature lagoonal facies, including those where the contact between terrestrial (usually marsh) and lagoonal facies is erosional.
2. Selected sites (n = 33) where the terrestrial to lagoonal facies contact is less likely to be erosional.
3. Estimated by correcting the thickness for compaction (a factor of 2.5) and assuming that the accretion rate approximately tracked the rate of RSL rise.
4. Note that mean values always exceed median values (typically due to one or a few sites with relatively large numbers); therefore, median values are used in the interpretation.

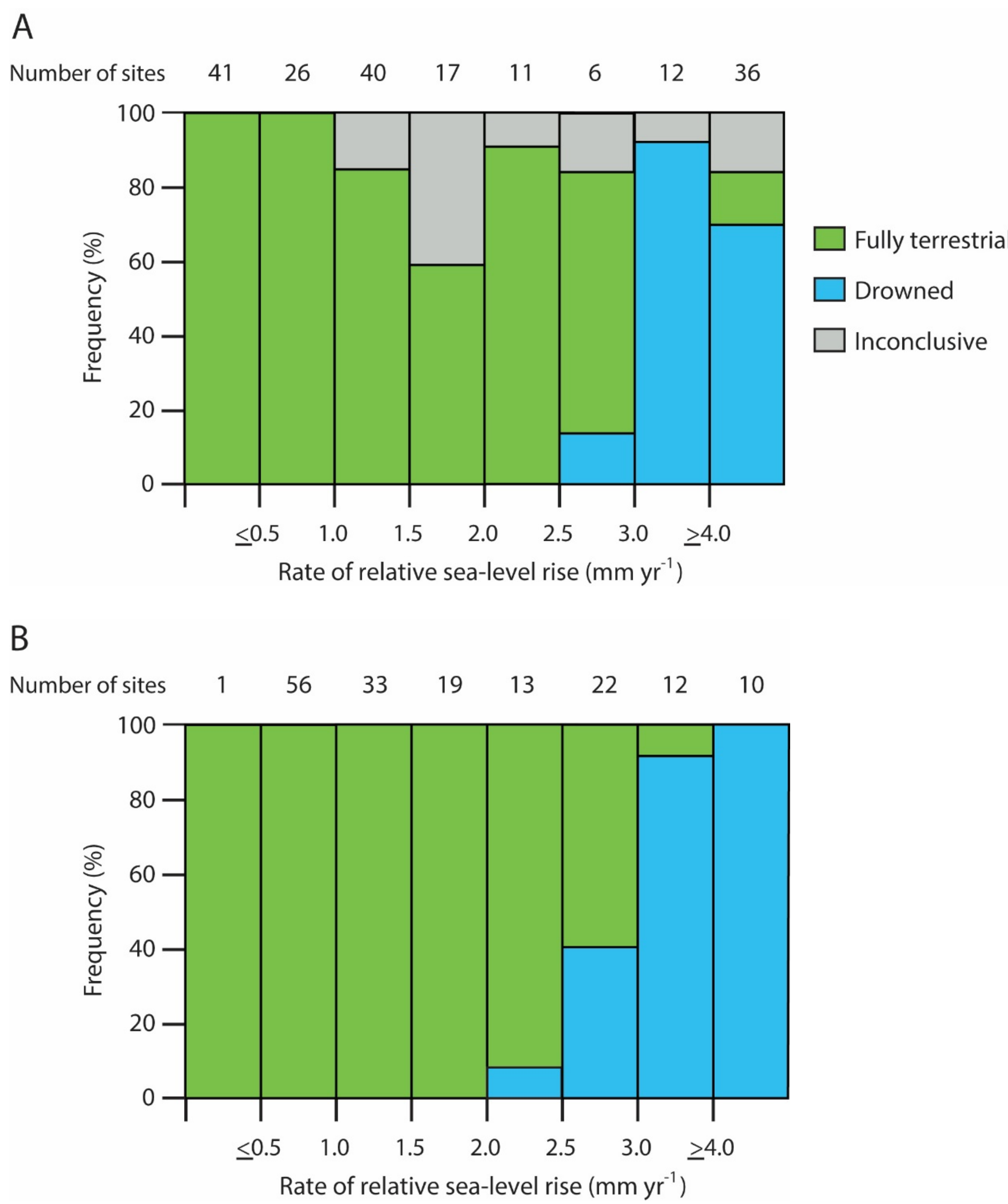

Figure 3.8. Relationship between the rate of relative sea-level rise and marsh persistence for the western (a) and eastern (b) study areas. The relative proportion of facies successions is determined for eight increments of rates of RSL rise to identify the tipping point for marsh drowning. The trend seen in Fig. 3.5, with a dominance of drowning when rates exceed 3.0 mm/yr, is also seen in the two study areas separately.

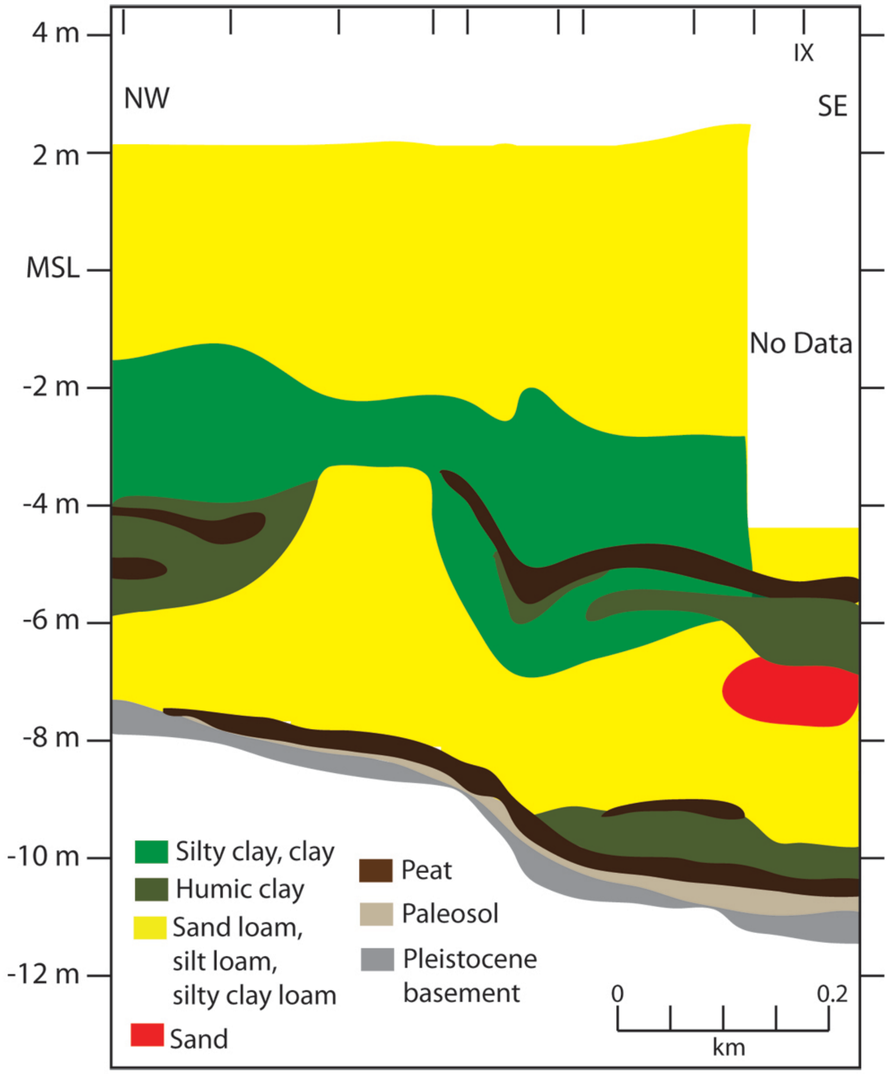

Figure 3.9. Cross-section of the Lutcher borehole transect. Regional stratigraphy of the Lutcher area. The location of the Lutcher IX core is indicated by the labeled tick mark at the top of the figure. Facies classification for Lutcher IX is provided in Fig 3.10.

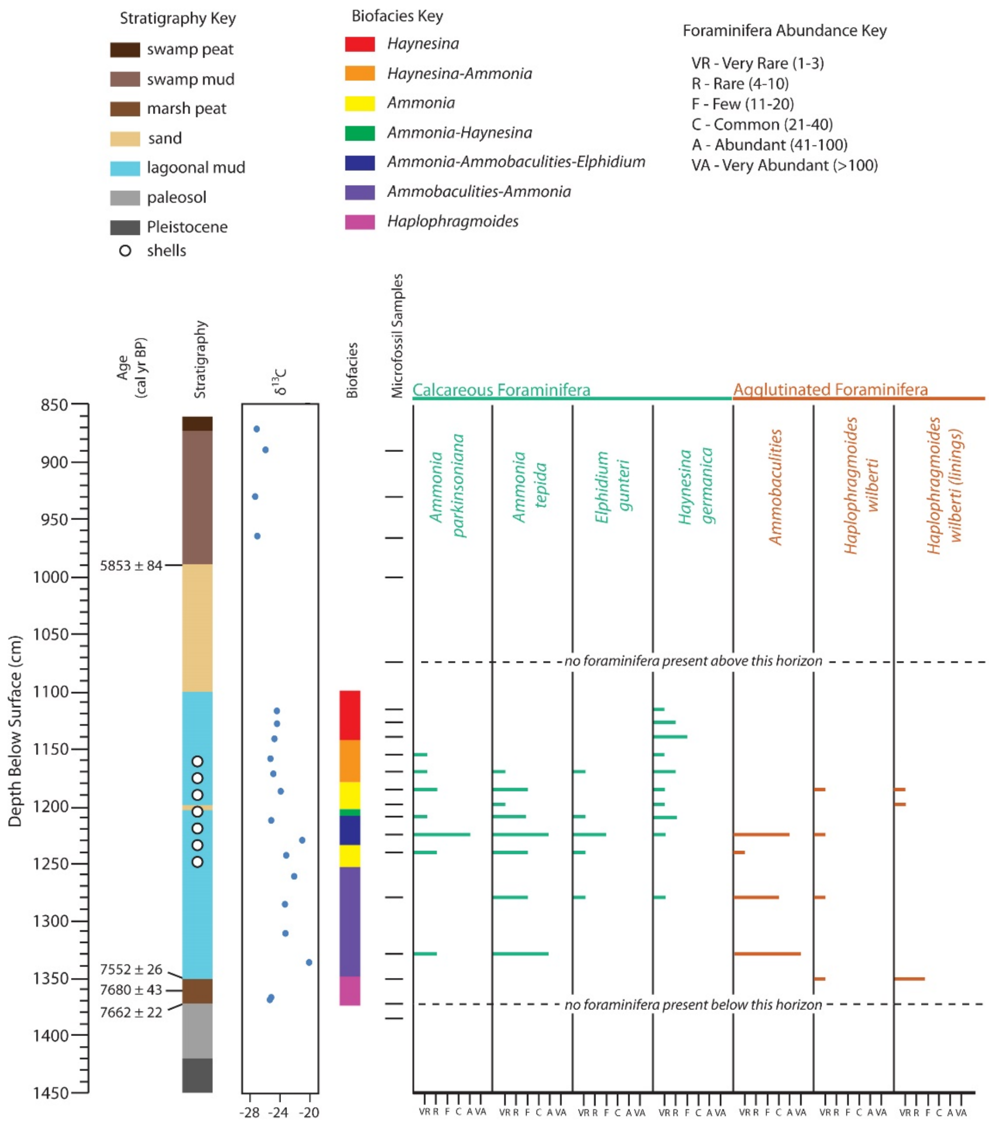

Figure 3.10. Stratigraphy, ^{14}C dating, foraminiferal assemblages, and δ^{13}C values to characterize paleo-environmental change at the Lutcher IX site. Stratigraphic column to the left shows sedimentary facies including the initial, basal peat at 1350-1372 cm. Weighted mean ^{14}C ages are indicated to the left of the stratigraphic column. Biofacies zones are based upon foraminiferal assemblages. δ^{13}C results are shown as ‰ VPDB. The relative abundance of calcareous (teal lines) and agglutinated (orange lines) foraminifera is also shown (modified from Steinmetz, 2015).

(Eichler, 2007). Above the basal peat, 8 foraminiferal biofacies zones were identified in ~2.5 m of sediments (Fig. 3.10). Each of these foraminiferal assemblages represent brackish conditions with varying salinities (e.g. Kane, 1967; Eichler, 2007; Murray, 1991; Poag, 1978, Horton, 1999) and suggest that the basal peat is overlain by lagoonal facies. The appearance of other paleo-fauna, in particular Rangia at 1240 cm depth confirms marsh drowning.

A 100 cm thick sandy layer occurs at 1100 cm depth in the borehole. The lack of foraminifera from the base of the sandy unit through the overlying clayey units suggests that with the deposition of the thick sand layer the borehole had transitioned out of a brackish environment into a freshwater, terrestrial environment. These results are confirmed by stable carbon isotope analysis which show the top of the basal peat with a $\delta^{13}C$ value of -20‰ (indicative of brackish conditions) that gradually transition into a $\delta^{13}C$ value near the upper peat of -26‰ (indicative of fresh conditions) (Fig. 3.10).

At Lutcher IX, the local RSL rise rate that lead to drowning was approximately 4.5 mm/yr (Fig. 3.3), a rate greater than the 3 mm/yr threshold rate for drowning identified earlier in this study. It is important to note that the relationship between paleo-elevation and age found for the basal-peat derived SLIPs cannot be assumed to hold true for non-basal peats or organic-rich units. This is because the paleo-elevation of SLIPs is considered fixed as the basal peats rest on the highly consolidated, virtually compaction-free Pleistocene substrate that underlies the region, whereas peats located at higher elevations within the borehole are underlain by compressible Holocene muds and organic-rich facies and their paleo-elevation cannot be considered fixed. As a first order approximation of the rate of RSL rise at the time of terrestrial re-establishment we might compare the re-established peat to basal peats of similar age (~5.8 cal kyr B.P.) which were exposed to RSL rise rates of ~1.5 mm/yr. However, it is conceivable that the actual local rate of RSL rise was higher due to the compaction of underlying strata.

3.4. Discussion

3.4.1 Tipping points related to RSLR

Previous work (Li et al., 2012) has suggested that transgressive stratigraphic successions with very thin basal peat units (<10 cm) were rapidly drowned, while those with thicker terrestrial facies were more gradually drowned. Our ^{14}C results from the Lutcher IX site confirm this, demonstrating that the thin basal peat (~20 cm) represents a marsh that persisted on the order of ~50-150 years (see ^{14}C results above) before the appearance of lagoonal mud facies (Fig. 3.10), indicating marsh drowning. We can use the distribution of terrestrial package thicknesses prior to drowning (Appendix B, Table B1) to classify boreholes with drowned facies successions as either gradually drowned (basal terrestrial deposit thickness >0.3 m) or rapidly drowned (basal terrestrial deposit thickness <0.3 m). Using this method, we find that for paleo-marshes with drowned facies successions with a RSL rise rate between ~3 and 7.5 mm/yr, marshes are nearly equally likely to drown gradually (55%) as they were to drown rapidly (45%). For paleo-marshes with a RSL rise rate that exceeds 7.5 mm/yr however, 94% of sites exhibit a rapidly downing facies succession. This suggests that at a RSLR rate of >7.5 mm/yr yet another tipping point is reached and rapid drowning becomes the dominant form of state change from marsh to open water. As a test of the robustness of this result, we can observe the geographic distribution (Fig. 3.8) of sites that exhibit drowning facies successions. We find that in the Mississippi Delta, sites located >100 km apart with similar basal ages show very similar facies successions (Fig. 3.4).

Marsh resilience is tightly associated with the rate of RSL rise (Figs. 3.5 and 3.8). Marshes that were exposed to RSL rise rates of <2 mm/yr exhibit terrestrial facies (predominantly marsh mud) that persist throughout the borehole (Fig. 3.4), indicating that elevation gain kept pace with, or exceeded, the rate of RSL rise on centennial to millennial timescales. Above this rate, marshes show evidence of gradual drowning at RSL rise rates of more than ~3 mm/yr, where many of the sites exhibit a >0.3 m interval of terrestrial deposition between the basal unit and the eventual appearance of lagoonal mud facies.

Stratigraphic interpretation of our boreholes shows that at RSLR rates of over ~7.5 mm/yr, marshes drown rapidly. Our interpretation is that at rates of RSL rise between approximately 3 and 7.5 mm/yr marshes are, for a time, able to withstand rising water levels before their rate of elevation gain falls below the rate of RSL rise and therefore becomes insufficient for them to persist. Strikingly, the lower end of this range is very close to current global sea-level rise rates **(**USGCRP, 2017**)** and far less than present-day RSL rise in the Mississippi Delta (13 ± 9 mm/yr) (Chapter 2), which indicates a strong dependence on the timescale of observation.

We note that Holocene conditions in the Mississippi Delta may have favored marsh persistence as compared to modern conditions. Modern SSC measurements of 20-70 mg L^{-1} (Kirwan et al., 2010) are significantly lower than extreme-event SSC values - up to 150 mg L^{-1} during the 2011 flood in Atchafalaya Bay (Falcini et al., 2012) – which are thought to more closely represent the SSC conditions that dominated the Mississippi Delta through the Holocene. Early Holocene atmospheric CO_2 concentrations, however, were about 65% of present-day values which would not act to increase the organic contribution to marsh accretion (Langley et al., 2009). The present-day regional microtidal range (<0.5 m) may limit marsh resilience by limiting inundation-derived sedimentation. However, the regional tidal range may have been higher prior to 8 kyr ago (Hill, et al., 2011) which would enhance marsh resilience.

Measurements of modern shallow subsidence rates in the Mississippi Delta (mean = 7.1 ± 8.7 mm/yr) (Chapter 2) are in line with recent findings (Törnqvist et al, 2008; Meckel et al., 2006) that compaction of Holocene strata is a major contributor to regional land-surface subsidence. Studies (Kaye and Barghoorn, 1964; Van Asselen, 2011) have shown that autocompaction, which is initiatied through the accretion of high porosity, low bulk density wetland sediments (Wang et al., 2016), increases the local rate of RSL rise to values well above the initial threshold rates (~3 to ~7.5 mm/yr) obtained from our compaction-free RSL rise record. This results in marshes being closer to the tipping point that triggers drowning than the initial rate of RSL rise calculated for the basal peat would suggest (Kaye and Barghoorn, 1964).

3.4.2 Re-establishment of terrestrial conditions after drowning

Marshes that are lost to rapid RSL rise rates typically re-establish after the initial drowning, as evidenced by the terrestrial conditions at borehole sites with thick lagoonal packages. However, how long this process takes is not well understood. The radiocarbon age of the Lutcher IX re-established terrestrial layer is ~5.8 cal kyr B.P., suggesting that marsh re-establishment occurred approximately ~1.7 kyr after the initial conversion to open water. Whereas this estimate of time before marsh re-establishment is derived from just a single borehole, we can determine the thickness of the sediment package between drowning and re-establishment to see how it compares to the thickness of similar packages from core logs at other sites.

As all cores were collected on land, terrestrial re-establishment occurred in all boreholes with gradual or rapidly drowned facies successions (n=51 cores with core descriptions that extend to the present-day surface). The thickness of the sediment package between marsh drowning and terrestrial re-establishment for Lutcher IX is 2.5 m. This is comparable to the mean thickness (2.09 ± 0.95 m) of this interval between drowning and re-establishment for all boreholes exhibiting gradually or rapidly drowned facies. Whereas additional chronological analyses are needed to determine the time it took for each drowned site to re-establish, our results suggest that this is likely on the order of centuries to millennia in the Mississippi Delta region.

It is important to note, however, that our results indicate the re-established marsh is not identical to the basal marsh that once occupied this site. Both $\delta^{13}C$ and foraminiferal analysis suggest that the Lutcher IX site underwent an overall shift from brackish marsh to freshwater marsh over time, which indicates that larger scale environmental shifts (such as changes in the distance from active Mississippi River distributaries) may also have a strong influence on re-equilibration processes.

3.5 Conclusions

On annual to decadal timescales, observations clearly indicate that coastal marshes respond to rapid RSL rise rates through surface-elevation gain in order to persist in the landscape (Chapter 2). Paleo-environmental records, however, indicate that it is common for marshes to convert to open water and re-establish centuries to millennia later in this region. We interpret the strong correlation between the rate of RSL rise and the conversion to open water for cores in the earliest part of our record as evidence that this process is dominated by ecosystem response to RSL rise, though this does not rule out the possibility that some of our “drowned” sites may in fact have experienced lateral marsh edge erosion. Rapid drowning is the typical response for marshes facing rates of RSL rise similar to those predicted for the end of the 21st century (USGCRP, 2017), suggesting that large-scale loss of marshes due to drowning in coming decades is a real threat. It is important to note that the particular conditions (such as SSC and tidal range) needed to support marsh persistence likely vary with location and therefore specific threshold rates of RSL rise reported here are not likely to be transferable to other coastal marsh settings. We also note that uncertainties in the facies analysis could potentially shift threshold rates resulting in tipping points downward (i.e. undifferentiated mud may in some cases actually be drowned facies and in others they represent fully terrestrial facies). The value of this study, however, is in recognizing the large disparity between rates of RSL rise that affect marsh persistence over annual to decadal vs. centennial to millennial timescales.

Degradation of Mississippi Delta marshes due to land-use changes and other impacts (Day et al., 2007) has resulted in reduced resilience which makes them more likely to experience rapid shifts in environmental conditions (Scheffer et al., 2001) (e.g., drowning and conversion to open water). This contrasts with the apparent short-term resilience of wetlands to much higher rates of RSL rise as shown through observational (Chapter 2) and modeling results (Kirwan and Megonigal, 2013; Morris et al., 2002). Given modern RSL rise rates in the Mississippi Delta that exceed the threshold rate for rapid flooding and unfavorable modern conditions (e.g. degraded wetlands and limited possibility for landward migration), we suggest that the long-term fate of Mississippi Delta marshes may be less favorable than previously thought, requiring increased attention and urgency in coastal protection planning and in restoration efforts.

4. Organic carbon storage rates in clastic strata outpace rates in organic-rich strata in the Mississippi Delta

4.1 Abstract

Modern wetlands – both coastal and inland - have long been recognized for their rapid rates of organic carbon (OC) accumulation on short (annual to decadal) timescales. Recent work has found higher energy, clastic-dominated, land-building deposits exhibit high rates of OC accumulation over similar timescales of observation, challenging the conventional wisdom that OC accumulation rates are highest in deposits that are rich in organic matter. It remains unknown, however, whether these short-term rates of OC accumulation are representative of OC storage rates on longer (centennial to millennial) timescales for organic and clastic-dominated depositional environments. Here we use the sedimentary record of the last ~6000 years from an inland, freshwater swamp setting in the central Mississippi River delta plain to investigate OC storage rates for peats and clastic overbank deposits (flood-basin and crevasse-splay deposits). We compare OC storage rates between depositional environments to gain insight into the potential role of alluvial OC storage in the global carbon cycle. We use these data to test a pair of hypotheses: first, that OC storage rates are higher in organic-rich deposits than in clastic deposits within this inland alluvial setting and second, that in lower energy inland alluvial settings, OC storage rates are higher than those recently found in higher energy, coastal deltaic settings.

Our results show that mean rates of long-term OC storage rates are up to ~2.5 times more rapid in clastic deposits (~75-150 g/m^2/yr) than in organic-rich deposits (~35-150 g/m^2/yr), a surprising result that is strongly influenced by episodic clastic accretion rates 1-2 orders of magnitude higher than accretion rates of organic-rich strata. We find that in our inland, freshwater swamp study area within the delta plain, long-term OC storage rates in clastic deposits are comparable to short-term OC storage rates for clastic deltaic deposits. Our results suggest that despite relatively low OC content, alluvial deposition of fluvially-derived

clastic sediments is likely an important contribution to the global residual terrestrial OC sink, and may be an important unintended but direct benefit of fluvial sediment-based coastal restoration projects.

4.2 Introduction

Fluvial transport of organic carbon (OC) from terrestrial settings to the deep ocean is an important part of the global carbon cycle (Schlesinger and Melack, 1981; Degens et al., 1991). Erosion by rivers facilitates the delivery of previously stored OC to the ocean where it may be oxidized or re-buried. Rivers also actively transport OC laterally in alluvial systems (Cole et al., 2007; Battin et al., 2009) which can result in labile contemporary and resistant ancient OC being re-deposited in floodplains and deltas (e.g., Stallard, 1998; Walling et al., 2006; Ye et al., 2015; Shields et al., 2017). This process of transport, erosion, and deposition therefore links short-term (modern) and long-term (geologic) carbon cycling processes (Hedges and Keil, 1995; Burdige, 2005). For at least three decades, researchers quantifying fluxes between global carbon reservoirs have recognized that annual emissions are not entirely balanced by oceanic and atmospheric uptake (e.g., Kolchugina and Vinson, 1993; Fan et al., 1998; Hoffman et al., 2013, Jones et al., 2013) and that an unidentified residual terrestrial sink must take up ~3 Pg/yr of carbon that is not accounted for otherwise (LeQuéré et al., 2016).

In order to function as a long-term sink for OC, a sedimentary system requires two properties. First, OC must accumulate at a rate that outpaces removal or remineralization during deposition. Second, in order to facilitate OC storage, the post-depositional rate of degradation or removal of OC must be minimal. Here, we make the important distinction between OC accumulation (a syndepositional process) which takes place over shorter (annual to decadal) timescales and OC storage, which is linked to the balance between OC accumulation and post-depositional degradation and takes place over longer (centennial to millennial) timescales.

Alluvial strata make up the majority of the Earth's terrestrial sedimentary record (e.g., Allen and Allen, 1991), and previous studies have quantified OC accumulation and storage in alluvial systems (or portions thereof), suggesting that up to 66% of OC in these environments is terrestrial in origin (Keil et al., 1997). However, highly variable OC accumulation rates, deposit types, and system dynamics mean that estimating the overall alluvial contribution to global terrestrial OC storage is difficult. In coastal marshes, rapid burial under anoxic conditions ensures high rates (~200 $g/m^2/yr$) of OC storage (Chmura et al., 2003; Baustian et al., 2017). Freshwater swamp environments have been shown to accumulate OC at ~100 $g/m^2/yr$ (e.g., Craft et al., 2008; Villa and Mitsch, 2014). While conventional interpretations of floodplain deposition dictate that OC is primarily accumulated and stored in organic-rich deposits, other alluvial depositional facies may account for a significant component of the missing OC sink (e.g., Hoffmann et al. 2009; Cierjacks et al. 2010; Wohl et al. 2012; Wohl et al., 2015; Sutfin et al. 2016).

The Mississippi River feeds the largest alluvial system in North America, draining ~40% of the United States. This alluvial system encompasses a variety of depositional environments, including swamps and marshes, in its alluvial reach (the Lower Mississippi Valley and the Mississippi Delta). The variety of depositional settings in the Mississippi Delta has therefore resulted in a stratigraphy comprised to a significant extent of clastic fluvial sediments (mostly silts and clays, with lesser amounts of sand) and organic-rich deposits including swamp and marsh peats (Fisk, 1960; Frazier and Osanik, 1969; Kosters et al., 1987; Kosters, 1989), making the Mississippi Delta a prime location to investigate OC storage in a variety of alluvial facies.

Here we compare the OC storage rates of clastic and organic-rich deposits in an inland, freshwater setting in the central Mississippi River delta plain (Fig. 4.1a) – a depositional environment that has not been previously evaluated for OC storage rates - using three sediment cores that are 4-10 m long. We analyze overbank deposits to evaluate the OC storage associated with clastic deposition, while underlying organic-rich strata enable us to evaluate OC storage in peat-forming wetlands. First, we compare OC storage rates in organic-rich deposits and clastic deposits within this inland alluvial setting. We then discuss the role of OC storage in these settings within the context of the missing terrestrial carbon sink and suggest that alluvial deposition may play an important role. We also consider the possible implications for coastal restoration in Louisiana within this context.

4.3 Methods

4.3.1 Sample collection and stratigraphy

We collected three sediment cores from the alluvial ridge of Bayou Lafourche (Fig. 4.1b), an abandoned precursor of the present-day Mississippi River, using a Geoprobe 6610 DT drilling system.

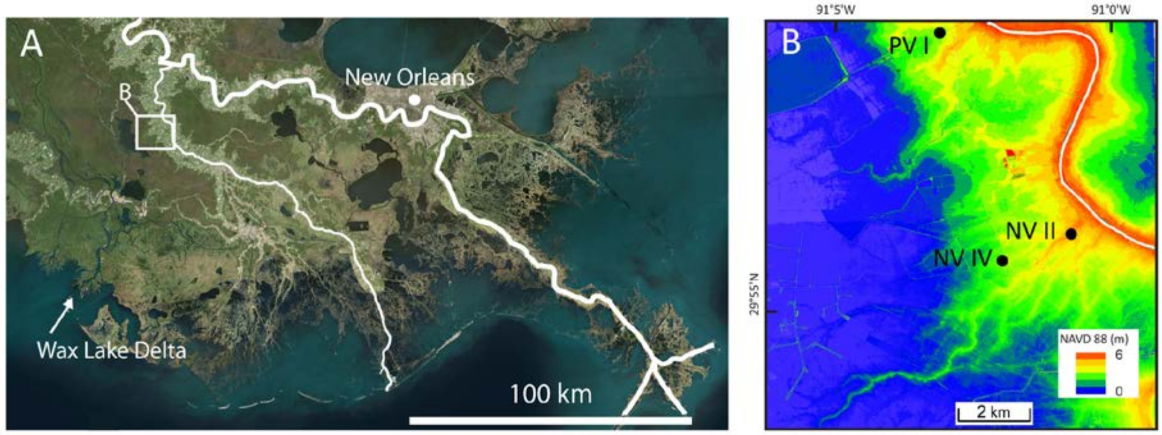

Figure 4.1. Regional (A) and study area (B) location maps. The study area is located along Bayou Lafourche (thin white line), a distributary of the Mississippi River (thick white line) in southern Louisiana. The Wax Lake Delta (study area of Shields et al., 2017) is also shown. Within the study area, three sediment cores were collected for this study: Paincourtville I (PV I), Napoleonville II (NV II), and Napoleonville IV (NV IV).

Sediment texture, color, and the presence or absence of visible organic matter were described in the field at 10 cm increments using the US Department of Agriculture classification system. We focused on a relatively large crevasse splay near Napoleonville, Louisiana, and a smaller crevasse splay near Paincourtville, Louisiana. We collected ~10 m long cores from each crevasse splay (Paincourtville I – PV I and Napoleonville II – NV II; Figs. 4.2a and 4.3a, respectively) which capture the representative stratigraphy of the region: overbank deposits underlain by a laterally extensive wood peat bed (Törnqvist et al., 1996; Shen et al., 2015). We also collected an additional, shorter (~4 m long) core (Napoleonville IV – NV IV; Fig. 4.4a) primarily targeting the underlying wood peat bed to increase the number of samples within the organic-rich strata.

4.3.2 Bulk density and OC content measurements

In each of the three cores, samples of known volume were collected for bulk density (either 5 or 10 mL) and OC content (1 mL) measurements, at ~20 cm intervals. For each bulk density sample, the known volume of sediment was dried at 60 °C overnight (8-16 hours) before weighing. To prepare sediment samples for OC content analysis, they were dried overnight (8-16 hours) at 60 °C, crushed and homogenized with a ceramic mortar and pestle, and then acid-treated with 10% HCl for 24 hours to remove inorganic carbonate material. Acid-treated samples were then centrifuged and the sediment brought to a neutral pH by rinsing (4x) in deionized water. The re-dried and re-homogenized, decarbonated samples were then transferred into tin capsules. Combustion elemental analysis was used to determine OC content (% by mass) of each sample using a Vario MicroCube elemental analyzer. Loss-on-ignition (LOI) analyses were also conducted on sediments at 20 cm increments and a discussion of the comparison between the LOI results and the OC measurements can be found in Appendix C (Figs. C1-C2).

4.3.3 ^{14}C dating

To obtain ^{14}C ages for the peat beds in the NV II and NV IV cores (Table 4.1), plant macrofossils or charcoal fragments were picked from the top and base of the wood peat bed. Multiple subsamples were dated in most cases, following the methods of Törnqvist et al. (1996). At NV IV, an additional sample was collected from a thin organic-rich layer above the wood peat bed. All ^{14}C samples were pre-treated with an

Table 4.1. Radiocarbon data.

Sample name	Material dated	Depth below land surface (cm)	^{14}C age (yr BP)	UTM (N)[1]	UTM (E)[1]	Lab number
Paincourtville I-1a	1 Taxodium distichum twig	920-922[2]	1469 ± 35	3319240	686920	UtC-3871
Paincourtville I-1b	1 Taxodium distichum cone	920-922[2]	1486 ± 55	3319240	686920	UtC-3872
Paincourtville I-2	10 Scirpus cf. robustus nuts	1056-1058[2]	3780 ± 59	3319240	686920	UtC-3873
Paincourtville I-3	5 Carex sp. nuts	1140-1142[2]	4869 ± 51	3319240	686920	UtC-3874
Napoleonville II-5a	1 Taxodium distichum cone fragment	1066-1068	1415 ± 20	3312800	690540	UCIAMS-137467
Napoleonville II-5b	1 Taxodium distichum cone fragment	1066-1068	1430 ± 20	3312800	690540	UCIAMS-137468
Napoleonville II-6a	4 charcoal fragments	1241-1243	4280 ± 20	3312800	690540	UCIAMS-137465
Napoleonville II-6b	6 charcoal fragments	1241-1243	4195 ± 25	3312800	690540	UCIAMS-137466
Napoleonville IV-4a	4 charcoal fragments	871-873	1965 ± 35[3]	3312020	688520	UCIAMS-137469
Napoleonville IV-4b	>20 unidentified macrofossils	871-873	4265 ± 20[3]	3312020	688520	UCIAMS-137470
Napoleonville IV-4c	2 charcoal fragments	871-873	1675 ± 15	3312020	688520	UCIAMS-187164
Napoleonville IV-4d	1 charcoal fragment	871-873	1690 ± 20	3312020	688520	UCIAMS-190601
Napoleonville IV-5a	6 charcoal fragments	1147-1149	3820 ± 45	3312020	688520	UCIAMS-137471
Napoleonville IV-5b	1 Taxodium distichum cone fragment	1147-1149	3740 ± 20	3312020	688520	UCIAMS-137472
Napoleonville IV-6	1 wood fragment	797-799	1305 ± 15	3312020	688520	UCIAMS-187165

[1]All sites are located in UTM zone 15R with reference to NAD 27.
[2] Depths differ from those originally published; sample depths were obtained by projecting the samples from Törnqvist et al. (1996) on corresponding facies boundaries in the newly obtained core for the present study.
[3]Rejected (see text for further discussion).

acid-base-acid rinse of HCl and NaOH at 75°C prior to combustion and then measured using accelerator mass spectrometry at the University of California, Irvine. Previously published ^{14}C ages for the PV I site were adopted from Törnqvist et al. (1996) (Table 4.1).

4.3.4 Age-depth modeling

We combine our new ^{14}C results with previously published optically stimulated luminescence (OSL) (Shen et al., 2015) and ^{14}C (Törnqvist et al., 1996; Table 4.1) data from the same sites to create integrated age-depth models for all three cores. OSL dating has been successfully used for developing chronologies in clastic sediments in the Mississippi Delta (Shen and Mauz, 2012; Chamberlain et al., 2018) and here we use this technique to date clastic overbank deposition from Bayou Lafourche (Shen et al., 2015). OSL ages from both the Napoleonville and Paincourtville sites point to distinct episodes of accretion between 1600 and 600 cal yr BP. OSL ages are typically reported relative to 2010 CE, whereas calibrated ^{14}C ages are reported relative to 1950 CE. To allow for a single age-depth model for each core that combines ages from these two dating techniques, we adjusted the OSL ages to be relative to 1950 CE. Previously published ^{14}C ages at Paincourtville (Törnqvist et al., 1996) were from samples collected at similar facies transitions as those encountered in the present study. We therefore projected the previously published ^{14}C ages from the PV I site onto the corresponding facies contacts in the new core that was used here.

Age-depth models were created using the Bayesian statistical accumulation model Bacon (Blaauw and Christen, 2011) to determine accretion rates for all the strata between chronological data points (OSL and ^{14}C ages). This approach assumes that accretion rates are always positive; i.e., that the rate of sediment accretion outpaces the rate of syndepositional or short-term erosion. Priors for accretion rates in different sections of the core were chosen based on existing ^{14}C and OSL data (Appendix C, Figs. C3-C5). Storage rates were calculated at 10 cm intervals within each core by Markov Chain Monte Carlo (MCMC) iterations. ^{14}C ages used to construct the age models were calibrated in Bacon using the IntCal13 curve (Reimer et al., 2013).

4.3.5 OC storage rates

Accretion rates are calculated at 10 cm intervals within each core. Since OC content and bulk density samples were taken at 20 cm intervals, values were interpolated between each sample (based on the values on either side) so that there was a value at every 10 cm interval. We can therefore determine OC storage rates at 10 cm intervals using the equation

$$\mathrm{Rate_{OC}} = \mathrm{Rate_{Acc}} \times \%\mathrm{OC} \times \rho_{\mathrm{bulk}}$$

where R_{Acc} is the sediment accretion rate (mm/yr), %OC is the OC content (% by mass), ρ_{bulk} is the bulk density (g/m^3), and $\mathrm{Rate_{OC}}$ is the OC storage rate (g/m^2/yr).

4.4. Results and Interpretation

4.4.1 Stratigraphy

The stratigraphy of the study area has been established by previous investigations (Fisk, 1952; Törnqvist et al., 1996; Shen et al., 2015) and includes an extensive wood peat bed (likely dominated by Taxodium distichum) overlain by clastic overbank deposits, including flood-basin and crevasse-splay deposits. Bayou Lafourche was active between ~1550 and 550 cal yr BP (Törnqvist et al., 1996; Shen et al., 2015; Chamberlain et al., 2018). The three sedimentary logs for PVI, NV II, and NV IV (Figs 4.2a-4.4a) all include the wood peat bed and, in PV I and NV II, are overlain by the clastic overbank deposits.

4.4.2 Bulk density and OC content

In each of the three cores, the bulk density varies as a function of sediment texture (Figs 4.2d, 4.3d, and 4.4d) with mean bulk density values ranging from 0.7 g/cm^3 for peats to 1.6 g/cm^3 for the sandy facies (Table 4.2). Organic-rich deposits in all three cores exhibit high OC content with mean values of 14% (PV I), 22% (NV II) and 20% (NV IV), whereas clastic deposits have mean OC contents ranging from 1-5%, varying significantly within each core (Figs. 4.2e, 4.3e and 4.4e).

Table 4.2 Organic carbon content and bulk density by sediment texture.

Sediment Texture	Bulk density (10^6 g/m^3)[2]	OC content (% by mass)[2]	Number of samples
Peat[1]	0.68 ± 0.17	17.92 ± 6.26	11
Clayey Peat[1]	0.89 ± 0.16	9.78 ± 4.37	15
Humic Clay[1]	1.08 ± 0.09	4.80 ± 2.19	8
Clay	1.23 ± 0.23	1.62 ± 2.20	14
Silty Clay	1.38 ± 0.25	0.96 ± 0.73	5
Silty Clay Loam	1.46 ± 0.19	1.30 ± 3.02	19
Silt Loam	1.49 ± 0.08	0.27 ± 0.20	10
Sandy Loam	1.58 ± 0.01	0.16 ± 0.14	2
Very Fine Sand	1.48 ± 0.01	0.20 ± 0.12	2

[1] Organic-rich facies.
[2] Uncertainties are reported as one standard deviation of the mean for each sediment texture.

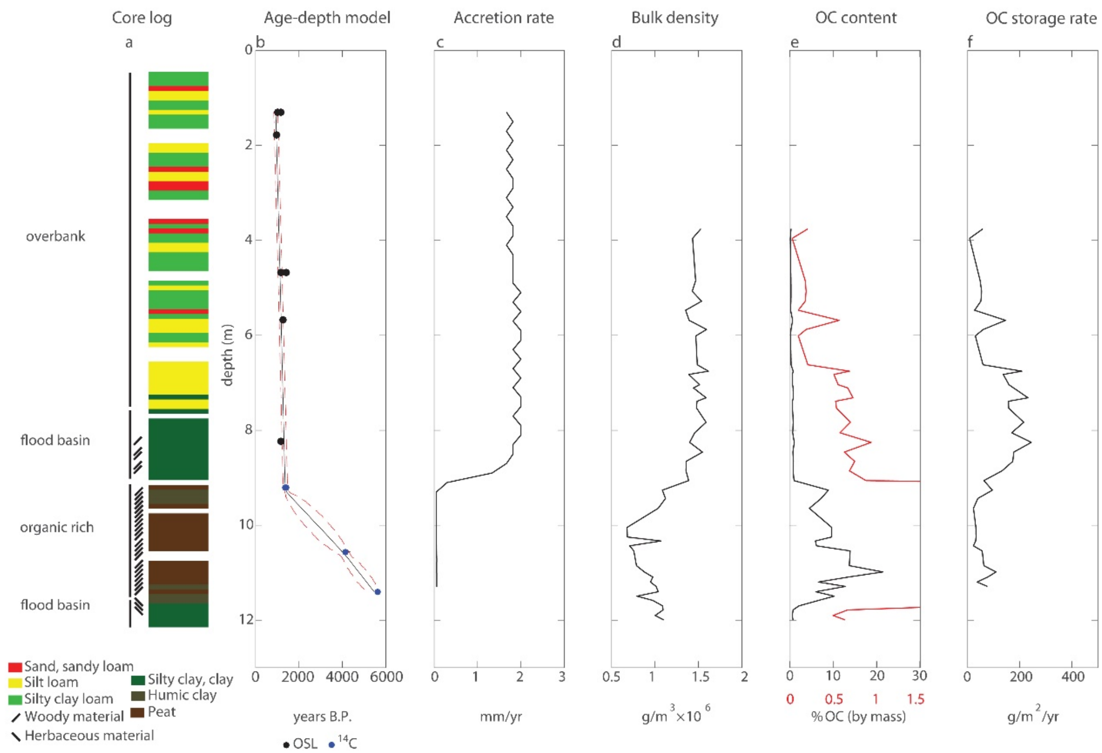

Figure 4.2. Stratigraphy and organic carbon storage rates at the Paincourtville I site. Core log (a) with (b) age-depth model, (c) accretion rate, (d) bulk density, (e) organic carbon content, and (f) organic carbon storage rate. All data can be found in Appendix C.

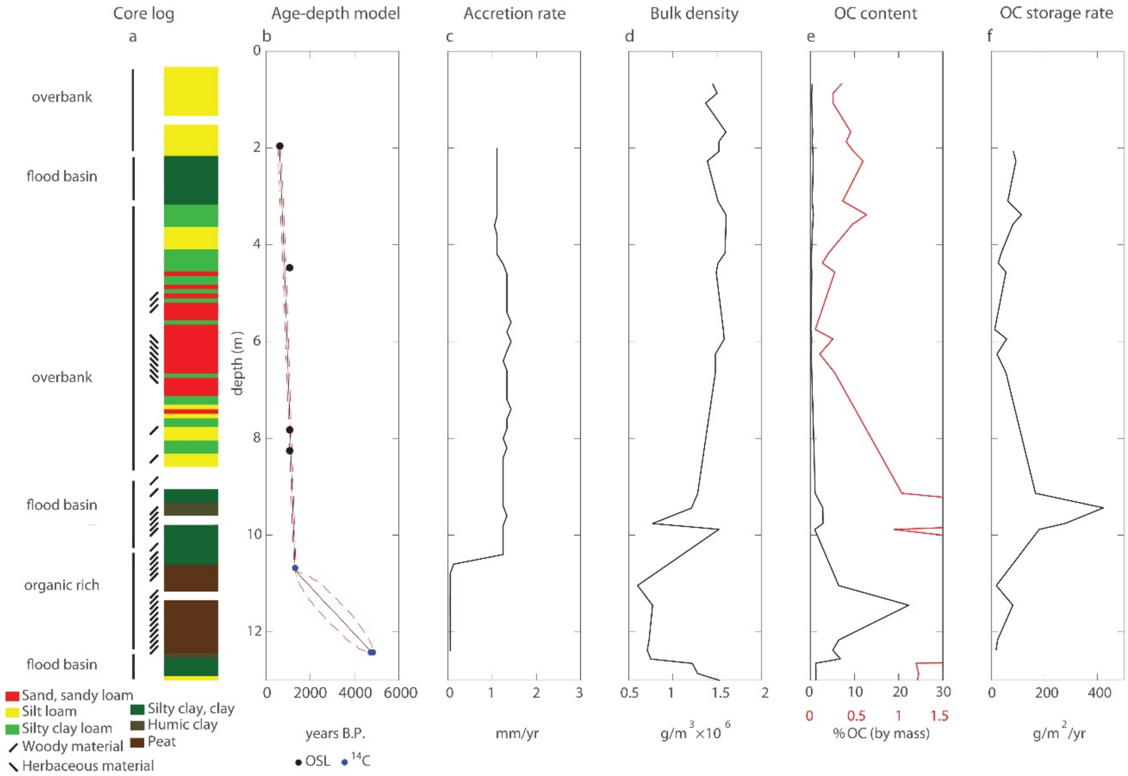

Figure 4.3. Stratigraphy and organic carbon storage rates at the Napoleonville II site. Core log (a) with (b) age-depth model, (c) accretion rate, (d) bulk density, (e) organic carbon content, and (f) organic carbon storage rate. All data can be found in Appendix C.

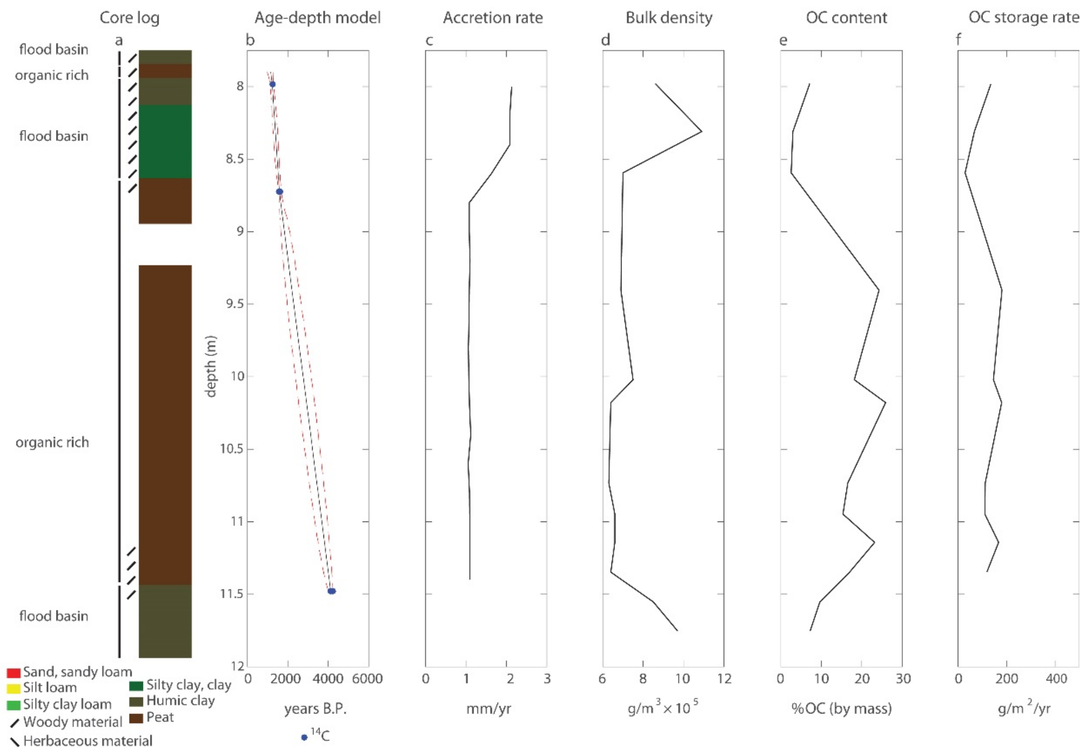

Figure 4.4. Stratigraphy and organic carbon storage rates at the Napoleonville IV site. Core log (a) with (b) age-depth model, (c) accretion rate, (d) bulk density, (e) organic carbon content, and (f) organic carbon storage rate. All data can be found in Appendix C.

4.4.3 Accretion rates

4.4.3.1 Paincourtville I

For PV I (Fig. 4.2), the accretion rate for the wood peat can be calculated using the ^{14}C ages from Törnqvist et al. (1996) (Table 4.1). Using these ^{14}C ages, we obtain accretion rates for the organic-rich portion of PV I of ~0.5 mm/yr. Our age model in the clastic portion of the PV I core uses five OSL-dated levels (Shen et al., 2015) to calculate a long-term, averaged accretion rate of ~20 mm/yr, but as discussed further below, this should be taken as a minimum value given the episodic nature of deposition in this area.

4.4.3.2 Napoleonville II

Using ^{14}C ages (Table 4.1) from the top and base of the wood peat at NV II (Fig. 4.3b) we calculate an accretion rate of ~0.5 mm/yr for the organic-rich portion of the NV II core, similar to the rate found in the organic-rich portion of PV I. OSL ages (Shen et al., 2015) were used to calculate accretion rates the clastic portion of NV II, ranging from ~12-15 mm/yr. These rates are at least an order of magnitude higher than accretion rates in the organic-rich portion of the record and they are higher than the median accretion rate of ~10 mm/yr for NV II obtained using a probabilistic model by Shen et al. (2015). That study, however, found that multiple depositional events could be distinguished (each with rates of up to ~30 mm/yr) which may explain this difference.

4.4.3.3 Napoleonville IV

For NV IV, ^{14}C ages (Table 4.1) were obtained for three organic-rich horizons. Our initial ^{14}C ages (NV IV-4a and NV IV-4b) for the top of the main peat bed were from unidentified seeds and charcoal fragments (Table 4.1), but the ^{14}C results were inconsistent. We re-sampled charcoal from the same horizon (NV IV-4c and NV IV-4d) and obtained consistent ages, allowing us to reject the initial samples as too old.

The accretion rate for the organic-rich portion of the NV IV core between the lowermost ^{14}C sample and the top of the wood peat bed is estimated at ~1 mm/yr. The accretion rate between the top of the wood peat bed and the uppermost ^{14}C sample (NV IV-6) is calculated to be ~2 mm/yr.

4.4.4 OC storage rates

The mean OC storage rate in organic-rich deposits for PV I is ~55 $g/m^2/yr$. This contrasts with ~130 $g/m^2/yr$ for the clastic deposits, ~2.5 times more rapid than in the organic-rich deposits. For NV II the rate of OC storage in the organic-rich deposits is ~35 $g/m^2/yr$ as compared to between ~75-150 $g/m^2/yr$ for the clastic deposits (mean OC storage rate of ~115 $g/m^2/yr$), which similarly outpaces the OC storage rate of the organic-rich deposits by a factor of ~2.5. We also observe that in both PV I and NV II the maximum rates of OC storage correspond to the clay beds between the peat and the overlying, siltier strata, with values of ~200 $g/m^2/yr$ and ~400 $g/m^2/yr$, respectively. One possible explanation for this result is the well-known association of OC with clay minerals in soils and other deposits (e.g., Amato and Ladd, 1992; Jenkinson, 1988), where OC essentially coats high surface area clays and, where it fills pores between the clay minerals, is protected and leads to higher OC content in clay-dominated deposits. While the flood-basin deposits contain 5-50% of the OC content of the peat (Table 4.1), they feature a distinct increase in sediment accretion rates (4.2c and 4.3c) and, as a result, an increase OC storage rates.

The organic-rich deposits from NV IV have the highest rate of OC storage among the peats examined in our study at ~150 $g/m^2/yr$. It is important, however, to note that our OC storage model produces minimum OC storage rates for the clastic strata. Shen et al. (2015) showed that overbank accretion rates at these sites could be up to an order of magnitude higher than the calculated rates and, if this is the case, it would mean that our clastic OC storage rates could in reality be as much as an order of magnitude higher than in the organic-rich portions of our cores.

4.5 Discussion

4.5.1 Sedimentology and OC storage rates

Despite the widely held view that organic-rich deposits are the primary OC repositories in wetland ecosystems, our results show that despite containing 4-20 times less OC (% by mass) than the organic-rich deposits, clastic deposits accumulate OC more rapidly, at rates of up to 400 $g/m^2/yr$. This result is strongly tied to the much more rapid accretion rates of the overbank deposits, in comparison to the organic-rich deposits. Since our calculated sediment accretion rates for clastic deposits are generally ~20 times higher than those for the organic-rich deposits, these results suggest that sediment accretion rate is a dominant influence on overall rates of OC storage.

Rates of OC storage in organic-rich deposits are also strongly linked with accretion rate and vary up to 3 times between individual sites. The rate of OC storage in the organic deposits of PV I and NV II ranged from ~35-55 g/m^2/yr. OC storage rates at NV IV were the highest calculated at ~150 g/m^2/yr, though this is likely explained by the fact that accretion rates were twice as high as the organic rich portions of NV II and PV I as well as the greater number of OC content samples that were located in high OC content peat facies. While we are unaware of any published rates for OC accumulation in Louisiana swamps, the average value of OC storage in organic-rich deposits for the three sites (~80 g/m^2/yr) is comparable, if somewhat slower, than the average OC accumulation rate for comparable, peat-forming modern swamps (~100 g/m^2/yr) in Georgia and Florida (Craft et al., 2008; Villa and Mitsch, 2014), indicating that spatial variability may be a factor in these settings.

Whereas our methodology allows us to calculate a long-term average accretion rate for clastic sediments at NV II, it is important to note that Shen et al. (2015) identified two distinct episodes of crevasse-splay formation in the study area, with emplacement that occurred over much shorter timescales. Our results, therefore, likely underestimate the true rates of OC storage in the clastic deposits as each of these high-energy, episodic events would have deposited material more rapidly than we are able to estimate with our age-depth model. Because the available OSL ages for NV II are not sufficient to resolve the depth within the core at which one depositional episode ceased and the next began, we use a plausible rate of 40 mm/yr (from Shen et al., 2015) to estimate the upper bounds of OC storage rates in this setting.

These findings have implications for the framework in which we interpret OC storage rates in a coastal deltaic setting, such as the Wax Lake Delta, in comparison to inland, freshwater swamps within the Mississippi River delta plain. Geologically, the formation and destruction of alluvial deposits is controlled by internal river processes as well as climate change on millennial and longer time scales. Currently, in coastal Louisiana at the mouth of the Mississippi River, changes in alluvial deposits happen much more quickly. Approximately 5000 km^2 of land has been lost over the past ~80 years (Couvillion et al., 2017) and continued loss is expected in the future given the vulnerability of coastal wetlands to relative sea-level rise (RSLR) (Chapters 2 and 3). However, land use changes impact the global carbon cycle through anthropogenic climate change (e.g. Houghton, 1995), including loss of coastal marshes due to sea level rise which may threaten future coastal marsh OC storage potential (e.g. DeLaune and White, 2012). One of the few areas of present-day land building in coastal Louisiana is the Wax Lake Delta (Fig. 4.1a), the product of an outlet channel cut into the lowermost Atchafalaya River in 1941. Recent work (Shields et al., 2017) in the Wax Lake Delta found OC accumulation rates of ~250 g C/m^2/yr in modern, muddy (>50% mud; Esposito et al., 2017) deltaic deposits and OC storage potential through continuous, self-organized building of land on decadal timescales. Whereas this OC accumulation rate implicitly includes short-term OC losses due to emissions and erosion, it remains unclear whether this rate is representative of the rates of OC storage after centuries or millennia of diagenesis have passed. While examples of land building are rare in the modern Mississippi River delta plain, the sedimentary record can be readily used to examine OC storage during past land-building events.

Our long-term average OC storage rate of ~75-150 g/m^2/yr in clastic deposits at inland sites is only 30-60% of the ~250 g /m^2/yr calculated for the Wax Lake Delta (Shields et al., 2017). However, when calculating OC storage rates using both our age-depth model and the probabilistic sediment accretion rates for individual episodic land-building events of Shen et al. (2015), we find that the OC storage rates of clastic deposits at our study sites may be as high as ~400 g/m^2/yr, i.e., higher than those observed in the Wax Lake Delta.

One important note, however, is that the OC storage that we find in our cores is calculated over century to millennium timescales, as compared to the much shorter (~60 years) observation period in the Wax Lake Delta. In addition, the OC in our cores was deposited and has been stored for periods ranging from ~1300 to ~5400 years, which may impact the rates we calculate. Whereas OC in our cores initially accumulated during deposition, it also has potentially been exposed to long-term diagenetic processes that could have preferentially removed OC over time, decreasing the total long-term OC storage at our sites. Our rates of OC storage can therefore be considered minimum estimates for this reason as well. Additional investigation is needed to determine if that means that the rapid rates (~250 g/m^2/yr) of OC storage reported by Shields et al. (2017) in the Wax Lake Delta is due in part to the relatively short time window, where processes of OC degradation on centennial to millennial timescales have not yet begun to affect the overall pool of OC storage.

4.5.2 Carbon cycling

We find that the rate of OC storage is strongly correlated with sedimentary facies and recognize that the original OC source may be a significant factor herein. This has key implications for carbon cycling and storage in alluvial systems. For instance, the primary source of OC in crevasse-splay deposits is likely to be allochthonous riverine particulate OC, which is frequently sourced from a location well upstream within the watershed (e.g., Hedges and Parker, 1976; Galy, et al., 2007). Recent work has shown that this allochthonous particulate OC in modern river systems can contain a significant proportion of carbon with an old ^{14}C age (Rosenheim and Galy, 2012). This older OC has already undergone partial degradation and consists of more chemically and thermally resistant compounds, so the remaining material that is deposited is more resistant to subsequent loss through diagenetic processes.

During high-discharge events in the Mississippi River, particulate OC can contain a higher proportion of “old” allochthonous OC that has been reworked from upstream alluvial strata (Rosenheim et al., 2013). In contrast, wetlands generate sedimentary OC in place (autochthonous) by wetland vegetation primary production, with smaller contributions from allochthonous OC emplaced during occasional deposition of clastic sediments. The peats produced by these low-energy wetlands can reach up to ~40% OC but preferentially contain “fresh” OC which has more labile compounds (Hedges and Keil, 1995). As a result, this autochthonous OC is more susceptible to degradation and early diagenesis, which has implications for degradation and preservation of OC. When coupled with our findings that OC accumulation rates in organic-rich deposits are only 15-25% of accumulation rates in clastic facies, these results suggest that clastic alluvial deposits outpace organic rich deposits for long-term OC storage, and could potentially account for a component of the missing terrestrial OC sink.

These results also have implications for ongoing coastal restoration efforts in Louisiana as there is an increased focus on using the Mississippi River, specifically its sediment supply, to the largest benefit: nourishing wetlands and building land (Coastal Protection and Restoration Authority, 2017). To combat the rapid land loss, the Louisiana Coastal Master Plan proposes several large sediment diversions along the lowermost Mississippi River. These diversions are intended to build land and maintain vegetated wetlands (e.g., Allison and Meselhe, 2010; Day et al., 2011) and therefore may impact future OC storage potential within the Mississippi River delta pain. An increase in the amount of sediment transported by the river and deposited on the delta plain, whether through sediment diversions - which may build land via processes similar to crevasse splays (Yuill et al., 2016; Esposito et al., 2017; Nienhuis et al., 2018) – or through Wax Lake Delta-style land forms will continue to accumulate OC at rapid rates and may increase the contribution of alluvial deposition to the unidentified terrestrial OC sink.

4.6 Conclusions

Our results suggest that the conventional notion that OC is primarily accumulated and stored in organic-rich floodplain strata may need revision. With accretion rates 1-2 orders of magnitude higher than organic-rich deposits, clastic deposits can accumulate significant amounts of OC rapidly through alluvial deposition of fluvially-derived sediments. This, when paired with the abundance of clastic alluvial deposits on a global scale, suggests that OC accumulation and storage may in fact be less concentrated in organic-rich deposits and more dispersed throughout clastic deposits. The fact that our results suggest alluvial deposition as a significant sink for the missing 3 Pg/yr of OC renders the areal comparison of clastic vs. organic-rich deposition in alluvial strata a high priority in carbon budgeting. We also stress that our results – with rates as high as ~400 g/m^2/yr - represent minimum rates of OC storage in clastic deposits and may in fact significantly underestimate the contribution of clastic alluvial OC storage.

Additionally, our results show that rates of long term (centennial to millennial) OC storage in inland, freshwater swamp ecosystems within the delta plain are comparable to – and in some locations exceed - the high rates of short term (annual to decadal) OC accumulation in coastal marshes and delta fronts. This result is important because whereas the OC accumulation rates may incorporate limited losses due to erosion and oxidation, the long-term OC storage rates incorporate century to millennium scale histories of diagenetic OC alteration and loss – meaning that our results again likely underestimate the rates of OC storage in these settings.

Whereas the Mississippi River and its floodplain have been altered by decades of levee building and altered hydrology, our results show that fluvially-derived deposition has led to the rapid storage of OC in clastic deposits. With ongoing plans for coastal restoration efforts in Louisiana to include large scale sediment diversions to maintain and build land, it is important to note that there will be associated OC accumulation that should be considered a direct, if perhaps unintended, result of these efforts. Depending on the status of carbon valuation efforts, this has the potential to be a component of financing coastal restoration efforts in the state.

5. Summary

Summary of Chapter 2: Vulnerability of Louisiana's coastal wetlands to present-day rates of relative sea-level rise

This chapter aims to answer the question "How vulnerable are modern wetlands to relative sea-level rise (RSLR)?" Our methodology relies on comparing vertical accretion data from 274 sites across coastal Louisiana to RSLR rates at those same locations to determine vulnerability to drowning as reflected by accretion surplus or deficit.

One significant contribution of our study is the unique way in which the rate of relative sea-level rise is calculated. Previous studies used tide gauge data to characterize the rate of RSLR. However, because tide gauges are anchored well below the land surface, they actually measure how water levels are changing relative to that sub-surface anchor elevation, rather than the marsh surface. We calculate rates of relative sea-level rise by combining site-specific measurements of shallow subsidence (based on rod surface-elevation table – marker horizon data) with GPS-derived deep subsidence rates and measurements of eustatic sea level rise from satellite altimetry, giving us a clearer picture of what is happening at the marsh surface – where the risk of drowning exists.

This study is the first large-scale analysis of surface elevation and vertical accretion data from the Coastwide Reference Monitoring System (CRMS) to characterize shallow subsidence and wetland vulnerability in coastal Louisiana. Using CRMS data we found that 35% of wetland sites in the Mississippi Delta and 58% in the Chenier Plain are vulnerable due to modern rates of RSLR (mean of 13 and 9 mm per year, respectively, for these two regions). This confirms previous studies that suggested RSLR rates >10 mm/yr are near the upper limit that Louisiana wetlands can withstand.

An important finding from our study is that there is a sub-regional trend of higher vulnerability for wetlands in the western Chenier Plain (64%) as compared to 58% of sites for the Chenier Plain as a whole.

Our results indicate that the very low vertical accretion rates at Chenier Plain sites explain much of this vulnerability, although there may be other factors at play as well. We recognize that there is a large number of variables and biogeochemical feedbacks that impact wetland surface elevation and that our methodology considers the cumulative result of these interactions, rather than the individual processes.

Another key finding from our study is that shallow subsidence is concentrated in the uppermost portions (5-10 m) of the Holocene package. This means that while deep subsidence rates may be influenced by the thickness of the Holocene package in any given location (resulting in variable deep subsidence rates in the Mississippi Delta, for example), the shallow subsidence rate is likely driven by short-term compaction that occurs within the most recent sedimentary deposits at a rate that is, on average, constant across coastal Louisiana (~6 mm/yr). This may also suggest that active compaction is mostly completed in the time that it takes for ~5-10 m of sedimentary material to aggrade in coastal Louisiana; future research could focus on defining the timeline for this to occur.

While this study is an examination of the vulnerability of wetlands to RSLR in present-day coastal Louisiana, there are many avenues of further research that would greatly improve our understanding of what drives wetland vulnerability and how these environments respond to environmental change. Future work can be undertaken to see if links exist between soil characteristics, such as bulk density and organic matter content, and shallow subsidence rates.

While an initial analysis of the relationship between shallow subsidence rates and these soil characteristics was completed as part of the preliminary work for this study, the bulk density and organic matter data were only available from the time prior to CRMS site establishment and were therefore not suitable to link with shallow subsidence rates 6-10 years after that initial measurement. The CRMS program is in the process of obtaining a second set of bulk density and organic matter measurements which would give insight into how these characteristics have changed over time and whether shallow subsidence rates might be correlated with any discernable trend in those variables.

Summary of Chapter 3. Holocene coastal marsh drowning and re-emergence in response to relative sea-level rise

The intention of this chapter is to determine the rates of RSLR that lead to marsh collapse and conversion of terrestrial ecosystems to open water and to provide an estimate of the time required for re-establishment of a terrestrial ecosystem. Our methodology relies on comparison between a high-resolution Holocene RSLR record and a stratigraphic analysis of facies successions from 355 sediment cores from across the Mississippi Delta to identify threshold rates of RSLR that lead to marsh drowning over the past ~8500 years. We also use stratigraphic analysis, ^{14}C dating, foraminiferal assemblage analysis, and stable isotope geochemistry to track and constrain the timing of paleo-environmental changes, including marsh collapse, conversion to open water, and terrestrial ecosystem reestablishment.

We use a set of 72 sea-level index points to establish a robust RSLR record (tracking the elevation of sea level through time) through the Holocene. We then use that relationship between age and elevation to expand our analysis to an additional 283 sites beyond the 72 sites with sea-level index points and investigate trends in this much larger data set.

This study uses a combination of in-depth geochemical and microfossil analyses to track paleo-environmental change at a single site, Lutcher IX, as well as ^{14}C analysis to evaluate how long it takes for re-establishment after drowning. Stratigraphic records from 51 cores with evidence of marsh drowning are analyzed and the thickness of deposition between drowning and re-establishment are compared to that found in the Lutcher IX core (which has geochronological control indicating ~1700 years for re-establishment) to make a reasonable estimate of the time required for re-establishment in marsh systems. While previous studies have established a framework to describe the theory behind marsh collapse, conversion to open water, and re-establishment of a terrestrial ecosystem, this is the first test of that framework using the sedimentary record. Our results suggest that this response in marsh systems occurs on the order of centuries to millennia.

One key outcome of this analysis is the identification of threshold rates of RSLR that lead to marsh drowning and conversion to open water in coastal Louisiana. When rates of RSLR exceed ~3 mm/yr, we find evidence of marsh drowning in ~80% of the study sites. We also find that when rates of RSLR exceed ~7.5 mm/yr, another tipping point is reached and 94% of sites drown rapidly. This is an important finding because, as was discovered in Chapter 2, modern marshes in the Mississippi Delta are already facing rates of RSLR of ~13 mm/yr. While the short-term (annual to decadal scale) observations of modern marsh conditions of Chapter 1 suggest that 35% of marshes are vulnerable due to current rates of RSLR rise, the results from the paleo-record would suggest that this is a vast underestimation of actual vulnerability on centennial timescales. To further refine the hysteresis analysis of this study would require additional in-depth geochemical and microfossil analyses of cores where hysteresis response is observed. By extending the analysis to additional sites beyond Lutcher IX, we can determine how robust our initial results of ~1700 years to marsh re-establishment may be.

Summary of Chapter 4. Organic carbon storage rates in clastic strata outpace rates in organic-rich strata in the Mississippi Delta

In this chapter, we test a pair of hypotheses: first, that OC storage rates are higher in organic-rich deposits than in clastic deposits within this inland alluvial setting and second, that in lower energy, inland deltaic settings, OC storage rates are higher than those recently found in higher energy, coastal deltaic settings. We rely on ^{14}C and OSL dating, elemental analysis, and bulk density measurements collected from three sediment cores collected near Bayou Lafourche, a former distributary of the Mississippi River, to calculate carbon storage rates for organic-rich and clastic strata and to determine the relative carbon storage efficiency of these deposits.

One significant contribution of our study is the surprising finding that while clastic strata contain significantly less OC (~1-5%) than organic strata (~14-22%), the clastic strata store carbon at at least ~2.5 times the rate of organic-rich strata. We find that the rapid accretion rates associated with overbank deposition that produce the clastic strata allow for much more rapid OC storage than the formation of organic-rich strata. We also find that OC storage rates in these inland, freshwater swamp settings are comparable to the short-term OC accumulation rates for coastal marshes (~200 g/m^2/yr) and delta front deposits such as those in the Wax Lake Delta (~250 g/m^2/yr over the past ~60 years), despite having been exposed to possible diagenetic alteration that could lead to OC loss (and therefore underestimated rates of OC storage). Our results suggest that OC storage within clastic alluvial deposits may have a larger role in the global carbon cycle than previously recognized, which may also have implications for future OC accumulation due to coastal restoration efforts.

Appendix A. Supplementary Information for Chapter 2

Table A1. Study database.

Digital file.

Table A2. Size of previously published rod-surface elevation table data sets. The list below includes the number of rod-surface elevation tables (RSETs) used in 63 previously published studies. Our data set (n = 274) is an order of magnitude larger than the largest regionally contiguous RSET data set[20]. Supplementary Table 1 is an extension of previously published RSET data compilations (Cahoon et al., 2015; Webb et al., 2013).

Study/Reference #	Number of RSETs	Location
		United States
Boumans et al., 2002b	6	California
Reed, 1995	unspecified	California
Wallace et al., 2005	8	California
Rooth and Stevenson, 2000	2	Chesapeake Bay
Kirwan et al., 2016	179	East Coast (and parts of Europe)
McKee, 2011	16	Florida and the Carribbean
Cahoon and Lynch, 1997	unspecified	Florida
Hendrickson, 1997	unspecified	Florida
Whenlan et al., 2005	9	Florida
Whelan et al., 2009	9	Florida
Cahoon et al., 2011	2	Louisiana
Lane et al., 2006	18	Louisiana
Rybczyk and Cahoon, 2002	6	Louisiana
Boumans et al., 1997	9	Louisiana
Cahoon et al., 2011	10	Louisiana
Ford and Grace, 1998	20	Louisiana
Guntenspergen et al., 1995	3	Louisiana
Bowron et al., 2011	6	Maine
Kroes and Hupp, 2010	6	Maryland
Delgado et al., 2013	12	Maryland
Childers et al., 1993	25	Maryland
Erwin et al., 2006	14	Massachusetts, New Jersey, and Virginia
Cahoon et al., 2000	1	Mississippi Delta Region
Day et al., 2011	12	Mississippi Delta Region
Ford et al., 1999	6	Mississippi Delta Region
McKee and Cherry, 2009	4	Mississippi Delta Region
Boumans, et al., 2002a	14	New Hampshire and Massachusetts
Roman et al., 2007	unspecified	New York
Mattheus et al., 2010	3	North Carolina
Cornu and Sadro, 2002	2	Oregon
Morris et al., 2002	3	South Carolina
Cahoon et al., 1995	4	Southern Region

Cahoon et al., 2008	22	Southern Region and Caribbean
Cahoon et al., 2011	15	Texas and Louisiana
Cahoon et al., 2004	12	Texas
Baldwin et al., 2009	10	Washington DC
Cahoon et al., 1999	unspecified	Washington
		Oceania
Rogers et al., 2006	69	Australia
Rogers et al., 2013	9	Australia
Rogers et al., 2005a	9	Australia
Rogers et al., 2005b	24	Australia
Howe et al., 2009	12	Australia
Lovelock et al., 2011	12	Australia (Brisbane)
Oliver et al., 2012	6	Australia (Minnamurra River)
Lovelock et al., 2014	9	Australia (Queensland)
Krauss et al., 2010	18	Micronesia
Stokes et al., 2009	12	New Zealand
Lovelock et al., 2015	153	Indo-Pacific Region
		North and Central America
Pacquette et al., 2004	16	Canada (Bay of Fundy)
Van Proosdij et al., 2006	3	Canada (Bay of Fundy)
Van Proosdij et al., 2010	5	Canada (Bay of Fundy)
McKee et al., 2007	9	Belize
Cahoon et al., 2003	18	Honduras
		Europe
Hensel et al., 1999	2	France (Rhone Delta)
Day et al., 1999	20	Italy (Venice Lagoon)
Day et al., 1998	10	Italy (Venice Lagoon)
Scarton et al., 2000	4	Italy (Venice Lagoon)
Ibáñez et al., 2010	6	Spain (Ebro Delta)
Ibáñez et al., 1997	4	Spain (Ebro Delta)
Day et al., 2011b	55	Spain, France, Italy
Vandenbruwaene et al., 2011	13	The Netherlands
Cahoon et al., 2000b	10	United Kingdom
French and Burningham, 2003	8	United Kingdom
Spencer et al., 2012	11	United Kingdom

Table A3. **Rates of surface-elevation change, vertical accretion, and shallow subsidence by wetland type.**

	Surface-elevation change rate (mm/yr)			Vertical accretion rate (mm/yr)			Shallow subsidence rate (mm/yr)				
	Mean	Median	sd	Mean	Median	sd	Mean	Median	sd	n	%
All	3.8	4.1	7.4	10.7	9.5	7.8	6.9	6.0	7.9	274	100
F[1]	4.4	4.7	10.7	12.2	10.3	7.6	7.8	8.7	10.7	31	11
I[2]	2.5	2.0	7.5	9.9	9.5	6.3	7.4	7.1	5.8	83	30
B[3]	3.0	3.5	5.4	8.7	8.6	4.5	5.7	5.3	4.8	74	27
Sa[4]	6.3	7.7	8.4	13.6	10.0	12.5	7.3	3.4	12.3	57	21
Sw[5]	4.1	3.9	3.4	10.5	9.5	4.7	6.4	6.1	4.9	29	11
MD	5.7	5.8	7.2	12.8	11.3	8.4	7.1	6.0	8.7	185	100
F	8.1	7.0	10.5	14.8	15.0	7.8	6.7	8.7	12.7	19	10
I	5.4	5.1	7.2	13.7	12.7	6.2	8.2	8.0	4.8	42	23
B	4.6	4.4	4.8	10.6	10.3	4.1	5.9	5.5	4.3	45	24
Sa	6.9	8.1	8.8	14.5	11.6	13.0	7.6	3.4	13.0	50	27
Sw	4.1	3.9	3.4	10.5	9.5	4.7	6.4	6.1	4.9	29	16
CP	-0.2	-0.5	6.3	6.3	5.9	3.7	6.5	5.8	6.3	89	100
F	-1.6	-3.0	8.4	8.0	7.5	5.0	9.6	9.8	6.7	12	13
I	-0.6	-1.0	6.7	6.0	6.0	3.6	6.6	6.2	6.7	41	46
B	0.5	1.5	5.4	5.8	4.5	11.6	5.3	5.1	5.6	29	29
Sa	1.7	1.3	2.8	7.0	6.3	3.5	5.3	3.7	4.1	7	8
Sw	N/A	N/A	N/A	N/A	N/A	N/A	N/A	N/A	N/A	0	0

1. Fresh marsh.
2. Intermediate marsh.
3. Brackish marsh.
4. Saline marsh.
5. Swamp.

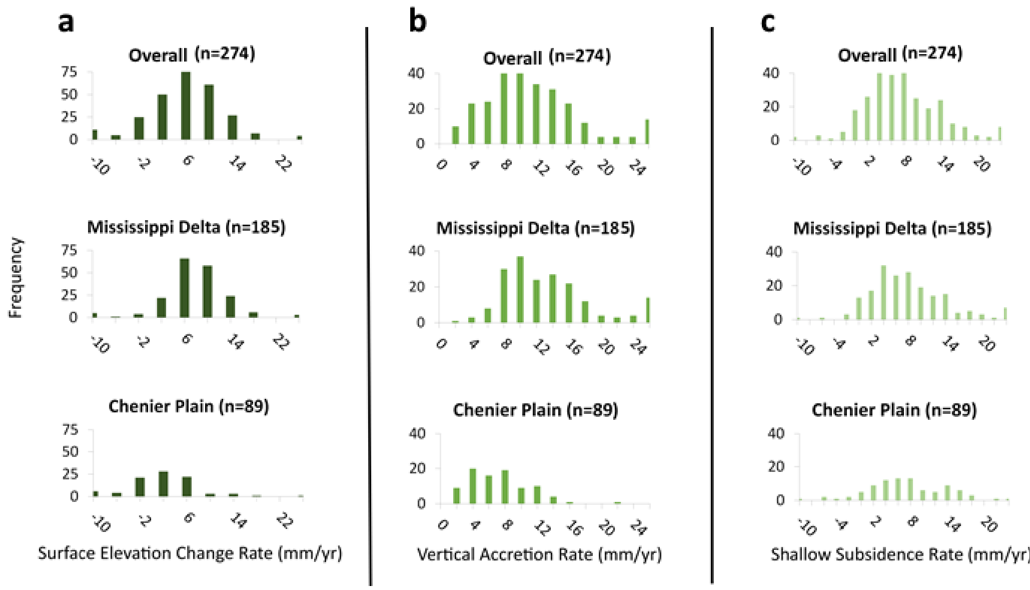

Figure A1. Frequency histograms with rates of (a) surface-elevation change, (b) vertical accretion, and (c) shallow subsidence.

Table A4. GPS-measured and predicted deep subsidence rates in the Mississippi Delta. Vertical velocity data were obtained from 13 GPS stations (data from Karegar et al., 2015) within the Mississippi Delta that were used to create a linear model (Fig. 4) of deep subsidence rates. Predicted vertical velocity is obtained by solving this linear equation as a function of latitude. Only GPS sites within the Mississippi Delta with ≥5 years of observation were included.

GPS Station	Lat	Long	Length of observation (yr)	GPS foundation depth (m)	GPS measured vertical velocity (mm/yr)	Predicted vertical velocity (mm/yr)	GPS minus predicted vertical velocity (mm/yr)
BVHS	-89.41	29.34	11.93	>20	-5.7	-5.27	0.43
COVG	-90.10	30.48	10.02	>15	-0.8	-1.04	-0.24
DSTR	-90.38	29.96	8.38	unknown	-2.0	-2.97	-0.97
ENG1	-89.94	29.8	18.54	~3	-2.3	-3.26	-0.96
GRIS	-89.96	29.27	8.89	unknown	-5.6	-5.53	0.07
HAMM	-90.47	30.51	13.45	>15	-1.0	-0.92	0.08
HOUM	-90.72	29.59	10.67	>15	-3.9	-4.34	-0.44
LMCN	-90.66	29.25	11.26	36.5	-6.5	-5.61	0.89
LWES	-90.35	29.90	6.67	unknown	-2.7	-3.19	-0.49
MSSC	-89.61	30.38	9.23	unknown	-1.5	-1.41	0.09
NDBC	-89.61	30.36	13.18	unknown	-1.3	-1.48	-0.18
SJB1	-91.11	30.40	5.36	unknown	-1.5	-1.33	0.17
1LSU	-91.18	30.41	11.21	<15	-2.9	-1.30	1.60

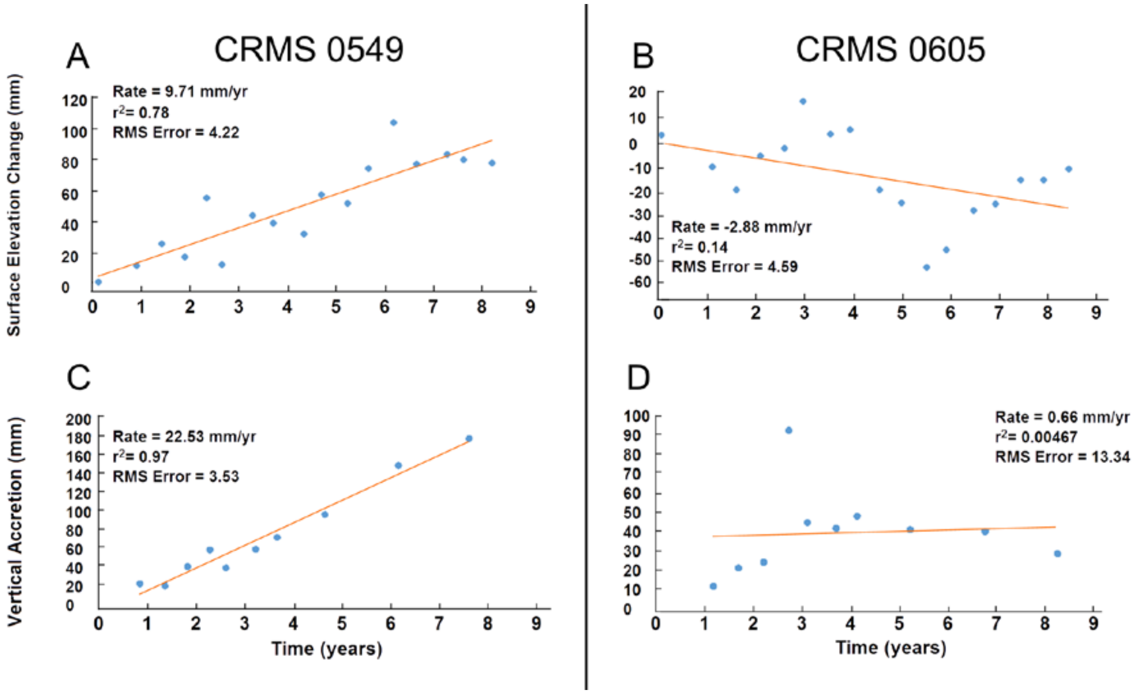

Figure A2. **Methodology to determine rates of surface-elevation change and vertical accretion.** Following each site visit, individual measurements are averaged and plotted vs. time. A linear regression is carried out to determine the rate of surface-elevation change (a, c) and vertical accretion (b, d). For both SEC and VA records, mean site visit (i.e., static) measurements are indicated by the blue dots and the orange line indicates a linear regression analysis of the record which yields the eventual (i.e., long-term) SEC or VA rate. Short-term perturbations in the accretion history at individual CRMS sites contribute to within-site variability. It is important to note that due to the MH methodology, individual events that deviate from the overall trend of accretion at a CRMS site are necessarily time-averaged between site visits, and so the relative importance of individual events is dependent on the frequency of sampling.

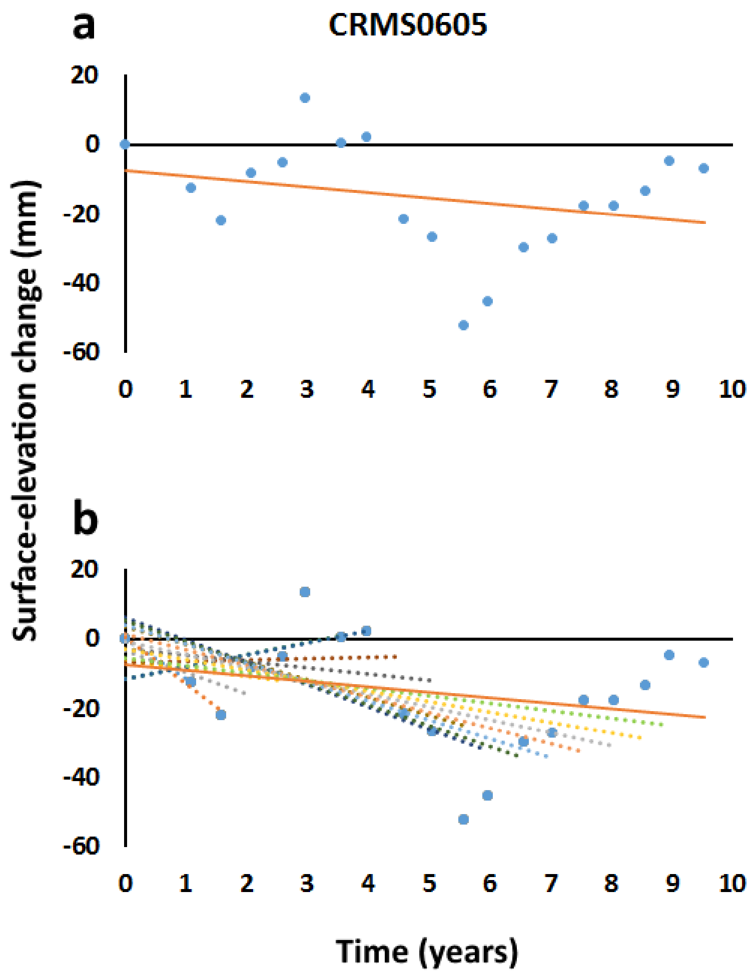

Figure A3. Comparison of eventual and site visit surface-elevation change linear regression analyses for site 0605. The step-wise establishment of CRMS sites has resulted in variable durations of observation among sites. We determined the eventual (i.e., long-term) surface-elevation change rate for site 0605 with blue dots indicating site visit surface elevation measurements and the solid orange line indicating the linear regression (i.e., the eventual SEC rate) for this record (a), i.e., similar to Supplementary Fig. 2c. We then determined linear regressions for site visit SEC rates at each time step (i.e., approximately every six months through the duration of observation) with each of the dotted lines representing a site visit SEC rate of different length and the solid orange line representing the eventual SEC rate (b). Short-term site visit SEC rates (≤4 years of observation) produce highly variable campaign SEC rates that may deviate significantly from the eventual SEC rate. Longer-term site visit SEC rates (≥5 years of observation) approximate the eventual SEC rate.

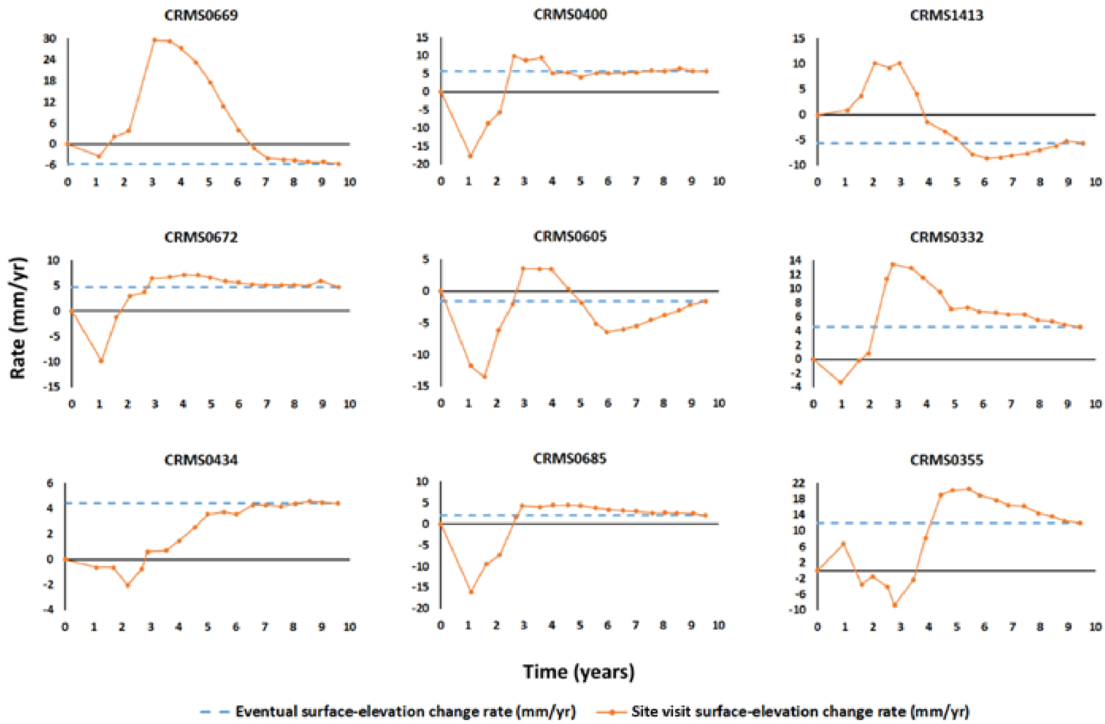

Figure A4. Comparison of eventual and site visit surface-elevation change for the 9 longest records. The difference between each site visit SEC rate (orange line) and the eventual SEC rate (dashed blue line) is plotted for the 9 sites with the longest duration of observation. The difference at each time step is tracked over the full duration of observation for each of the 9 selected sites. We find that in most cases, the difference between the site visit SEC rate and the eventual SEC rate approaches its minimum after 5 years of observation (and sometimes earlier). All sites included in this analyses have been monitored for 6 years or more. It is important to note that this analysis fundamentally assumes that SEC rates at a given site approach a "true" value over time and that these rates are appropriately represented by a linear relationship as time progresses. While this is not necessarily correct, it constitutes a more stringent assessment of required length of observation record than what has commonly been used[47].

Table A5. Effect of removing noisy surface-elevation change and vertical accretion records. Descriptive statistics for rates of surface-elevation change and vertical accretion and for the Mississippi Delta and Chenier Plain sub-regions were calculated using the full data set as well as a smaller, reduced error data set. We compare the descriptive statistics of these two data sets to evaluate the effect that noisy data may have on the results. In the reduced error data set, sites with a root mean squared (RMS) error in the 90th percentile (i.e., the noisiest records) for surface-elevation change and/or vertical accretion were removed. Removal of high RMS error records generally removed exceptionally low minimum and/or high maximum values and lowered the standard deviation.

	Full data set n=274	**Reduced error data set n=227**	**Full data set n=274**	**Reduced error data set n=227**
	Overall			
	Surface-elevation change rate (mm/yr)		Vertical accretion rate (mm/yr)	
Mean	3.8	3.7	10.7	10.5
Median	4.1	4.1	9.5	9.5
Standard deviation	7.4	6.0	7.8	7.8
Minimum	-41.0	-18.0	0.2	0.9
Maximum	46.0	31.9	83.7	83.7
	Mississippi Delta			
	Surface-elevation change rate (mm/yr)		Vertical accretion rate (mm/yr)	
Mean	5.7	5.6	12.8	12.6
Median	5.8	5.8	11.3	11.2
Standard deviation	7.2	5.1	8.4	8.5
Minimum	-41.0	-18.9	1.6	2.0
Maximum	46.0	31.9	83.7	83.7
	Chenier Plain			
	Surface-elevation change rate (mm/yr)		Vertical accretion rate (mm/yr)	
Mean	-0.2	-0.9	6.3	6.1
Median	-0.5	-0.6	5.9	5.5
Standard deviation	6.3	5.1	3.7	3.4
Minimum	-17.3	-17.3	0.2	0.9
Maximum	22.5	12.2	20.6	14.7

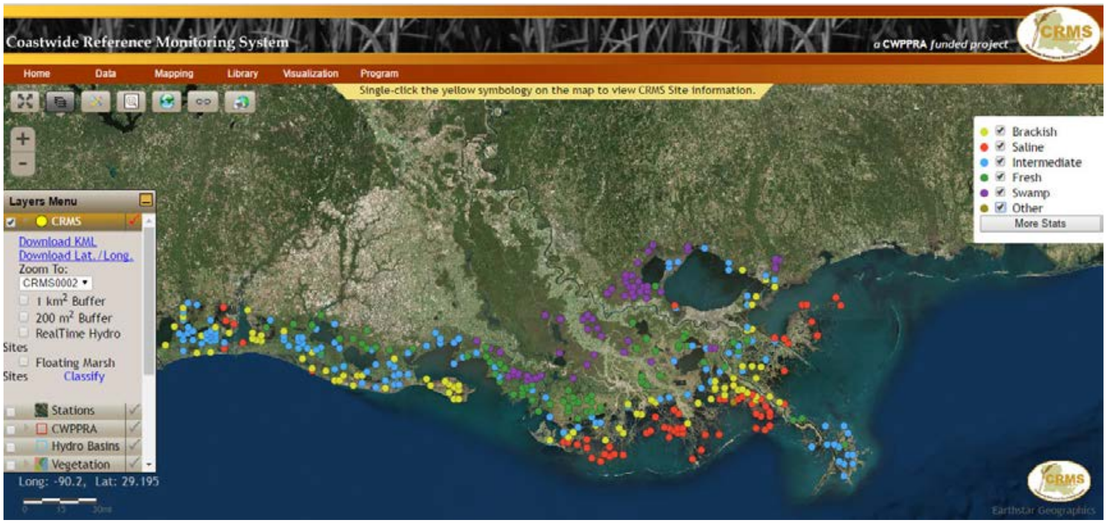

Figure A5. Distribution of wetland types in coastal Louisiana. Data are taken from the Coastwide Reference Monitoring System[66] and wetland types are based upon an established classification system[67]. Here all 391 CRMS sites (including the 274 sites used in this study) are represented.

Appendix B. Supplementary Information for Chapter 3.

Table B1. Study database.

Digital file.

Appendix C. Supplementary Information for Chapter 4.

Appendix C analysis: Loss-on-ignition vs. elemental analysis comparison

Many studies have explored the link between sediment texture and organic-matter content through loss-on-ignition measurements (Kearns and Davison, 1983; Kosters, et al., 1987). Organic matter differs from OC. Organic matter includes OC, in addition to other elements that make up organic compounds (e.g. H, N, S, and O). For example, leaf litter is 100% organic matter, but typically only 40-50% OC. Organic matter is generally a good proxy for OC but there are a number of considerations such as the greater amount of OC associated with sediment textures that have a greater surface area to mass ratio (e.g., clays) (Kearns and Davison, 1983; Kosters et al., 1987) that impact the actual organic matter to OC ratio; therefore, variations in the conversion factor warrant discussion. The relationship can vary widely based on several factors, including the origin of the OC and the depth of burial (e.g., Allen et al., 1974; Schnitzer and Khan, 1978; Perie and Ouimet, 2008; CPRA, 2012).

A factor of 1.724 – equivalent to organic matter containing 58% OC - has often been used as a general conversion factor between organic matter and OC (see Allen, 1974), although this assumption has been challenged by empirical and theoretical studies (Schumacher, 2002; Zhong and Wu, 2009; Pribyl, 2010). Louisiana-specific values for the relationship between organic matter and OC content were measured in coastal marsh sediments and reported by the Coastal Protection and Restoration Authority (CPRA, 2012). The results (Fig. C1) show that for Louisiana marsh sediments at shallow depths (<50 cm) the organic matter to OC conversion factor is 2.2, representing ~45% OC in organic matter. This suggests that more precise values can be obtained by using a local, experimentally derived conversion factor than when using the generalized factor of 1.742.

As part of this study, we measured organic matter content within our three cores using loss-on-ignition. Each sample was weighed and dried overnight (8-16 hours) at 100 °C. These dried samples were then crushed and homogenized with a ceramic mortar and pestle, weighed, and then heated to 550°C for 24 hours to ignite and remove all organic matter. The samples were then weighed and the amount of organic matter lost (% by mass) was calculated. We then compared the organic matter values to the OC values we determined using Elemental Analysis (see Methods) to determine a conversion factor for each core (Fig. D2). Though we find some variation between the conversion factor in the cores, the OC content of organic matter in our study cores falls between ~48-57%, suggesting that there is spatial variability (as much as ~10%) in the amount of organic matter that is comprised of OC. This result means that quantifying the OC content of sedimentary deposits may require specific measurements in the study location to obtain more precise values.

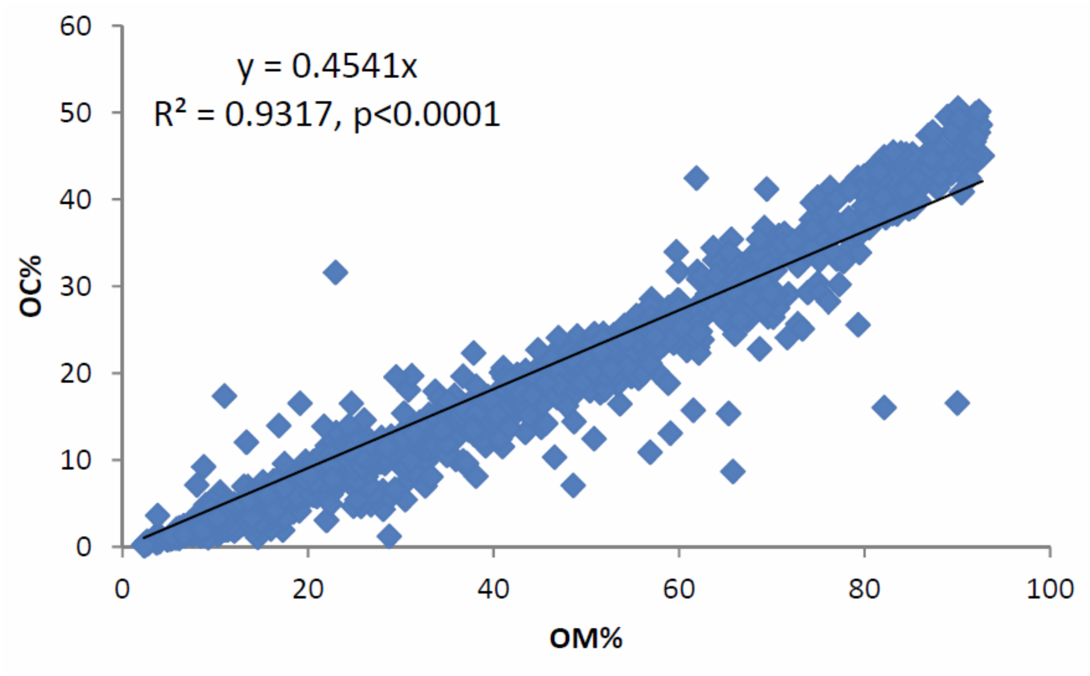

Figure C1. The relationship between organic matter (derived from loss-on-ignition analyses) and OC content for coastal Louisiana marsh sediments (CPRA, 2012).

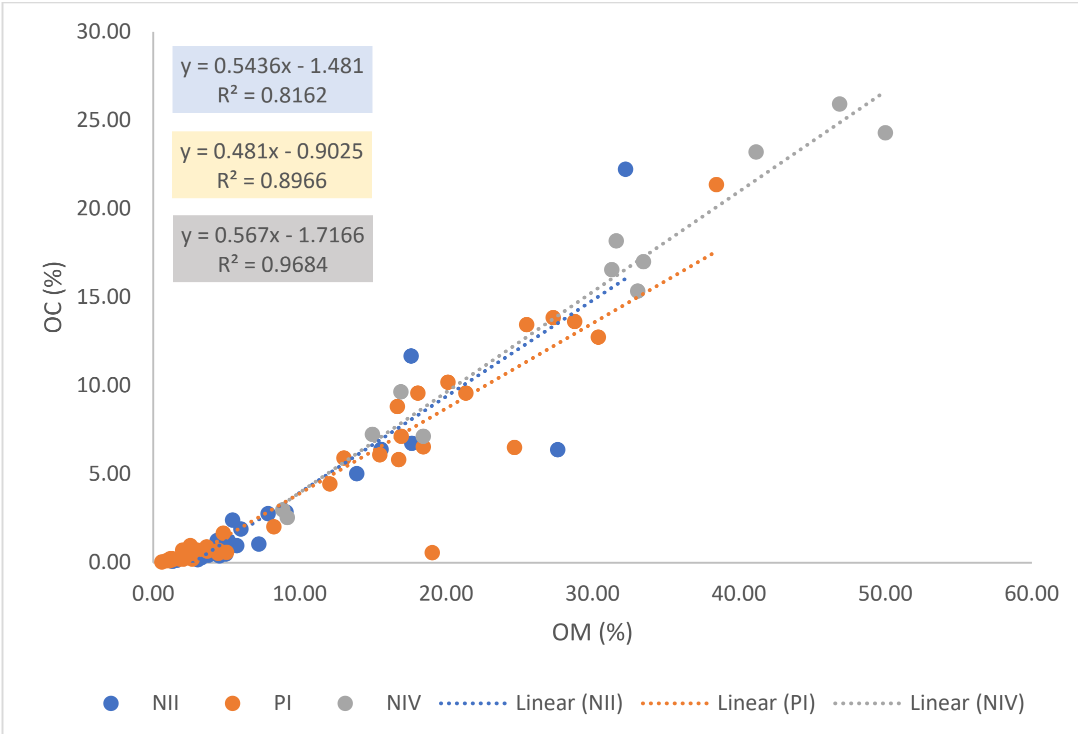

Figure C2. The relationship between organic matter (derived from loss-on-ignition analyses) and OC content for the Napoleonville II, Napoleonville IV, and Paincourtville I cores.

Appendix C. Bacon age-depth model outputs

OSL and ^{14}C ages are reported in years B.P. This involved converting the OSL ages (which were previously reported with reference to 2010 C.E.) from Shen et al. (2015) to B.P. by subtracting 60 years from the ages to convert them so they are with reference to 1950 C.E. as ^{14}C ages commonly are reported. Radiocarbon ages were calibrated within a Bayesian accumulation model (*Bacon)* Blaauw and Christen, 2011) using the IntCal13 curve (Reimer, et al., 2013). *Bacon* is used to construct age-depth models by calculating accretion rates at regular intervals within each core using Markov Chain Monte Carlo (MCMC) iterations. In cores NV II and PV I, a “hiatus” (hiatus mean = 10 yr) was included above the peat bed to clear the memory of the model to accommodate the rapid change in accretion rate at the point where deposition changes from organic to clastic sediments. This is important because within *Bacon* the accretion rate is informed by all accretion rates occurring previously and there is a fundamental difference in the mechanisms that control organic deposition (decayed plant material) and clastic deposition (flooding) in this system. Priors for accretion rates in different sections of each core were estimated based on existing ^{14}C and OSL data (Figs. C3, C4, and C5).

Accretion rates for each core were calculated in Matlab using the *Bacon* age model output. The *Bacon* output data were sampled at 10 cm depth intervals. The difference in years at each of the sampled 10 cm intervals in the core was calculated and then divided by 10 cm to produce an accretion rate.

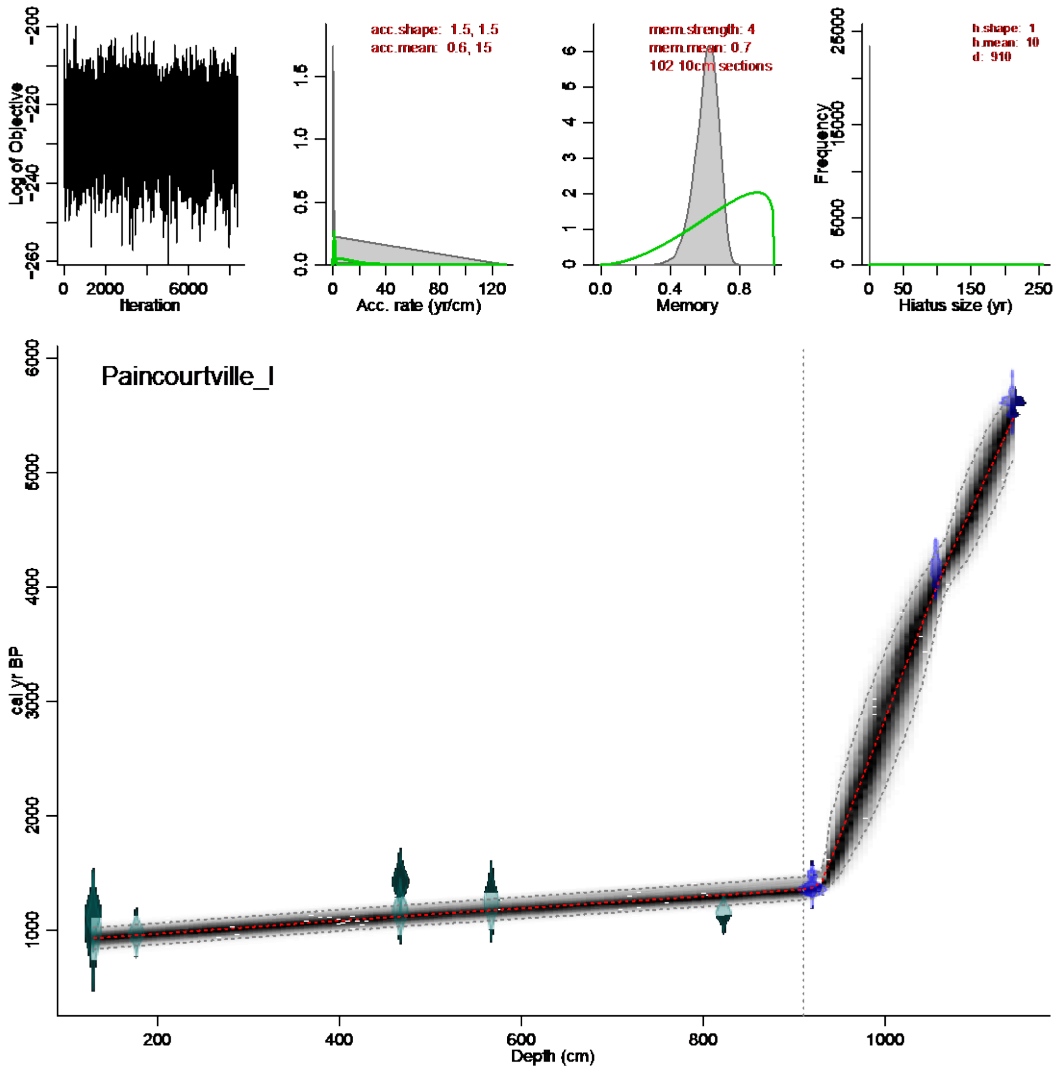

Figure C3. Priors and age-depth model for Paincourtville I. The lower panel shows the calibrated ^{14}C ages (transparent blue), the converted OSL ages (transparent green) and the age-depth model. For the age-depth model the grey shading indicates the likelihood of calendar ages and the grey dotted lines shows 95% confidence intervals. The red curve shows the optimal age-depth model based on the weighted mean age for each depth. The smaller, upper panels show the iterations of MCMC runs (upper left) and the prior (green curves) and posterior (grey histograms) distributions for the accretion rate (upper center) and memory (upper right) of the model.

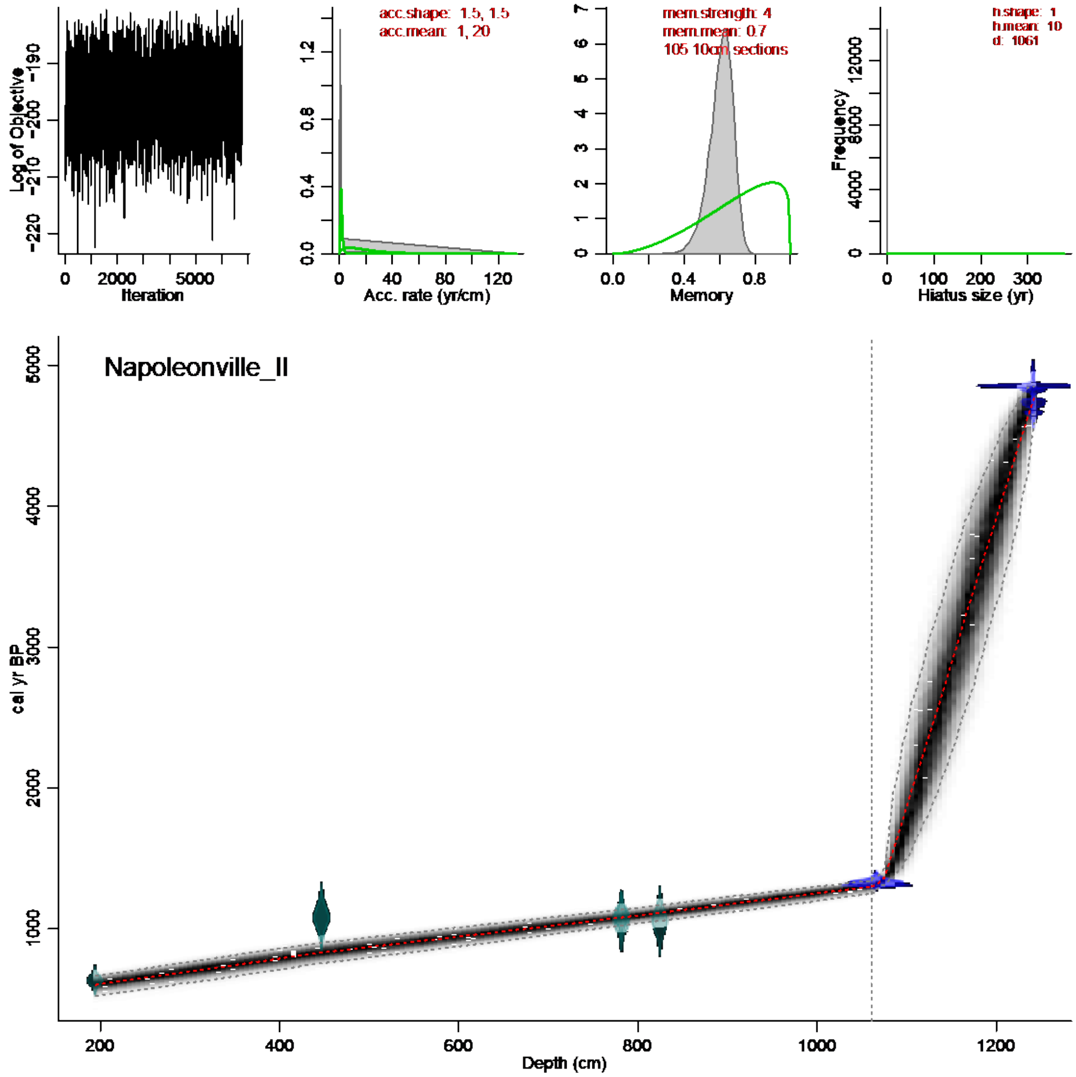

Figure C4. Priors and age-depth model for Napoleonville II. The lower panel shows the calibrated ^{14}C ages (transparent blue), the converted OSL ages (transparent green) and the age-depth model. For the age-depth model the grey shading indicates the likelihood of calendar ages and the grey dotted lines shows 95% confidence intervals. The red curve shows the optimal age-depth model based on the weighted mean age for each depth. The smaller, upper panels show the iterations of MCMC runs (upper left) and the prior (green curves) and posterior (grey histograms) distributions for the accretion rate (upper center) and memory (upper right) of the model.

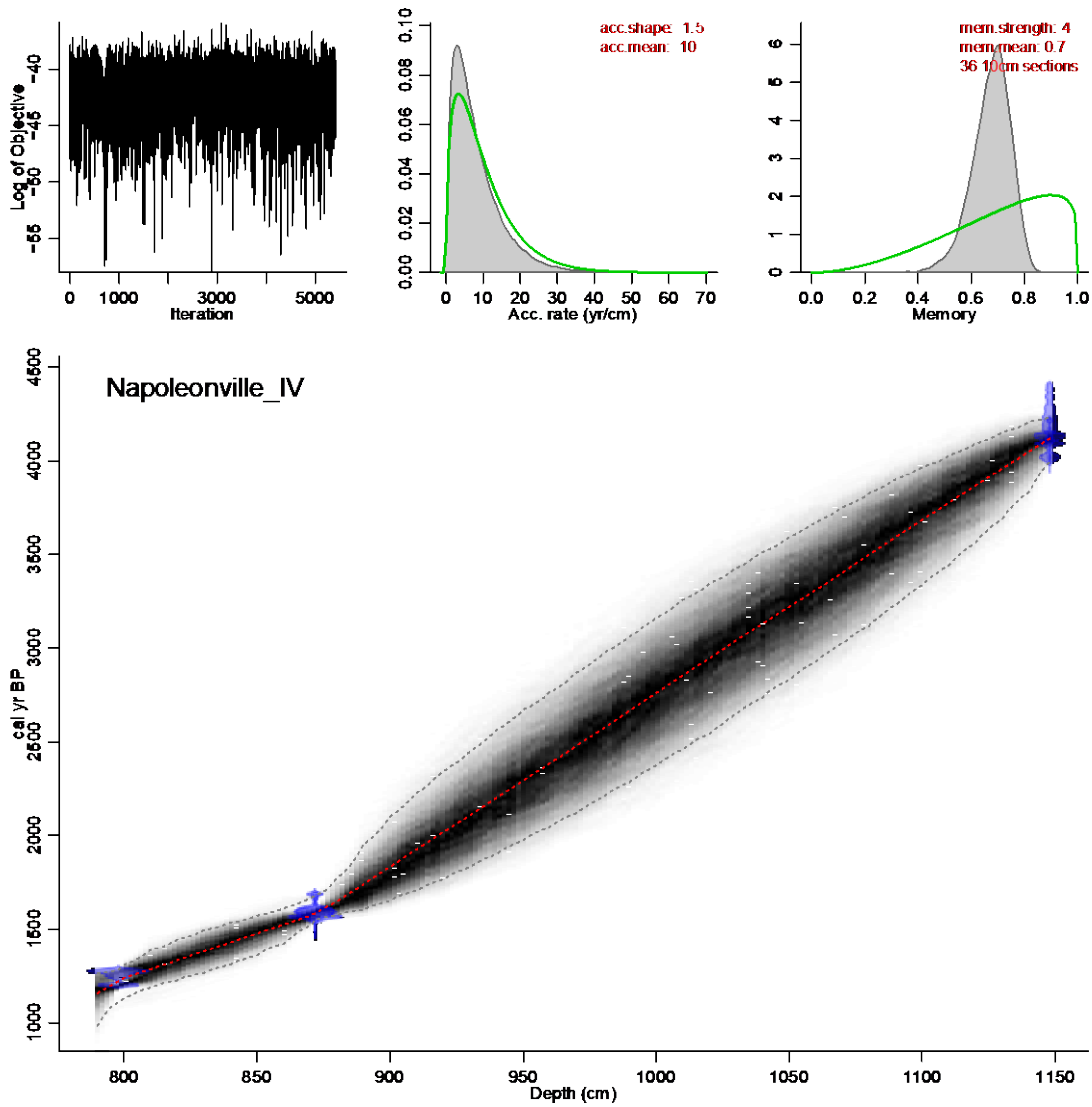

Figure C5. Priors and age-depth model for Napoleonville IV. The lower panel shows the calibrated ^{14}C ages (transparent blue) and the age-depth model. For the age-depth model the grey shading indicates the likelihood of calendar ages and the grey dotted lines shows 95% confidence intervals. The red curve shows the optimal age-depth model based on the weighted mean age for each depth. The smaller, upper panels show the iterations of MCMC runs (upper left) and the prior (green curves) and posterior (grey histograms) distributions for the accretion rate (upper center) and memory (upper right) of the model.

Table C1. Age-depth model data output from Bacon software using IntCal13 calibration curve.

Digital file.

Table C2. Accretion rates calculated using Bacon software.

Napoleonville II		**Napoleonville IV**		**Paincourtville I**	
depth (m)	mm/yr	depth (m)	mm/yr	depth (m)	mm/yr
2	11.1	8	0.0021	1.3	1.67
2.2	11.1	8.2	0.0021	1.5	1.82
2.4	11.1	8.4	0.0021	1.7	1.67
2.6	11.1	8.6	0.0016	1.9	1.82
2.8	11.1	8.8	0.0011	2.1	1.67
3	11.1	9	0.0011	2.3	1.82
3.2	11.1	9.2	0.0011	2.5	1.67
3.4	11.1	9.4	0.0011	2.7	1.82
3.6	10.5	9.6	0.0011	2.9	1.82
3.8	11.1	9.8	0.0011	3.1	1.67
4	11.1	10	0.0011	3.3	1.82
4.2	11.1	10.2	0.0011	3.5	1.67
4.4	12.5	10.4	0.0011	3.7	1.82
4.6	13.3	10.6	0.0011	3.9	1.82
4.8	13.3	10.8	0.0011	4.1	1.67
5	13.3	11	0.0011	4.3	1.82
5.2	13.3	11.2	0.0011	4.5	1.82
5.4	13.3	11.4	0.0011	4.7	1.82
5.6	14.3			4.9	1.82
5.8	13.3			5.1	2.0
6	14.3			5.3	1.82
6.2	13.3			5.5	2.0
6.4	12.5			5.7	1.82
6.6	13.3			5.9	2.0
6.8	13.3			6.1	2.0
7	13.3			6.3	1.82
7.2	13.3			6.5	2.0
7.4	14.3			6.7	1.82
7.6	13.3			6.9	2.0
7.8	13.3			7.1	1.82
8	12.5			7.3	2.0
8.2	13.3			7.5	2.0
8.4	12.5			7.7	1.82

Napoleonville II		Napoleonville IV		Paincourtville I	
depth (m)	mm/yr	depth (m)	mm/yr	depth (m)	mm/yr
8.6	12.5			7.9	2.0
8.8	12.5			8.1	2.0
9	12.5			8.3	1.82
9.2	12.5			8.5	1.82
9.4	12.5			8.7	1.67
9.6	13.3			8.9	1.33
9.8	12.5			9.1	3.0
10	12.5			9.3	0.5
10.2	12.5			9.5	0.5
10.4	12.5			9.7	0.5
10.6	1.3			9.9	0.5
10.8	0.5			10.1	0.5
11	0.5			10.3	0.5
11.2	0.5			10.5	0.5
11.4	0.5			10.7	0.6
11.6	0.5			10.9	0.6
11.8	0.5			11.1	0.6
12	0.5			11.3	0.6
12.2	0.5				
12.4	0.5				

Table C3. Bulk density and organic carbon content.

Napoleonville II

depth (m)	bulk density (g/m3)	% OC (by mass)
0.67	1.45	0.36
0.87	1.50	0.26
1.07	1.37	0.26
1.67	1.60	0.46
1.87	1.52	0.41
2.07	1.52	0.49
2.27	1.39	0.60
3.10	1.51	0.37
3.38	1.60	0.64
3.58	1.60	0.48
4.17	1.59	0.21
4.38	1.51	0.14
4.57	1.49	0.28
5.75	1.57	0.06
5.95	1.58	0.26
6.26	1.48	0.11
6.65	1.48	0.28
9.14	1.28	1.04
9.44	1.21	2.76
9.76	0.77	2.84
9.88	1.52	0.95
11.04	0.60	6.37
11.45	0.77	22.22
12.17	0.73	6.39
12.38	0.71	5.01
12.56	0.75	6.73
12.65	1.22	1.20
12.86	1.28	1.23
13.06	1.63	1.21
13.26	1.56	1.47
13.45	1.28	1.20
13.60	1.39	1.89
13.83	0.99	11.67
13.98	1.20	2.39

Napoleonville IV

depth (m)	bulk density (g/m3)	% OC (by mass)
7.98	0.86	7.13
8.31	1.09	2.97
8.59	0.70	2.54
9.40	0.69	24.27
10.02	0.75	18.16
10.18	0.64	25.90
10.73	0.63	16.55
10.95	0.66	15.34
11.14	0.66	23.18
11.35	0.64	16.99
11.55	0.85	9.64
11.75	0.97	7.24

Paincourtville I

depth (m)	bulk density (g/m3)	% OC (by mass)
3.76	1.53	0.21
3.96	1.43	0.03
4.85	1.47	0.18
5.07	1.43	0.19
5.28	1.54	0.18
5.47	1.35	0.10
5.68	1.39	0.57
5.88	1.59	0.19
6.01	1.47	0.10
6.62	1.49	0.21
6.76	1.62	0.69
6.82	1.39	0.51
7.04	1.51	0.56
7.11	1.44	0.67
7.32	1.59	0.73
7.39	1.48	0.53
7.53	1.48	0.54
7.83	1.59	0.70
8.05	1.46	0.58
8.25	1.40	0.94
8.46	1.55	0.63
8.65	1.36	0.75
8.85	1.36	0.69
9.06	1.39	0.88
9.26	1.08	8.81
9.44	1.12	7.13
9.64	1.04	4.43
10.05	0.68	9.57
10.25	0.68	9.56
10.33	1.07	5.81
10.43	0.71	6.07
10.54	0.76	13.83
10.85	0.79	13.62
10.98	0.88	21.36
11.09	0.97	13.44
11.20	0.95	6.49
11.29	1.01	12.72
11.40	1.04	5.89
11.49	0.79	10.18
11.58	0.98	6.54
11.70	1.09	2.02
11.78	1.09	0.67
11.90	1.00	0.50
11.99	1.10	0.64

Table C4. Organic carbon accumulation rate outputs from Bacon software.

Napoleonville II		Napoleonville IV		Paincourtville I	
depth (m)	g/m2/yr	depth (m)	g/m2/yr	depth (m)	g/m2/yr
2.07	82.76	8.31	67.44	3.76	58.36
2.27	92.67	8.59	29.15	3.96	7.63
3.10	62.06	9.40	181.03	4.85	48.06
3.38	113.72	10.02	145.91	5.07	53.59
3.58	81.35	10.18	179.86	5.28	50.77
4.17	37.08	10.73	112.12	5.47	26.71
4.38	26.11	10.95	110.49	5.68	145.53
4.57	55.04	11.14	167.20	5.88	59.93
5.75	12.78	11.35	118.84	6.01	29.42
5.95	57.60			6.62	59.07
6.26	21.33			6.76	208.26
6.65	55.25			6.82	136.72
9.14	166.45			7.04	158.70
9.44	422.73			7.11	176.48
9.76	279.93			7.32	231.94
9.88	180.26			7.39	157.37
11.04	18.94			7.53	157.38
11.45	81.10			7.83	215.49
12.17	23.42			8.05	169.09
12.38	17.98			8.25	244.65
				8.46	177.27
				8.65	173.38
				8.85	132.03
				9.06	62.36
				9.26	94.99
				9.44	39.07
				9.64	22.40
				10.05	31.61
				10.25	32.01
				10.33	30.78
				10.43	22.02
				10.54	55.98
				10.85	62.05
				10.98	109.02
				11.09	77.21
				11.20	36.28
				11.29	76.00

6. References

Allen, P. A., and Allen, J. R. (1991). Basin analysis: Principles and application to petroleum play assessment. John Wiley & Sons. 451 p.

Allen, S. E., et al. (1974). Chemical analysis of ecological materials. Blackwell Scientific Publications. 1974 p.

Allison, M. A., and Meselhe, E. A. (2010). The use of large water and sediment diversions in the lower Mississippi River (Louisiana) for coastal restoration. Journal of Hydrology, 387(3-4), 346-360.

Amato, M., and Ladd, J. N. (1992). Decomposition of 14C-labelled glucose and legume materials in soil: Properties influencing the accumulation of organic residue C and microbial biomass C. Soil Biology and Biochemistry, 24(5), 455-464.

Baldwin, A. H., et al. (2009). Evaluation of restored tidal freshwater wetlands. In: Perillo, G.M.E., et al. (Eds.) Coastal wetlands: an integrated ecosystem approach. Elsevier. 30 p.

Battin, T. J., et al. (2009). The boundless carbon cycle. Nature Geoscience, 2(9), 598.

Baustian, M. M., et al. (2017). Relationships between salinity and short-term soil carbon accumulation rates from marsh types across a landscape in the Mississippi River Delta. Wetlands, 37(2), 313-324.

Blaauw, M., and Christen, J. A. (2011). Flexible paleoclimate age-depth models using an autoregressive gamma process. Bayesian analysis, 6(3), 457-474.

Blum, M. D., and Roberts, H. H. (2009). Drowning of the Mississippi Delta due to insufficient sediment supply and global sea-level rise. Nature Geoscience, 2(7), 488-491.

Blum, M. D., and Roberts, H. H. (2012). The Mississippi delta region: past, present, and future. Annual Review of Earth and Planetary Sciences, 40, 655-683.

Boumans, R. M. J., et al. (1997). The effect of intertidal sediment fences on wetland surface elevation, wave energy and vegetation establishment in two Louisiana coastal marshes. Ecological Engineering, 9(1-2), 37–50.

Boumans, R. M. J., et al. (2002a). Modeling habitat change in salt marshes after tidal restoration. Restoration Ecology, 10(3), 543-555.

Boumans, R. M. J., et al. (2002b). Sediment elevation dynamics in tidal marshes: Functional assessment of accretionary biofilters. Final Report to NOAA/UNH Cooperative Institute for Coastal and Estuarine Environmental Technology (CICEET) Technical Report, Durham, NH.

Bourne, J. (2000). Louisiana's vanishing wetlands: Going, going... Science, 289(5486), 1860–1863.

Bowron, T., et al. (2011). Macro-tidal salt marsh ecosystem response to culvert expansion. Restoration Ecology, 19(3), 307–322.

Breshears, D. D., et al. (2005). Regional vegetation die-off in response to global-change-type drought. Proceedings of the National Academy of Sciences, 102(42), 15144-15148.

Buffler, R. T. (1991). Early evolution of the Gulf of Mexico basin. 1-15.

Burdige, D. J. (2005). Burial of terrestrial organic matter in marine sediments: A re-assessment. Global Biogeochemical Cycles, 19(4), GB4011, 1-7.

Cahoon, D. R., et al. (1995). Estimating shallow subsidence in microtidal salt marshes of the southeastern United States: Kaye and Barghoorn revisited. Marine Geology, 128(1-2), 1-9.

Cahoon, D. R., and Lynch, J. C. (1996). Improved cryogenic coring device for sampling wetland soils. Journal of Sedimentary Research, 66(5), 1025–1027.

Cahoon, D. R., and Lynch, J. C. (1997). Vertical accretion and shallow subsidence in a mangrove forest of southwestern Florida, USA. Mangroves and Salt Marshes, 1(3), 173–186.

Cahoon, D. R., et al. (1999). The influence of surface and shallow subsurface soil processes on wetland elevation: a synthesis. Current Topics in Wetland Biogeochemistry, 3, 72-88.

Cahoon, D. R., et al. (2000a). A method for measuring vertical accretion, elevation, and compaction of soft, shallow-water sediments. Journal of Sedimentary Research, 70(5), 1250- 1253.

Cahoon, D. R., et al. (2000b). Vertical accretion versus elevational adjustment in UK saltmarshes: an evaluation of alternative methodologies. In Pye, K. and Allen, J. R. L. (Eds.). Coastal and Estuarine Environments: sedimentology, geomorphology and geoarchaeology. Geological Society, London, 223-238.

Cahoon, D. R., et al. (2006). High-precision measurements of wetland sediment elevation: II. The rod surface elevation table. Journal of Sedimentary Research, 72(5), 734–739.

Cahoon, D. R., et al. (2003). Mass tree mortality leads to mangrove peat collapse at Bay Islands, Honduras after Hurricane Mitch. Journal of Ecology, 91(6), 1093-1105.

Cahoon, D. R, et al., (2004). Ecogeomorphology of Spartina patens-dominated tidal marshes: solid organic matter accumulation, marsh elevation dynamics, and disturbance. Coastal and Estuarine Studies, 59, 247-266.

Cahoon, D. R. (2006) A review of major storm impacts on coastal wetland elevations. Estuaries and Coasts, 29(6), 889-898.

Cahoon, D. R., et al. (2011). Sediment infilling and wetland formation dynamics in an active crevasse splay of the Mississippi River delta. Geomorphology, 131(3-4), 57–68.

Cahoon, D. R. (2015). Estimating relative sea-level rise and submergence potential at a coastal wetland. Estuaries and Coasts, 38(3), 1077-1084.

Carlson, A. E., et al. (2008). Rapid early Holocene deglaciation of the Laurentide ice sheet. Nature Geoscience, 1(9), 620.

Cierjacks, A., et al. (2010). Carbon stocks of soil and vegetation on Danubian floodplains. Journal of Plant Nutrition and Soil Science, 173(5), 644-653.

Chamberlain, E. L., et al. (2018). Anatomy of Mississippi Delta growth and its implications for coastal restoration. Science Advances, 4(4), eaar4740.

Childers, D. L., et al. (1993). Seasonal movements of sediment elevation in three mid-Atlantic estuaries. Journal of Coastal Research, 9, 986-1003.

Chmura, G. L., et al. (1987). An inventory of 13C abundances in coastal wetlands of Louisiana, USA: vegetation and sediments. Oecologia, 74(2), 264-271.

Chmura, G. L., et al. (2003). Global carbon sequestration in tidal, saline wetland soils. Global Biogeochemical Cycles, 17(4), 1-22.

Coastal Protection and Restoration Authority (CPRA) of Louisiana. 2016. Coastwide Reference Monitoring System-Wetlands Monitoring Data. Retrieved from Coastal Information Management System (CIMS) database. http://cims.coastal.louisiana.gov. Accessed 04/15/2016.

Coastal Protection and Restoration Authority of Louisiana (CPRA) (2012). Louisiana's Comprehensive Master Plan for a Sustainable Coast.

Coastal Protection and Restoration Authority of Louisiana (CPRA) (2017). Louisiana's Comprehensive Master Plan for a Sustainable Coast.

Cole, J. J., et al. (2007). Plumbing the global carbon cycle: integrating inland waters into the terrestrial carbon budget. Ecosystems, 10(1), 172-185.

Cornu, C. E., and Sadro, S. (2002). Physical and functional responses to experimental marsh surface elevation manipulation in Coos Bay's South Slough. Restoration Ecology, 10(3), 474-486.

Costanza, R., et al. (2014). Changes in the global value of ecosystem services. Global Environmental Change, 26, 152–158.

Couvillion, B. R., et al. (2011). Land area change in coastal Louisiana from 1932 to 2010: U.S. Geological Survey scientific investigations map 3164, scale 1:265,000, 12 p.

Couvillion, B. R., and Beck, H. (2013). Marsh collapse thresholds for coastal Louisiana estimated using elevation and vegetation index data. Journal of Coastal Research, 63(sp1), 58-67.

Couvillion, B.R., et al. (2017). Land area change in coastal Louisiana 1932 to 2016: U.S. Geological Survey Scientific Investigations Map 3381, 16 p. pamphlet, https://doi.org/10.3133/sim3381.

Culver, S. J., et al. (2012). Distribution of foraminifera of the Setiu estuary and lagoon, Terengganu, Malaysia. Journal of Foraminieral Research, 42(2): 109-133.

Craft, C., et al. (2008). Latitudinal trends in organic carbon accumulation in temperate freshwater peatlands. Wastewater treatment, plant dynamics and management in constructed and natural wetlands. Springer. 23-31.

Davidson, N. C. (2014). How much wetland has the world lost? Long-term and recent trends in global wetland area. Marine and Freshwater Research, 65(10), 931–941.

Day, J. W., et al. (1998). Relative sea level rise and Venice lagoon wetlands. Journal of Coastal Conservation, 4(1), 27-34.

Day, J. W., et al. (1999). Soil accretionary dynamics, sea-level rise and the survival of wetlands in Venice lagoon: a field and modelling approach. Estuarine, Coastal and Shelf Science, 49(5), 607-628.

Day, J. W. et al. (2000). Pattern and process of land loss in the Mississippi Delta: A spatial and temporal analysis of wetland habitat change. Estuaries, 23(4), 425-438.

Day, J. W. et al. (2007). Restoration of the Mississippi Delta: Lessons from Hurricanes Katrina and Rita. Science, 315(4), 1679-1684.

Day, J. W., et al. (2011a). Vegetation death and rapid loss of surface elevation in two contrasting Mississippi delta salt marshes: The role of sedimentation, autocompaction and sea-level rise. Ecological Engineering, 37(2), 229-240.

Day, J. W., et al. Sustainability of Mediterranean deltaic and lagoon wetlands with sea-level rise: the importance of river input. Estuaries and Coasts, 34(3), 483-493.

DeConto, R. M., and Pollard, D. (2016). Contribution of Antarctica to past and future sea-level rise. Nature, 531(7596), 591–597.

Degens, E. T., et al. (1991). SCOPE 42: Biogeochemistry of major world rivers. UK: Wiley.

DeLaune, R. D., et al. (1983). Relationship of marsh elevation, redox potential, and sulfide to Spartina alterniflora productivity. Soil Science Society of America Journal, 47(5), 930-935.

DeLaune, R. D., et al. (1994). Peat collapse, ponding and wetland loss in a rapidly submerging coastal marsh. Journal of Coastal Research, 1021-1030.

DeLaune, R. D., and White, J. R. (2012). Will coastal wetlands continue to sequester carbon in response to an increase in global sea level?: a case study of the rapidly subsiding Mississippi river deltaic plain. Climatic Change, 110(1-2), 297-314.

Delgado, P., et al. (2013) Sustainability of a tidal freshwater marsh exposed to a long-term hydrologic barrier and sea level rise. Estuaries and Coasts, 36(3), 585-594.

Eichler, P. P. B., et al. (2007). Modern Foraminiferal Biofacies in Subtropical Esturarine Channel, Pertioga, Sao Paulo, Brazil. The Journal of. Foraminiferal Research, 37(3): 234-247.

Erwin, R. M., et al. (2006). Surface elevation dynamics in vegetated Spartina marshes versus unvegetated tidal ponds along the mid-Atlantic coast, USA, with implications to wetlands. Estuaries and Coasts, 29(1), 96-108.

Esposito, C. R., et al. (2017). Efficient retention of mud drives land building on the Mississippi Delta plain. Earth Surface Dynamics, 5(3), 387-397.

Fagherazzi, S., et al. (2012). Numerical models of salt marsh evolution: Ecological, geormorphic, and climatic factors. Reviews of Geophysics, 50(1), RG1002.

Fagherazzi, S. (2013). The ephemeral life of a salt marsh. Geology, 41(8), 943-944.

Falcini, F., et al. (2012). Linking the historic 2011 Mississippi River flood to coastal wetland sedimentation. Nature Geoscience, 5(11), 803–807.

Fisk, H. N. (1938). Geology of Grant and LaSalle parishes (No. 10). Department of Conservation, Louisiana Geological Survey.

Fisk, H. N. (1944). Geological investigation of the alluvial valley of the lower Mississippi River: Mississippi River Waterways Exper. Sta., Vicksburg, Miss., 2.

Fisk, H. N. (1952). Geological investigation of the Atchafalaya Basin and the problem of Mississippi River diversion. Waterways Experiment Station. 145 p.

Fisk, H. N., and McFarlan, E. (1955). Late Quaternary deltaic deposits of the Mississippi River (local sedimentation and basin tectonics). Geological Society of America Special Papers, 62, 279-302.

Fisk, H. N., et al. (1954). Sedimentary framework of the modern Mississippi delta. Journal of Sedimentary Research, 24(2).

Fisk, H. N. (1960). Recent Mississippi River sedimentation and peat accumulation. Congrès Avanc Étud Stratigr carb, 1958, 187-199.

FitzGerald, D. M., et al. (2008). Coastal impacts due to sea-level rise. Annual Review of Earth and Planetary Sciences, 36, 601-647.

Folse, T. M. et al. (2014). A standard operating procedures manual for the coast-wide reference monitoring system-wetlands: Methods for site establishment, data collection, and quality assurance/quality control. Louisiana Coastal Protection and Restoration Authority. Baton Rouge, LA. 228 p.

Ford, M. A., and Grace, J. B. (1998). Effects of vertebrate herbivores on soil processes, plant biomass, litter accumulation and soil elevation changes in a coastal marsh. Journal of Ecology, 86(6), 974–982.

Ford, M. A., et al. (1999). Restoring marsh elevation in a rapidly subsiding salt marsh by thin-layer deposition of dredged material. Ecological Engineering, 12(3-4), 189-205.

Frazier, D. E., and Osanik, A. (1969). Recent peat deposits-Louisiana coastal plain. Geological Society of America Special Papers, 114, 63-86.

Frazier, D. E. (1974). Depositional episode: their relationship to the Quaternary stratigraphic framework in the northwestern portion of the Gulf basin. The University of Texas at Austin, Bureau of Economic Geology, Geological Circular, 74(1), 28.

French, J. R., and Burningham, H. (2003). Tidal marsh sedimentation versus sea-level rise: A Southeast England estuarine perspective. Proceedings Coastal Sediments 3, 1-14.

Galy, V., et al. (2008a). Loading and fate of particulate organic carbon from the Himalaya to the Ganga-Brahmaputra delta. Geochimica et Cosmochimica Acta, 72(7), 1767–1787.

Gonzalez, J. L., and Törnqvist, T. E. (2009). A new Late Holocene sea-level record from the Mississippi Delta: evidence for a climate/sea level connection?. Quaternary Science Reviews, 28(17), 1737-1749.

Gunderson, L. H., et al. (2002). Resilience of large-scale resource systems. Scope-Scientific Committee on Problems of the Environment International Council of Scientific Unions, 60, 3-20.

Guntenspergen, G., et al. (1995). Disturbance and recovery of the Louisiana coastal marsh landscape from the impacts of Hurricane Andrew. Journal of Coastal Research, SI 21, 324-339.

Hedges, J. I., and P. L. Parker (1976). Land-derived organic matter in surface sediments from the Gulf of Mexico. Geochimica et Cosmochimica Acta, 40(9), 1019-1029.

Hedges, J. I., and Keil, R. G. (1995). Sedimentary organic matter preservation: an assessment and speculative synthesis. Marine Chemistry, 49(2-3), 81-115.

Hensel, P. E., et al. (1999). Wetland vertical accretion and soil elevation change in the Rhône River delta, France: the importance of river flooding. Journal of Coastal Research, 15, 668-681.

Heinrich, P., et al. (2015). Investigation and GIS development of the buried Holocene-Pleistocene surface in the Louisiana coastal plain. Louisiana Geological Survey and Louisiana State University for the Louisiana Coastal Protection and Restoration Authority. Baton Rouge, LA. 140 p.

Hendrickson, J. C. (1997). Coastal wetland response to rising sea-level: quantification of short- and longterm accretion and subsidence, northeastern Gulf of Mexico. MS Thesis, Florida State University, Tallahassee, FL.

Hill, D. F., et al. (2011). High-resolution numerical modeling of tides in the western Atlantic, Gulf of Mexico, and Caribbean Sea during the Holocene. Journal of Geophysical Research: Oceans, 116(C10).

Hoegh-Guldberg, O. (1999). Climate change, coral bleaching and the future of the world's coral reefs. Marine and Freshwater Research, 50(8), 839-866.

Hoffmann, T., Glatzel, S., & Dikau, R. (2009). A carbon storage perspective on alluvial sediment storage in the Rhine catchment. Geomorphology, 108(1), 127-137.

Hoffmann, T., et al. (2013). Humans and the missing C-sink: erosion and burial of soil carbon through time. Earth Surface Dynamics, 1(1), 45.

Holling, C. S. (1973). Resilience and stability of ecological systems. Annual Review of Ecology and Systematics, 4(1), 1-23.

Horton, B. P. (1999). The distribution of contemporary intertidal foraminifera at Cowpen Marsh, Tees Estuary, UK: implications for studies of Holocene sea-level changes. Palaeogeography, Palaeoclimatology, Palaeoecology, 149(1-4), 127-149.

Houghton, R. A. (1995). Land-use change and the carbon cycle. Global Change Biology, 1(4), 275-287.

Howe, A. J., et al. (2009). Surface evolution and carbon sequestration in disturbed and undisturbed wetland soils of the Hunter estuary, southeast Australia. Estuarine, Coastal and Shelf Science, 84(1), 75-83.

Ibañez, C., et al. (1997). Morphologic development, relative sea level rise and sustainable management of water and sediment in the Ebre Delta, Spain. Journal of Coastal Conservation, 3(1), 191-202.

Ibáñez, C., et al. (2010). Vertical accretion and relative sea level rise in the Ebro delta wetlands (Catalonia, Spain). Wetlands, 30(5), 979-988.

Jenkinson, D. S., (1988). Soil organic matter and its dynamics. Russel's Soil Conditions and Plant Growth. Longman. 33 p.

Jelgersma, S. (1961). Holocene sea level changes in the Netherlands. PhD dissertation, Leiden University.

Kane, H. E. (1967). Recent microfaunal biobiofacies in Sabine Lake and environs, Texas and Louisiana. Journal of Paleontology, 41 (4): 947-964.

Karegar, M. A., et al. (2015). A three-dimensional surface velocity field for the Mississippi Delta: Implications for coastal restoration and flood potential. Geology, 43(6), 519-522.

Kaye, C. A., and Barghoorn, E. S. (1964). Late Quaternary sea-level change and crustal rise at Boston, Massachusetts, with notes on the autocompaction of peat. Geological Society of America Bulletin, 75(2), 63-80.

Kearns, F. L., and Davison, A. T. (1983). Field classification system of organic-rich sediments. Mineral Matter in Peat: Its Occurrence, Form and Distribution: Los Alamos National Laboratory, Los Alamos, New Mexico, 147-157.

Keil, R. G., et al. (1997). Loss of organic matter from riverine particles in deltas. Geochimica et Cosmoschimica Acta, 61(7), 1507-1511.

Kirwan, M. L., et al. (2010). Limits on the adaptability of coastal marshes to rising sea level, Geophysical Research Letters, 37, L23401.

Kirwan, M. L., and Guntenspergen, G. R. (2012). Feedbacks between inundation, root production, and shoot growth in a rapidly submerging brackish marsh. Journal of Ecology, 100(3), 764–770.

Kirwan, M. L., and Megonigal, J. P. (2013). Tidal wetland stability in the face of human impacts and sea-level rise. Nature, 504(7478), 53–60.

Kirwan, M. L., et al. (2016). Overestimation of marsh vulnerability to sea level rise. Nature Climate Change, 6(3), 253–260.

Kohl, B., et al. (2004). Foraminiferal Biostratigraphy and Paleoenvironments of the Pleistocene Lagniappe delta and related Section, Northeastern Gulf of Mexico. Late Quaternary Stratigraphic Evolution of the Northern Gulf of Mexico Basin, SEPM Special Publication 79, 189-216.

Kolb, C. R., and Van Lopik, J. R. (1958). Geology of the Mississippi River deltaic plain, southeastern Louisiana. U., S. Army Engineer Waterway Experiment Station, Corps of Engineers, Vicksburg. MS, Technical Report, 3-483.

Kolchugina, T. P., and Vinson, T. S. (1993). Carbon sources and sinks in forest biomes of the former Soviet Union. Global Biogeochemical Cycles, 7(2), 291-304.

Kolker, A. S., et al. (2011). An evaluation of subsidence rates and sea-level variability in the northern Gulf of Mexico. Geophys. Res. Lett. 38, L21404.

Kosters, E. C., et al. (1987). Sedimentary and botanical factors influencing peat accumulation in the Mississippi Delta. Journal of the Geological Society, 144(3), 423-434.

Kosters, E. C. (1989). Organic-clastic facies relationships and chronostratigraphy of the Barataria interlobe basin, Mississippi delta plain. Journal of Sedimentary Research, 59(1), 98-113.

Krauss, K.W., et al. (2010). Surface elevation change and susceptibility of different mangrove zones to sea-level rise on Pacific high islands of Micronesia. Ecosystems, 13(1), 129-143.

Kroes, D. E., and Hupp, C.R. (2010). The effect of channelization on floodplain sediment deposition and subsidence along the Pocomoke River, Maryland. Journal of the American Water Resources Association, 46(4), 686-699.

Lane, R. R., et al. (2006). Wetland surface elevation, vertical accretion, and subsidence at three Louisiana estuaries receiving diverted Mississippi River water. Wetlands, 26(4), 1130–1142.

Langley, J. A., et al. (2009). Elevated CO2 stimulates marsh elevation gain, counterbalancing sea-level rise. Proceedings of the National Academy of Sciences, 106(15), 6182-6186, doi:10.1073/pnas.0807695106.

Le Quéré, C., et al. (2016). Global carbon budget 2016. Earth System Science Data, 8(2).

Letetrel, C. et al. Estimation of vertical land movement rates along the coasts of the Gulf of Mexico over the past decades. Cont. Shelf Res. 111, 42–51 (2015).

Li, Y.-X., et al. (2012). Synchronizing a sea-level jump, final Lake Agassiz drainage, and abrupt cooling 8200 years ago. Earth and Planetary Science Letters, 315, 41-50.

Love, R. et al. (2016). The contribution of glacial isostatic adjustment to projections of sea-level change along the Atlantic and Gulf coasts of North America. Earth's Future, 4(10), 440-464.

Lovelock, C. E., et al. (2011). The role of surface and subsurface processes in keeping pace with sea level rise in intertidal wetlands of Moreton Bay, Queensland, Australia. Ecosystems, 14(5), 745-757.

Lovelock, C. E., et al. (2014). Contemporary rates of carbon sequestration through vertical accretion of sediments in mangrove forests and saltmarshes of South East Queensland, Australia. Estuaries and Coasts 37(3), 763 -771.

Lovelock, C. E. et al. (2015). The vulnerability of Indo-Pacific mangrove forests to sea-level rise. Nature, 526(7574), 559–565.

Maldonado, J. K., et al. (2013). The impact of climate change on tribal communities in the US: displacement, relocation, and human rights. Climatic Change, 120(3), 601-614.

Mattheus, C. R., (2010). Impact of land-use change and hard structures on the evolution of fringing marsh shorelines. Estuarine, Coastal and Shelf Science, 88(3), 365-376.

McFarlane, E. (1961). Radiocarbon dating of late Quaternary deposits, south Louisiana. Geological Society of America Bulletin, 72(1), 129-158.

McKee, K. L., et al. (2007). Caribbean mangroves adjust to rising sea level through biotic controls on change in soil elevation. Global Ecology and Biogeography, 16(5), 545-556.

McKee, K. L., and Cherry, J. A. (2009). Hurricane Katrina sediment slowed elevation loss in subsiding brackish marshes of the Mississippi River delta. Wetlands, 29(1), 2-15.

McKee, K. L. (2011). Biophysical controls on accretion and elevation change in Caribbean mangrove ecosystems. Estuarine, Coastal and Shelf Science, 91(4), 475–483.

Meckel, T. A., et al. (2006). Current subsidence rates due to compaction of Holocene sediments in southern Louisiana. Geophysical Research Letters, 33, L11403.

Mendelssohn, I. A., et al. (1981). Oxygen deficiency in Spartina alterniflora roots: metabolic adaptation to anoxia. Science, 214(4519), 439-441.

Mitrovica, J. X., et al. (2009). The sea-level fingerprint of West Antarctic collapse. Science, 323(5915), 753.

Morris, J. T., et al. (2002). Responses of coastal wetlands to rising sea level. Ecology, 83(10), 2869-2877.

Murray, J. W. (1973). Distribution and Ecology of Living Benthic Foraminiferids. Heinemann Educational Books Limited.

Murray, J. W. (1991). Ecology and Paleoecology of Benthic Foraminifera. Longman Scientific and Technical, Longman Group UK Limited.

Murray, J. (2006). Ecology and Applications of Benthic Foraminifera, Cambridge Univ. Press, 426 p.

Nienhaus, J. et al. (2018). A new subsidence map of coastal Louisiana. GSA Today, 27(9), G337GW.1

Nevitt, J. M. (2009). Perspectives on the Stability of Coastal Wetlands in the Mississippi Delta: A Comparison of Paleo-environmental Proxies (Unpublished bachelor's thesis). Tulane University.

Oliver, T. S. N., et al. (2012). Measuring, mapping and modelling: an integrated approach to the management of mangrove and saltmarsh in the Minnamurra River estuary, southeast Australia. Wetlands Ecology and Management, 20(4), 353–71.

Ortiz, A. C., et al. (2017). Land loss by pond expansion on the Mississippi River Delta Plain, Geophysical Research Letters, 44(8), GL073079.

Pacquette, C. H., et al. (2004). Changes in saltmarsh surface elevation due to variability in evapotranspiration and tidal flooding. Estuaries, 27(1), 82-89.

Paola, C. et al. (2011). Natural Processes in Delta Restoration: Application to the Mississippi Delta. Annual Review of Marine Science, 3, 67–91.

Penland, S., et al. (1988). Transgressive depositional systems of the Mississippi delta plain: a model for barrier shoreline and shelf sand development. Journal of Sedimentary Research, 58(6), 932-949.

Penland, S., and Ramsey, K.E. (1990). Relative sea-level rise in Louisiana and the Gulf of Mexico: 1908-1988. Journal of Coastal Research, 6, 323-342.

Perie, C., and Ouimet, R. (2008). Organic carbon, organic matter and bulk density relationships in boreal forest soils. Canadian Journal of Soil Science, 88(3), 315-325.

Phleger, F. B. (1970). Foraminiferal populations and marine marsh processes. Limnology and Oceanography, 15(4): 522-534.

Poag, C. W. (1978). Paired foraminiferal ecophenotypes in Gulf Coast estuaries: ecological and paleoecological implications. Gulf Coast Association of Geological Societies, 28: 395-421.

Ramsey, C. B. (2009). Bayesian analysis of radiocarbon dates. Radiocarbon, 51(5), 337-360.

Reed, D. J. (1995). The response of coastal marshes to sea-level rise: Survival or submergence? Earth Surface Processes and Landforms, 20(1), 39–48.

Reed, D. J. (2002). Understanding tidal marsh sedimentation in the Sacramento-San Joaquin Delta, California. Journal of Coastal Research, 36(sp1), 605-611.

Reimer, P. J., et al. (2013). IntCal13 and Marine13 radiocarbon age calibration curves 0-50,000 years cal BP. Radiocarbon, 55(4), 1869-1887.

Roberts, H. H. (1997). Dynamic changes of the Holocene Mississippi River delta plain: the delta cycle. Journal of Coastal Research, 605-627.

Roberts, H. H., et al. (2015). Floods and Cold Front Passages: Impacts on coastal marshes in a river diversion setting (Wax Lake Delta area, Louisiana). Journal of Coastal Research, 31(5), 1057 – 1068.

Rogers, K., et al. (2005a). Surface elevation dynamics in a regenerating mangrove forest ad Homebush Bay, Australia. Wetlands Ecology and Management, 13(5), 587-598.

Rogers, K., et al. (2005b). Mangrove encroachment of salt marsh in Port Bay, Victoria: the role of sedimentation, subsidence and sea level rise. Estuaries, 28(4), 551-559.

Rogers, K., et al. (2006). Vegetation change and surface elevation dynamics in estuarine wetlands of southeast Australia. Estuarine, Coastal and Shelf Science, 66(3-4), 559-569.

Rogers, K., et al. (2013). Sedimentation, elevation and marsh evolution in a southeastern Australian estuary during changing climatic conditions. Estuarine, Coastal and Shelf Science, 133, 172-181.

Roman, C. T., et al. (2007). Evaluation of marsh development processes at Fire Island National Seashore (New York): recent and historic perspectives. Technical Report NPS/NER/NRTR – 2007/089, National Park Service.

Rooth, J., and Stevenson, J. (2000). Sediment deposition patterns in Phragmites australis communities: Implications for coastal areas threatened by rising sea-level. Wetlands Ecology and Management, 8(2-3), 173-183.

Rosenheim, B. E., and Galy, V. (2012). Direct measurement of riverine particulate organic carbon age structure. Geophysical Research Letters, 39(19), GL052883.

Rosenheim, B. E., et al. (2013). River discharge influences on particulate organic carbon age structure in the Mississippi/Atchafalaya River System. Global Biogeochemical Cycles, 27(1), 154-166.

Russell, R. J. (1936). Physiography of lower Mississippi River delta. Louisiana Geological Survey.

Russell, R. J. (1940). Quaternary history of Louisiana. Geological Society of America Bulletin, 51(8), 1199-1233.

Rybczyk, J. M., and Cahoon, D. R. (2002). Estimating the potential for submergence for two wetlands in the Mississippi River Delta. Estuaries, 25(5), 985-998.

Saucier, R. T. (1964). Quaternary geology of the lower Mississippi Valley. (No. 6). Arkansas Archeological Survey.

Saucier, R. T. (1994). Geomorphology and Quarternary Geologic History of the Lower Mississippi Valley. Volume 2. Army Engineer Waterways Experiment Station, Vicksburg, MS, Geotechnical Lab.

Scarton, D., et al. (2000). Effects of an intertital sediment fence on sediment elevation and vegetation distribution in a Venice (Italy) lagoon salt marsh. Ecological Engineering, 16(2), 223-233.

Scheffer, M., and Carpenter, S. R. (2003). Catastrophic regime shifts in ecosystems: linking theory to observation. Trends in Ecology & Evolution, 18(12), 648-656.

Scheffer, M., et al. (2001). Catastrophic shifts in ecosystems. Nature, 413(6856), 591-596.

Schlesinger, W. H., and Melack, J. M. (1981). Transport of organic carbon in the world's rivers. Tellus, 33(2), 172-187.

Schnitzer, M. and Khan, S. U. (1978). Soil organic matter. Elsevier.

Shen, Z., and Mauz, B. (2012). Optical dating of young deltaic deposits on a decadal time scale. Quaternary Geochronology, 10, 110-116.

Shen, Z., et al. (2012). Rapid and widespread response of the Lower Mississippi River to eustatic forcing during the last glacial-interglacial cycle. Geological Society of America Bulletin, 124(5-6), 690-704.

Shen, Z., et al., (2015). Episodic overbank deposition as a dominant mechanism of floodplain and delta-plain aggradation. Geology, 43(10), 875-878.

Shields, M. R., et al. (2017). Carbon storage in the Mississippi River delta enhanced by environmental engineering. Nature Geoscience, 10(11), 846-851.

Spencer, T., et al. (2012). Surface elevation change in natural and re-created intertidal habitats, eastern England, UK, with particular reference to Frieston Shore. Wetlands Ecology and Management, 20(1), 9-33.

Stallard, R. F. (1998). Terrestrial sedimentation and the carbon cycle: coupling weathering and erosion to carbon burial. Global Biogeochemical Cycles, 12(2), 231-257.

Steinmetz, B. (2015). Assessing Mississippi Delta marsh stability through a paleoenvironmental analysis using foraminiferal assemblages (Unpublished bachelor's thesis). Tulane University.

Steneck, R. S., et al. (2002). Kelp forest ecosystems: biodiversity, stability, resilience and future. Environmental Conservation, 29(4), 436-459.

Steyer, G. D. et al. (2003). A proposed coast-wide reference monitoring system for evaluating Wetland restoration trajectories in Louisiana. Environmental Monitoring and Assessment. 81, 107–117.

Stokes, D. J., et al. (2009). Surface elevation changes and sediment characteristics of intertidal surfaces undergoing mangrove expansion and mangrove removal, Waikaraka Estuary, Tauranga Harbour, New Zealand. International Journal of Ecology and Development, 12, 88-106.

Sutfin, Nicholas A., et al. (2016). Banking carbon: a review of organic carbon storage and physical factors influencing retention in floodplains and riparian ecosystems. Earth Surface Processes and Landforms, 41(1), 38-60.

Törnqvist, T. E., et al. (1996). A revised chronology for Mississippi River subdeltas. *Science*, 274(5291), 1693-1696.

Törnqvist, T. E., (2004a). Tracking the sea-level signature of the 8.2 ka cooling event: New constraints from the Mississippi Delta. Geophysical Research Letters, 31(23), GL021429.

Törnqvist, T. E., (2004b). Deciphering Holocene sea-level history on the US Gulf Coast: A high-resolution record from the Mississippi Delta. Geological Society of America Bulletin, 116(7-8), 1026-1039.

Törnqvist, T. E. et al. (2008). Mississippi Delta subsidence primarily caused by compaction of Holocene strata. Nature Geoscience, 1(3), 173–176.

Trowbridge, A. C. (1930). Building of Mississippi delta. AAPG Bulletin, 14(7), 867-901.

Tweel, A. W., and Turner, R. E. (2012). Landscape-scale analysis of wetland sediment deposition from four tropical cyclone events. PLoS One 7, e50528.

Tye, R. S., and Kosters, E. C. (1986). Styles of interdistributary basin sedimentation: Mississippi delta plain, Louisiana.

USGCRP, 2017: Climate Science Special Report: Fourth National Climate Assessment, Volume I. U.S. Global Change Research Program, Washington, DC, USA, 470 pp, doi: 10.7930/J0J964J6.

Van Asselen, S. (2011). The contribution of peat compaction to total basin subsidence: implications for the provision of accommodation space in organic-rich deltas. Basin Research 23, 239-255, doi:10.1111/j.1365-2117.2010.00482.x.

Vandenbruwaene, W., et al. (2011). Sedimentation and response to sea-level rise of a restored marsh with reduced tidal exchange: comparison with a natural tidal marsh. Geomorphology 130(3-4), 115-126.

Van de Plassche, O. (1986). Introduction, in Sea-Level Research: a Manual for the Collection and Evaluation of Data. Geo Books. 1-26.

Van Proosdij, D., et al. (2006). Seasonal and annual variations in the volumetric sediment balance of a macro-tidal salt marsh. Marine Geology, 225(1-4), 103-127.

Van Proosdij, D., et al. (2010). Ecological re-engineering of a freshwater impoundment for salt marsh restoration in a hypertidal system. Ecological Engineering, 36(10), 1314-1332.

Vetter, L., et al. (2017). Short organic carbon turnover time and narrow 14C age spectra in early Holocene wetland paleosols. Geochemistry, Geophysics, Geosystems, 18(1), 142-155.

Villa, J. A., and Mitsch, W. J. (2015). Carbon sequestration in different wetland plant communities in the Big Cypress Swamp region of southwest Florida. International Journal of Biodiversity Science, Ecosystem Services, and Management, 11(1), 17-28.

Visser, J. M., et al. (2002). The impact of a severe drought on the vegetation of a subtropical estuary. Estuaries, 25(6), 1184–1195.

Wallace, K., et al. (2005). Evolution of tidal creek networks in a high sedimentation environment: A 5-year experiment at Tijuana Estuary, California. Estuaries, 28(6), 795-811.

Walling, D. E., et al. (2006). River flood plains as carbon sinks. IAHS PUBLICATION, 306, 460.

Wang, H., Steyer, et al. (2014). Forecasting landscape effects of Mississippi River diversions on elevation and accretion in Louisiana deltaic wetlands under future environmental uncertainty scenarios. Estuarine, Coastal and Shelf Science, 138, 57-68.

Webb, E. L. et al. (2013). A global standard for monitoring coastal wetland vulnerability to accelerated sea-level rise. Nature Climate Change, 3(5), 458–465.

Whelan, K.R.T., et al. (2005). Groundwater control of mangrove surface elevation: shrink-swell of mangrove soils varies with depth. Estuaries 28(6), 833–843.

Whelan, K.R.T., et al. (2009). Smith, T.J., Anderson, G.H., & Ouellette, M.L. Hurricane Wilma's impact on overall soil elevation and zones within the soil profile in a mangrove forest. Wetlands, 29(1), 16-23.

Wohl, E., et al. (2012). The hydrology of the humid tropics. *Nature Climate Change*, 2(9), 655.

Wohl, E., et al. (2015). "The science and practice of river restoration." Water Resources Research, 51(8), 5974-5997.

Wolstencroft, M., et al. (2014). Understanding subsidence in the Mississippi Delta region due to sediment, ice, and ocean loading: Insights from geophysical modeling. Journal of Geophysical Research, Solid Earth 119(4), 3838–3856.

Yu, S.-Y., et al. (2012). Quantifying Holocene lithospheric subsidence rates underneath the Mississippi Delta. Earth and Planetary Science Letters, 331, 21-30.

Yuill, B. T., et al. (2016). Morphodynamics of the erosional phase of crevasse-splay evolution and implications for river sediment diversion function. Geomorphology, 259, 12-29.

Biography

Krista L. Jankowski received a B.A. in Geology and Political Science from Macalester College (St. Paul, MN) in 2007, and an M.A. in Climate & Society from Columbia University (New York, NY) in 2010. She was named a 2017 National Academies of Science Gulf Research Program Science Policy Fellow and is currently a Coastal Resources Scientist Supervisor on the Master Plan Development Team at the Louisiana Coastal Protection and Restoration Authority.